DISS. ETH Nr. 19170

Linking Cholesterol Sensing at the Plasma Membrane to its Production at the Endoplasmic Reticulum

A B H A N D L U N G
zur Erlangung des Titels

DOKTOR DER WISSENSCHAFTEN

der

ETH Zürich

vorgelegt von

Herbert Polzhofer

Mag. rer. nat. Unversität Wien

geboren am 15. Dezember 1980

von Österreich

Angenommen auf Antrag von:

Prof. Dr. Lucas Pelkmans

Prof. Dr. Ernst Hafen

Prof. Dr. Christoph Thiele

Zürich 2010

[...] und also setzen wohl auch die kleinen Alltagsleistungen in ihrer gesellschaftlichen Summe und durch ihre Eignung für diese Summierung viel mehr Energie in die Welt als die heroischen Taten; ja die heroische Leistung erscheint geradezu winzig, wie ein Sandkorn, das mit ungeheurer Illusion auf einen Berg gelegt wird.
Robert Musil, Der Mann ohne Eigenschaften

Contents

1 Summary **1**

2 Zusammenfassung **3**

3 Introduction **5**

3.1 Atherosclerosis 5

3.2 Cholesterol homeostasis in the body 6

3.3 Cholesterol has a very special chemistry 8

3.3.1 Cholesterol-lipid interaction in the membrane 9

3.4 Endocytosis and the itinerary of cargo in the cell 10

3.4.1 Mechanisms of Endocytosis 10

3.4.2 The itinerary of endocytic cargo 16

3.4.3 Distribution of cholesterol in different organelles 18

3.4.4 Sites of cholesterol transport 19

3.5 Cholesterol homeostasis in the cell 24

3.5.1 Cholesterol is synthesized by the mevalonate pathway 24

3.5.2 Transcriptional control of cholesterol production 25

3.5.3 Regulation of HMGCR stability 26

3.6 Bibliography 31

4 Aim of the Thesis **49**

5 HMGCR is regulated by endocytosis **51**
5.1 Abstract . . . 51
5.2 Introduction . . . 52
5.3 Results . . . 54
5.4 Discussion . . . 61
5.5 Material and Methods . . . 64
5.5.1 Materials . . . 64
5.5.2 Methods . . . 64
5.6 Bibliography . . . 68
5.7 Figure Legends . . . 72
5.8 Figures . . . 76

6 Discussion **85**
6.1 Question and Hypothesis . . . 85
6.1.1 Endocytosis and HMGCR degradation . . . 88
6.1.2 Molecular regulators of HMGCR . . . 89
6.1.3 Is AMFR transported? . . . 91
6.2 Conclusion and Outlook . . . 92
6.2.1 Dissect the role of AMFR . . . 94
6.2.2 Identify the molecular players of HMGCR . . . 94
6.3 Bibliography . . . 100

7 Material and methods **103**
7.1 Materials . . . 103
7.2 Methods . . . 111
7.2.1 Cloning of HMGCR-GPF, AMFR-GFP and AMFR-myc . . . 111
7.2.2 Insertion of a LAP cassette into HMGCR on a BAC . . . 112
7.2.3 Cell Culture . . . 113

7.2.4 Drug Treatments 113
7.2.5 Image-based Assays 114
7.2.6 Cell Fractionation and Immunoblot Analysis 115
7.2.7 siRNA treatment of A431-HMGCR-GFP cells 116
7.2.8 qrtPCR of ABCA1, AMFR and VCP 117
7.2.9 Image analysis and statistical analysis 118

8 FAK controls transcription of ABCA1 **119**
Abstract 119
Introduction 120
Discussion 127
8.1 Figure legends 133
8.2 Figures 137

9 Acknowledgements **143**

List of Figures

3.1 The primary pathways of human plasma lipoproteins 7
3.2 The chemical structure of cholesterol 9
3.3 Intracellular cholesterol transport 23
3.4 Regulation of de novo cholesterol synthesis 30

5.1 Tyrosine kinases and Dynamins regulate HMGCR degradation . . . 77
5.2 HMGCR-GFP is regulated similar to endogenous HMGCR 78
5.3 An image-based fluorescent reporter assay 79
5.4 A candidate based siRNA 80
5.5 How cells sense their overall cholesterol content 81
5.6 Efficient and tight induction of the dynamin 82
5.7 AMFR does not change its localization upon sterol depletion 83

6.1 Overview of comparative screen 97

7.1 Vectormaps of generated constructs 110

List of Tables

3.1 An overview of different endocytic pathways 16

7.1 Antibodies 104
7.2 Chemicals 105
7.3 siRNAs used for candidate screen 106
7.4 Primers for ABCA1 108
7.5 Primers for HMGCR 109

1 Summary

Excess of cholesterol is an important cause of complex diseases such as arteriosclerosis, heart attack and stroke. Cholesterol is an essential constituent of mammalian cell membranes, which changes the fluidity of membranes and serves as a signaling molecule. Changes in the cholesterol concentration of cell membranes have important consequences for membrane ruffling, endocytosis and cellular motility.

The rate-limiting enzyme of cholesterol production is the 3-hydroxy-3-methylglutaryl-CoenzymeA-reductase (HMGCR), which is located in the membrane of the smooth endoplasmic reticulum (ER). Newly synthesized cholesterol is transported by vesicular and non-vesicular traffic to all membranous compartments of the cell. Its primary site of accumulation is the plasma membrane (PM), where 85% of all unesterified cholesterol is stored. Conversely, ER membranes contain relatively low levels of cholesterol. To ensure correct cholesterol homeostasis, it is imperative that cells are able to monitor the cholesterol levels of their membranes and feed this information back to the site of cholesterol synthesis in the smooth ER. Thus, the amount of cholesterol in the cell can be adjusted by regulating the rate-limiting enzyme HMGCR. Currently, the mechanism that relays the information from the PM to the ER is unknown. This work provides the first evidence that endocytosis is involved in regulating HMGCR levels by sensing of cholesterol in the plasma membrane. Furthermore, the assay that I developed will make it easy to screen for further regulators of HMGCR turnover. The identification of such regulators would have important medial implication for the treatment of cholesterol homeostasis-related diseases.

2 Zusammenfassung

Überschüssiges Cholesterin ist eine wichtige Ursache von komplexen Krankheiten wie Arteriosklerose, Herzinfarkt und Schlaganfall. Cholesterin ist ein wesentlicher Bestandteil der Zellmembranen von Säugetieren, es verändert die Fluidität der Membranen und dient als Signalmolekül. Änderungen in der Cholesterin-Konzentration von Zellmembranen haben wichtige Auswirkungen auf Membran „ruffles“, Endozytose und zellulärer Motilität.
Das geschwindigkeitsbestimmende Enzym der Cholesterinproduktion ist die 3-Hydroxy-3-methyl-CoenzymeA-Reduktase (HMGCR), ein Transmembranprotein des glatten endoplasmatischen Retikulums (ER). Neu synthetisiertes Cholesterin wird durch vesikulären und nicht-vesikulären Transport zu allen membranösen Kompartimenten der Zelle transportiert. Der primäre Ort der Akkumulation ist die Plasmamembran (PM), wo 85% alles unveresterten Cholesterins gespeichert ist. Im Gegensatz dazu enthalten ER-Membranen relativ niedrige Mengen an Cholesterin. Um ein korrektes Cholesteringleichgewicht in der gesamten Zelle herzustellen, ist es unerlässlich, dass eine Zelle den „Cholesterinspiegel„ in der Plasmamembran misst und diese Informationen an den Ort der Cholesterinproduktion im glatten ER weiterleitet. Nur so kann die Cholesterinpoduktion and die Gesamtmenge angepasst werden. Derzeit ist der Mechanismus der die Informationen aus der PM ans ER übermittelt unbekannt.

Eine Möglichkeit wäre, dass die Konzentration des Cholesterins durch Endozytose weitergeleitet wird. Ich habe die Folgen des Eingreifens in endozytischen vesikulären Transport auf die Expression und den Abbau von HMGCR untersucht.

Zu diesem Zweck clonierte ich an den cytosolischen C-Terminus von HMGCR, das auf einem Bacterial Artificial Chromosome (BAC) codiert war, ein Grün Fluoreszierendes Protein (GFP). Dadurch konnte ich die Änderung von physiologische HMGCR-levels von einzelnen Zellen mit zeitlicher Auflösung unter dem Mikroskop zu verfolgen. Wenn Zellen in Gegenwart eines Inhibitors von de novo Cholesterinsynthese ohne externes Cholesterin kultiviert wurden, stiegen HMGCR-levels dramatisch an, wenn Cholesterin zugegeben wurde, fielen die HMGCR levels rapide ab. Ich fand heraus, dass chemische Inhibitoren von Dynamin (Mediatoren für die Vesikel Abschnürung) und Tyrosinkinasen den Cholesterin-abhängigen HMGCR Abbau hemmten. Entscheidend ist, dass die Hemmung des vesikulären Transports vom Golgi complex zur PM und der Abbau von Mikrotubuli keine Wirkung auf HMGCR hatten. Darüber hinaus bewirkte die Hemmung der Tyrosinkinasen eine Cholesterin-unabhängige Degradation HMGCR, was eine Rolle von Tyrosinkinasen für die Stabilität von HMGCR bedeutet. Um den Dynamin-abhängigen Abbau von HMGCR zu untersuchen, habe ich die Proteinmengen von 18 Genen mit RNAi Technologie reduziert. Diese Gene waren entweder als Regulatoren von HMGCR bekannt oder an Endozytose und Membrantransport beteiligt. RNAi der schweren Untereinheit von Clathrin, Adapterprotein 2 μ-Untereinheit oder Dynamin 2 reduzierten den HMGCR Aufbau. Beim Cholesterin-induzierter HMGCR Abbau könnte Eps15 beteiligt sein.

Meine Arbeit liefert erste Beweise für eine Rolle von Endozytose in der Regulation von HMGCR. Ferner ermöglicht der von mir entwickelte Assay, weitere Regulatoren von HMGCR zu finden. Die Identifikation solcher Regulatoren würden wichtige Implikationen für die Behandlung von Krankheiten des Cholesteringleichgewichts haben.

3 Introduction

3.1 Atherosclerosis

Myocardial infarction, cerebral infarction (stroke) and gangrene are strongly linked to one common cause: Atherosclerosis. This chronic, slowly progressive and cumulative condition is a hardening of arteries by the formation of multiple plaques on the inside walls of the arteries (Ross, 1995). These plaques can breach and the resulting clot reduces the diameter of the arteries eventually closuring the artery completely thus finally blocking blood supply. Lesions of atherosclerosis represent the principal cause of death in the United States, Europe and part of Asia (Ross, 1995)

Atherogenesis in its early stage is marked by deposition of lipid-filled monocyte-derived macrophages and varying numbers of T lymphocytes. Atherosclerotic lesions in their advanced state consist of three components: the atheroma, a soft yellowish material at the center of plaques nearest to the lumen of the artery, a core of cholesterol crystals on the inside of plaques and calcification at the outer base.

From early on it became clear that atherosclerosis is tightly linked to levels of blood lipoproteins and its contents. (Castelli et al., 1986; Wilson et al., 1983,?)High levels of low-density lipoprotein (LDL) in the blood have been correlated with an increased risk of atherosclerosis, whereas high levels of high-density lipoproteins have been correlated with a protective effect. Research on the role of lipids and cholesterol in atherosclerosis has been performed for almost a century; for exam-

ple (Anitschkow, 1915). Cholesterol metabolism serves as the textbook example how insights into the molecular mechanisms enable us to treat a disease. However, despite of having a treatment for some cholesterol related diseases, we start seeing even more implications with other diseases and important questions like how cholesterol affects cells in atherosclerotic lesions or how cholesterol is transported within the cell remain unanswered. Therefore physical properties of cholesterol, its functions and its regulation, the transport within the cell and through the body, are still of main interest even more as cholesterol's role in Alzheimer's disease and cancer becomes increasing obvious (Wolozin et al., 2006; Wolozin, 2004).

3.2 Cholesterol homeostasis in the body

As cholesterol as a basic constituent of animal membranes, all food made from animal products contains cholesterol, with levels being highest in egg yolks, poultry and beef. Fat and cholesterol uptake from food takes place in the duodenum (Chang et al., 2006). Triacylglycerol (TAG) is hydrolyzed by lipase, which results in monoacylglycerol and fatty acids. Cholesterol and fatty acids are emulsified by bile salts and taken up by epithelial cells. There, fatty acids are re-esterified to TAG again and cholesterol is esterified by Acyl-coenzyme A:cholesterol acyltransferase (ACAT), resulting in neutral hydrophobic molecules. TAG and esterified cholesterol are arranged to spherical lipoprotein particles mainly consisting of neutral fats in their inside and apolipoproteinB (apoB) as the main protein constituent. These so called chylomicrons are exocytosed into the lymph vessel, where they reach the target cells. On the surface of the target cells, especially on adipocytes, TAG is converted to free fatty acids and glycerol by lipoprotein lipases. This leaves chylomicron remnants, which are loaded mainly by cholesterol. The liver as the crossing-point of cholesterol metabolism then takes up these chylomicron remnants. In order to deliver fatty acids and cholesterol to all peripheral tissue,

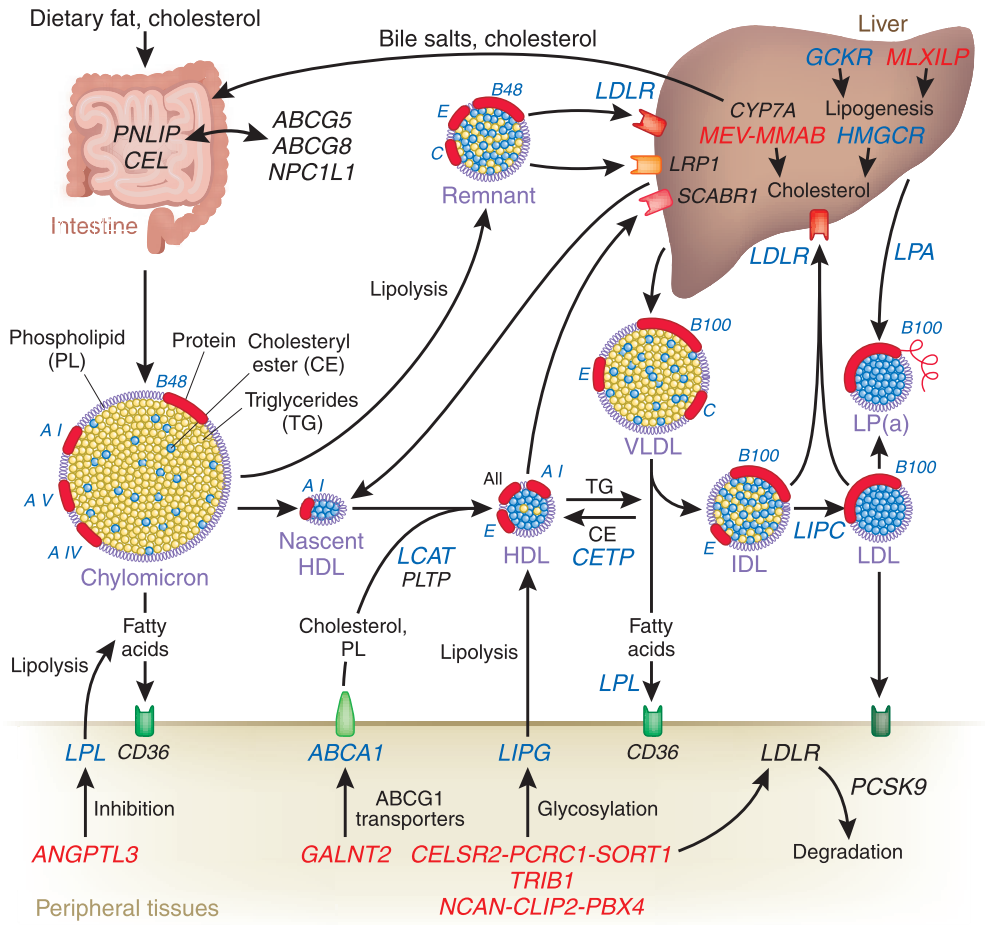

Figure 3.1: The primary pathways for the metabolism of human plasma lipoproteins. Triglyceride (TG)- rich lipoproteins are secreted by intestine (chylomicrons) and liver (VLDL). These undergo lipolysis in the circulation, thereby delivering fatty acids to tissues. Chylomicron remnants and about half of the VLDL remnants are then taken up by the liver. The remainder of the VLDL remnants is further metabolized to cholesterol-rich LDL, which constitutes the main cholesterol carrying particles in humans. LDL particles are taken up by peripheral tissues and the liver via the LDL receptor. HDL is formed in the circulation from lipid-poor apolipoproteins secreted by liver and intestine and from loading of TG, PL and cholesterol via a set of ABC-transporters. Figure modified from (Lusis and Pajukanta, 2008)

very low-density lipoproteins (VLDL) are both loaded with TAG and cholesterol. VLDL particles show the same lipolysis activities and consecutive enrichment in cholesterol as chylomicrons. The reduction of TAG leads to an intermediary density lipoprotein particle (IDL), which has higher concentrations of cholesterol but also contains TAG. When most TAG is lysed, the resulting low-density lipoprotein (LDL) is internalized by LDL-receptor mediated endocytosis, which delivers cholesterol (-esters) and the remaining TAG to the cell. Excess cholesterol in peripheral cells is pumped out of the cell via a multichargo-glycoprotein family called ATP cassette-binding proteins (ABC transporters). In the bloodstream, a second liver generated lipoprotein called high-density lipoprotein (HDL), with its main constituent ApoA-I is loaded with cholesterol. Free cholesterol is esterified inside the HDL particle by an energy-neutral reaction and transported back to the liver. The organism disposes cholesterol via the bile into the gut both as bile salts and as cholesterol. From there, cholesterol and bile salts can eventually be reabsorbed.

3.3 Cholesterol has a very special chemistry

Cholesterol is an isoprenoid with 3 hydrocarbon rings, a hydrocarbon side chain at C17 (Figure2) and consists of 27 carbon atoms with a hydroxyl group attached at C3. Due to its hydrophobicity it resides in its unesterified form almost exclusively in membranes. It is situated parallel to the fatty acid chains of the phospholipids, with its alkyl chain facing to the inside of the lipid bilayer and the hydroxyl group facing towards the aquatic environment. Notably, the chemical structure of cholesterol makes it special compared to other lipids in the membrane. It has only one hydroxyl group, which confers only little charge, a very rigid and almost planar ring structure and a relatively short alkyl chain (van Meer, 2005). Cholesterol does not only exist as unesterified cholesterol, but is stored in lipid droplets as esterified cholesterol. The ER residing enzyme ACAT performs this esterification.

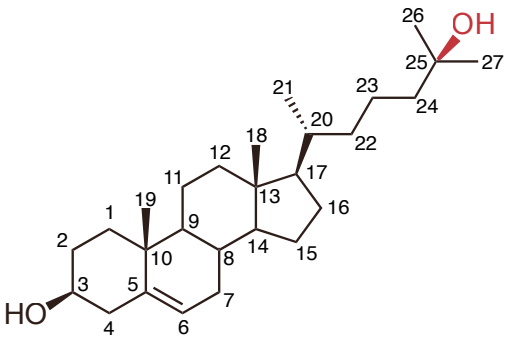

Figure 3.2: The chemical structure of cholesterol. The carbon numbering is according to the IUPAC recommendations. In red, an OH group of 25-hydroxycholesterol is added showing the chemical difference between cholesterol and 25-hydroxycholesterol.

3.3.1 Cholesterol-lipid interaction in the membrane

On the basis of these properties, several models of cholesterol-lipid interaction have been proposed and shown to exist at least in vitro. The umbrella model (Huang and Feigenson, 1999) underlines the hydrophobicity of cholesterol. In this model lipoproteins with bigger head groups protect the hydroxyl group of cholesterol from access to water. Thus, phospholipids with big head groups are favored as neighbors to phospholipids with smaller head groups (DiNitto et al., 2003). Another model, the condensed complex model, reasons that the rigid and planar structure of cholesterols ring system influences the ordering of neighboring lipids depending the degree of saturation in their acyl chains. Unsaturated acyl chains lead to higher cross sections (“a conical shape“) as compared with saturated hydrocarbon chains, which tend to be more cylindrical, can be bend more easily, and therefore have a lower chemical potential when mixed with cholesterol (Radhakrishnan and McConnell, 1999). Another result of the structure of cholesterol is its ability to change from one leaflet to the other (“flip-flop“) very fast due to its relatively low charged head group (Steck et al., 2002). The umbrella model and the condensed

complex model are not mutually exclusive and they both invoke attractive interaction between cholesterol and saturated phospholipids. Both models predict an abrupt increase of chemical activity when the sterol amount in membranes goes beyond the holding capacity of phospholipids. This has been shown experimentally (Lange et al., 2004).

Cholesterol increases lateral ordering of lipids, decreases fluidity and reduces permeability of polar molecules as summarized in (Simons and Vaz, 2004). The lipid raft theory states the existence of confined domains of cholesterol and sphingolipids that recruit special proteins and thus act as signaling platforms (Simons and Ikonen, 1997). This has been shown for the cross linking of IgE receptors and signaling to the Src-family kinase Lyn (Holowka et al., 2005). Still, the size, dynamics and even the existence of lipid rafts are disputed (Munro 2003).

As outlined before, cholesterol is a fundamental constituent of cellular membranes, but its hydrophobicity and its tendency to form crystals demand for tight regulation. Cells regulate their cholesterol content on at least three levels: (i) The uptake of cholesterol from outside of the cell via Low Density Lipoprotein (LDL) (ii) de novo synthesis (iii) active export from the cell via ABC transporter proteins. I have already summarized the transport of cholesterol through the body. I will now talk about transport processes in the cell with a special focus on cholesterol transport processes and cholesterol export and finally I will go into detail about de novo synthesis of cholesterol.

3.4 Endocytosis and the itinerary of cargo in the cell

3.4.1 Mechanisms of Endocytosis

Endocytosis can be regarded as the production of new internal membranes from the plasma membrane lipid bilayer (Doherty and McMahon, 2009). It intimately

regulates many processes, including nutrient uptake, cell adhesion and migration, receptor signaling (Miaczynska et al., 2004) pathogen entry (Marsh and Helenius, 2006) (Medina-Kauwe, 2007) neurotransmission (Söllner and Rothman, 1994), receptor down regulation, antigen presentation (Watts and Amigorena, 2001), cell polarity, mitosis, growth and differentiation, and drug delivery (Miaczynska et al., 2004; Marsh and McMahon, 1999). All of these processes require membranes to overcome the barrier of the cell's plasma membrane, in order to get internalized. This is biophysically very unfavorable. This biophysical problem has been solved by a number of different mechanisms. The internalized cargo, the uptake machinery and intracellular target can vary a lot. So far, is has not been possible to create a unified model and nomenclature for endocytic pathways, reflecting the highly varying dynamics and modularity of this system (Zwang and Yarden, 2009). Therefore, endocytic pathways have been defined by their structural components (e.g. clathrin, caveolin, GEEC), by their molecular dependencies (e.g. RhoA, Arf6) and their sensitivity to certain treatments (e.g. cholesterol extraction). I will shortly summarize the mayor pathways of endocytosis.

Clathrin-mediated Endocytosis

Clathrin-mediated endocytosis (CME) is a mayor pathway for the uptake of signaling molecules, nutrients and also pathogens. Furthermore, it has been implicated in intra-organelle transport. Clathrin-mediated endocytosis is marked by the formation of protein-coated invaginations at different membranes, so called clathrin-coated pits (CCP). The basic building block of the clathrin coat is a three-legged trimer, called triskelion, which consists of a 190 kD protein called clathrin heavy chain (CHC) and the 25 kD protein called clathrin light chain (CLC).

The main events in clathrin-mediated endocytosis are: (i) Membrane bending, which is accomplished by many membrane-curving protein domains in concert

with actin and clathrin recruitment. (ii) Scission, which requires the function of dynamin, actin and possibly myosin motor proteins. (iii) The uncoating of the vesicle, which is initiated by a burst of auxilin/GAK.

Even though a fibroblast takes up vast quantities of membranes by clathrin- mediated endocytosis at any given moment (Bretscher, 1982), the content of clathrin-coated vesicles (CCV) is still highly specific due to a wide number of cargo-specific receptors. Most known receptors are either tyrosine kinases or G-protein coupled receptors. The receptors have cytoplasmic tails, exposing internalization signals, thereby transmitting information from the outside of the cell to the inside. There are four types of internalization signals known (Traub and Lukacs, 2007) and each internalization signal recruits a different subset of adapter proteins and adapter proteins interact among each other and with the lipid environment. There are two types of adaptor proteins: the adaptor complex AP2 on the one hand, and a number of monomeric adaptors on the other hand. Apart from Eps15 and Eps15R, all adaptors are capable of binding, and probably recruiting, clathrin (Ungewickell and Hinrichsen, 2007). AP2 has a central position because basically all other CME proteins associate with one of the 4 subunits: α, $\beta 2$, $\mu 2$, $\sigma 2$ (Praefcke et al., 2004). It is therefore not surprising that knockdown of AP-2 subunits (especially α and µ2) could be shown to block transferrin uptake and reduce endocytic clathrin-coated structures (Motley et al., 2003). Nevertheless, specialized monomeric adaptors like Dab2 and epsin (Maurer and Cooper, 2006) where sufficient to mediate uptake of LDL in the absence of AP-2 (Motley et al., 2003). This shows the high complexity and variability of this pathway and shows the difficulties in defining strict pathways by single molecule dependencies (Boucrot et al., 2010).

After cargo loading, BAR domain containing proteins stabilize the membrane by introducing even more curvature, bind to clathrin and its adaptor proteins, and recruit dynamin to the neck of the vesicle. Dynamin is thought to bind PtdIns(4,5)P2

around the neck of the vesicle and constrict it thus leading to scission and release of the coated vesicle into the cytoplasm. Shortly before fission, many actin interacting proteins like cortactin (Engqvist-Goldstein et al., 2007) (Engqvist-Goldstein et al., 2007), N-WASP, Arp2/3 and actin (Benesch et al., 2005), endophilin and the 145 kD isoform of Sj1 (Perera et al., 2006) are recruited, underlining the importance of actin turnover in lateral movement of coated patches and vesicle fission (Merrifield et al., 2005).

As a final step the ATPase Hsc70 and its co-chaperone GAK/auxilin are recruited to the vesicles followed by an uncoating of the clathrin basket. It is thought that these two proteins mediate uncoating because depletion of GAK/auxilin decreases the exchange rate of clathrin on CCP (Lee, Zhao et al. 2005).

Clathrin-independent Endocytosis

Even though CME is associated with many internalization processes, many cargos are not affected by inhibition of CME components. These clathrin independent mechanisms are typically sensitive to cholesterol depletion and have been defined by internalized markers, their sensitivity to certain drugs and their dependence on cellular proteins like small G proteins, kinases and often dynamin. As these definitions are not mutual exclusive, overlapping pathways have been proposed. This also underlines our understanding of endocytosis as modular rather than a linear process.

Caveolin and Flotillin associated endocytosis

Caveolin-1 is implicated in the formation of caveolae, flask shaped invaginations (Rothberg et al., 1992). Caveolin is inserted into - and maybe through - the membrane in a hairpin structure. Caveolin-1 forms higher-order oligomers, binds cholesterol, fatty acids and the glycoshphingolipid GM1 (Fra et al., 1995), furthermore it

is palmitoylated. An example for the definition of caveolin dependent endocytosis is autocrine motility factor (AMF). AMF has been shown to be taken up selectively by binding to the caveolae residing AMF-receptor (AMFR) and accumulated in the ER within less than an hour (Benlimame et al., 1998). This uptake was insensitive to chlorpromazine (CME), brefeldin A (Golgi complex), nocodazole (microtubuli) and amiloride (macropinocytosis) treatment. However it localized in the PM to caveolae, was dynamin- and PI3K-dependent, methyl-ß-cyclodextrin (MßCD) and Genistein sensitive and increased upon knockdown of caveolin-1 (Le et al., 2002) (Kojic et al., 2008). AMFR is not only a receptor in the PM, but it also has E3 ligase activity in the ER. There, it is involved in the ubiquitination of 3-hydroxy-3-methylglutaryl CoA reductase (HMGCR). The details about this will be in the section about HMGCR stability. A number of other markers like cholera toxin B subunit (CTxB), SV40 virions (Pelkmans et al., 2001) and glycosylphosphadityinositol (GPI)-linked proteins have been shown partition into caveolin-1-positive structures (Kirkham and Parton, 2005) (Parton and Simons, 2007) (Cheng et al., 2006). All markers vary in their sensitivity to drugs. Internalization of only a few markers has been shown to be strictly caveolin-1 dependent (Parton and Simons, 2007). Caveolin-1 knockout mice are - even though short lived - macroscopically surprisingly normal (Park et al., 2003). Flotillin proteins are structurally related to caveolins. They share the hairpin fold and are also palmitoylated. It has been shown that flotillins are involved in the internalization of a portion of CTxB (Glebov et al., 2005), remarkably they are found in microdomains that are distinct from caveolae (Frick et al., 2007).

Clathrin and Caveolin-1 independent endocytosis

Cells can perform endocytosis in the absence of clathrin and caveolin, which once again underlines the extraordinary robustness of the endocytic system. These

processes are cholesterol dependent and have been shown to exist for the internalization of SV40 virions (Damm et al., 2005), GPI-linked proteins, IL2 receptors, growth hormones, endothelin and other molecules (Kirkham and Parton, 2005). The most prominent pathway is the clathrin-independent carrier (CLIC)/GPI-anchored protein-enriched early endosomal compartment (GEEC) pathway, which delivers cargo like fluid phase markers, CTxB and GPI-linked proteins to endosomes termed GPI-AP-enriched early endosomal compartments. This process is dependent on the BAR domain-containing GRAF1 and the small G protein cdc42.

Uptake of larger volumes

Macropinocytosis is a process thought to be mostly non-selective internalization of fluid and membranes. It has been reported to be involved in clearance of apoptotic bodies, immune defense and uptake of bacteria and viruses (Mercer and Helenius, 2009). Macropinocytosis is induced by receptor tyrosine kinases (RTKs) like epidermal growth factor (EGF), which leads to activation of a signaling cascade that in turn leads to massive rearrangements of the actin cytoskeleton to form protrusions from the membrane, circular ruffles and extended lamellipodia (Doherty and McMahon, 2009; Mercer and Helenius, 2009). A number of kinases that are known to play a role in other endocytic steps have been implicated to also act in macropinocytosis. These include Rac1, Pak1, Rab5, Arf6, and BARS proteins (Bar-Sagi and Feramisco, 1986; Mercer and Helenius, 2009).

Phagocytosis is mainly seen in very specialized cell types like macrophages, monocytes and neutrophils. The physiological role is the engulfment of particles, like bacteria and apoptotic cells. Phagocytosis also involves actin rearrangements and therefore is also dependent on actin modulating molecules like Rac1 and Cdc42 (Castellano et al., 2000).

Endocytic mechanisms	Morphology	Implicated cargoes[b]	Small G-protein dependence	Dynamin implicated?	Other proteins implicated
Clathrin mediated	Vesicular	RTKs, GPCRs, transferrin receptor, anthrax toxin	Rab5, Arf6 implicated	Well established	Clathrin, AP2, epsin, SNX9, synaptojanin, actin amphiphysin, plus many others
Caveolae-/ caveolin1-dependent	Vesicular/ tubulovesicular	CTxB, SV40, GPI-linked proteins	Unclear (cavelolins may regulate cdc42 activity)	Some evidence	Caveolins, PTRF, src, PKC, actin (many signaling proteins localize to these sites)
CLIC/GEEC	Tubular/ring like	Fluid phase markers, CTxB, GPI-linked proteins	Cdc42, Arf1	Not as yet	ARHGAP10, actin, GRAF1, other GRAFs
IL2Rβ pathway	Vesicular?	IL2Rβ, FCεRI, Kir3.4, γc-cytokine receptor	RhoA, Rac1	Implicated	PAK1, PAK2
Arf6 dependent	Vesicular/tubular	MHC class I proteins, CD59, carboxypeptidase E	Arf6	Not as yet	Unclear as yet
Flotillin dependent	Vesicular	CTxB, CD59, proteoglycans	Unclear	Implicated but unclear	Flotillin 1 and 2
Phagocytosis	Cargo shaped	Pathogens, apoptotic remnants	Arf6/cdc42/rac1/rhoA (depending on type)	Implicated	Actin, IQGAP1, amphiphysin1, Rho kinase, adhesion proteins
Macropinocytosis	Highly ruffled	Fluid phase markers, RTKs	Rac1	Not as yet (CtBP1/BARS implicated in scission)	Actin, PAK1, PI3K, Ras, Src, HDAC6
Circular dorsal ruffles	Highly ruffled	Fluid phase markers, RTKs	Unclear	Implicated	Cortactin, actin
Entosis	Cell shaped	Matrix-deligated cells	RhoA	Not as yet	Adherens junctions

[a]See the text for references.
[b]Abbreviations: CLIC, clathrin-independent carrier; GEEC, GPI-AP enriched early endosomal compartment; GPCRs, G protein–coupled receptors; GPI, glycosylphosphatidylinositol; MHC, major histocompatibility complex; RTK, receptor tyrosine kinase.

Table 3.1: An overview of known morphological and molecular characteristics of different endocytic pathways. Endocytic pathways show a high modularity in the cellular machinery as well as in the transported cargo. from (Doherty and McMahon, 2009)

3.4.2 The itinerary of endocytic cargo

Distinct cargos have divergent targets within the cell

The purpose of the endocytic event defines the destination of the cargo. Typically cargo is not directly transported from the plasma membrane to the target organelle, but typically travels via different sorting and distribution compartments within the cytoplasm, called endosomes. Endosomes are defined by structural markers (Rabs,

EEA1, Lamp1), by the cargo they contain (LDL, transferrin-receptor) and by time a cargo reaches the compartments (early and late endosomes). LDL, for example, binds to one of several LDL receptors and is internalized via clathrin-mediated endocytosis. After the clathrin coated pit pinches off, the resulting vesicle sheds its clathrin coat. The vesicle fuses with a rab5 and EEA1 positive compartment, forming the early endosome. There, it accumulates 30-40 fold in the first ten minutes. A drop in pH leads to dissociation of LDL particles from their receptors. The LDL receptors are transported back to the membrane and the remaining compartment matures into a Lamp1 positive late endosome and lysosome (Goldstein and Brown, 2009). Cholesteryl ester hydrolysis produces free cholesterol that can efflux from these compartments to other intracellular membranes via soluble luminal (NPC2) and membrane embedded (NPC1) proteins (Liscum and Sturley, 2004). I will discuss this cholesterol efflux in detail later. An illustrative example for the high specificity for the sorting inside the endocytic pathway was an experiment in which two receptors (Transferrin receptor and LDL receptor) were co-internalized and their accumulation in single endosomes was compared. Even though both receptors are internalized via clathrin dependent endocytosis, LDL receptor can accumulate in the same endosome from which Tfn receptor is constantly recycled back to the PM.

Cargos can have multiple targets within the cell

The functional roles of the different endocytosis pathways are mostly poorly established and are overlapping. This overlap becomes apparent when investigating clathrin independent uptake using CTxB. CTxB typically enriches in caveolae, but can also be found in flotillin-positive components of the early CLIC/GEEC pathway (Lundmark et al., 2008). This suggests that different uptake routes can transport the same cargo. Furthermore, internalization of both AMF and CTxB

has been reported to be caveolin dependent but the cargos did not co-localize when co-internalized. Another example of the intimate correlation of caveolin-1, flotillin and the CLIC/GEEC pathway is the activation of cdc42 when depleting caveolin-1. Endocytic pathways often have been defined using pathogens like viruses or toxins, because they are highly dependent on the host-cell machinery. They have been excellent tools because they are not present in standard conditions and provide functional readouts (infection vs. non-infection). Nevertheless the results from these studies cannot be directly translated into a physiological role of the investigated pathways. Pathogens might modulate pre-existing pathways to their needs (Marsh and Helenius, 2006) and even use different endocytic routes within the same cell, as shown for Influenza A (Rust et al., 2004). These three features summarize the modularity of endocytic processes: (i) a defined endocytic pathway may vary depending on the cargo internalized (iii) one type of cargo can be taken up by varying endocytic routes (iii) different cell types show very different uptake routes.

3.4.3 Distribution of cholesterol in different organelles

Cholesterol and phospholipids are distributed heterogeneously among the cellular membranes (Meer et al., 2008). Cholesterol levels are highest in the PM and the endocytic recycling compartment (ERC). The PM is estimated to contain 60% (Liscum and Munn, 1999) and the (ERC) 35% (FR and Zha, 1998) of the total cell cholesterol. Cholesterol levels in the ER are estimated to be 5% (Maxfield and Menon, 2006) and in lysosomes they are over all very low (Möbius et al., 2003). Golgi complex cholesterol levels are estimated to be intermediate (Meer et al., 2008).

Interestingly, the main entry points of cholesterol into the cell, (endosomes and lysosomes for LDL and ER for de novo synthesis (Goldstein et al., 2006)) have

low levels of cholesterol in their membranes, suggesting rapid transport out of these organelles (Maxfield and Wustner, 2002). Addition of dehydroergosterol (DHE), a naturally occurring fluorescent sterol, showed equilibration between the PM and the ERC within 2-3 minutes, which would require the transport of 106 sterol molecules per second (Maxfield and Mondal, 2006). As cholesterol is highly hydrophobic it does not diffuse through the cytosol, therefore this equilibration requires active transport.

3.4.4 Sites of cholesterol transport

There are at least two lipid transport mechanisms known: vesicular transport and soluble lipid transfer proteins (LTPs). LTPs are able to shuttle sterols between closely opposed membranes. X-ray crystal structures of several LTPs like NPC2 (Friedland et al., 2003; Xu et al., 2007), Osh4p (Im et al., 2005), StarD4 (Soccio et al., 2002), MLN64-START (Tsujishita and Hurley, 2000), reveal a common hydrophobic pocket that could bind single sterol molecules. Sterol binding LTPs have been shown to increase the transport rate between liposomes (Prinz, 2007; Infante et al., 2008b). However, the relationship between LTPs and vesicular transport is not very well understood.

Transport from the endoplasmic reticulum to the plasma membrane

Transport from newly synthesized cholesterol has been shown to be ATP-dependent but Golgi complex and microtubuli independent (Lusa et al., 2000) (Urbani and Simoni, 1990). Oxysterol-binding protein (OSBP)-related protein 2 (ORP2) has been proposed to perform this task, as its over-expression enhanced efflux of newly synthesized cholesterol from the ER to extracellular cyclodextrin (Hynynen et al., 2005). In S. Cervisiae, a strain missing six of the seven homologues of OSBP (Osh1p, Osh2p, Osh3p, Osh5p, Osh6p, Osh7p) and bearing a conditional defect

on the seventh (Osh4p) has been shown to reduce ER to PM ergosterol transport five-fold (Sullivan et al., 2006)underscoring the high redundancy of this process. Analysis of strains with single Osh-deficiencies could not show any strong enough effect. This, taken together with the small number of Osh molecules (2500 per cell), brings up further questions about their primary function. Other sterol carriers have also been proposed but they typically lack sterol specificity.

Transport from the plasma membrane to the endoplasmic reticulum

Measurement of cholesterol transport from the PM to the ER has been addressed using the esterification of cholesterol as a read-out, because ACAT, the enzyme that performs this step solely resides in the ER. Radiolabeled sterol was delivered to the PM and esterification was used as a measurement for transport to the ER (Tabas et al., 1988). In yeast, PM to ER transport of cholesterol was not inhibited in conditional mutant strains for key vesicular trafficking genes (Li and Prinz, 2004). In mammalian cells, this delivery has even been shown to be ATP independent (Skiba et al., 1996) (Pierini et al., 1998).

Sterol efflux from late endosomes and lysosomes

Late endosomes and lysosomes are the entry sites of LDL-derived cholesterol into the cell. Interestingly, sterols are not enriched in LE and LY, which means that there must be an efficient transport away from these organelles. In contrast to the highly redundant transport from the PM and the ER, the molecular players of cholesterol efflux from LE and LY are known with high certainty. Two proteins called NPC1 (Niemann-Pick Type C-1 protein) and NPC2 have been identified. Mutations of these genes lead to the retention of cholesterol and other lipids in LE/LY. This forms the molecular basis of the inherited autosomal recessive Niemann-Pick Type C disease (Maxfield and Tabas, 2005). Surprisingly, not

only LDL-derived sterols are trapped in the LE/LY of NPC cells, but also sterols from the PM and other membranes (Mukherjee and Maxfield, 2004), this implies a more general role of LE/LY, especially as NPC phenotype cells have apparently less cholesterol in their PM (Pipalia et al., 2007).

NPC1 is a multi-spanning transmembrane protein with 13 predicted transmembrane helices that fold into a putative sterol-sensing domain (SSD). The soluble luminal N-terminal domain has been reported to bind several species of sterols including 24-, 25-, 27-hydroxysterols(Infante et al., 2008a). However, a mutant that was defective in cholesterol binding (Q79A) could rescue the LE/LY cholesterol egress in NPC1 deficient cells (Infante et al., 2008a). Conversely, other single site mutations in the SSD (Y635C or P692S) could not rescue cholesterol egress (Watari et al., 1999). In other words, the molecular mechanism how NPC1 acts to facilitate the cholesterol efflux is unknown.

NPC2 is a small soluble protein in the lumen of LE/LY. NPC2 binds cholesterol and has been shown to facilitate cholesterol transfer between liposomes. It was suggested that NPC2 interacts with lipids of the membranes and thus brings cholesterol from the interior into the limiting membrane (Xu et al., 2008).

Importantly, NPC1 and NPC2 show a similar clinical and cellular phenotype, suggesting that these two proteins function together. A study investigating the sterol transport between phosphatidylcholine liposomes showed that the N-terminal domain of NPC1 and NPC2 act synergistically and accelerate cholesterol transfer (Infante et al., 2008b).

Cellular cholesterol efflux

Cholesterol release to extracellular acceptors such as apolipoproteinA-I (apoA-I) is an important mechanism for cellular cholesterol homeostasis and a large family of transmembrane proteins called ABC transporters has been attributed to this

process (Dean et al., 2001). Due to their large number (approx. 250), it is not well understood how ABC transporters function in transporting molecules such as phospholipids, sterols, bile acids, peptides and various drugs. It was shown that the ubiquitously expressed ABCA1 binds and transfers phospholipids and cholesterol to apoA-I. (Attie, 2007). Due to the lack of substrate specificity, it is controversial whether ABCA1 (i) transfers both cholesterol AND phospholipids, (ii) is required for cholesterol efflux at all or (iii) mediates cholesterol efflux in concert with yet another member of the ABC family, called ABCG1 (Lorenzi et al., 2006)(Vaughan and Oram, 2003). The interpretation becomes even more complex as ABCA1 has been shown to also co-localize with apoA-I in endosomes (Neufeld et al., 2004). However, macrophages of double knockout mice (ABCA1 -/- ABCG1 -/-) showed severe defects in cholesterol efflux (Hildebrand et al., 2008).

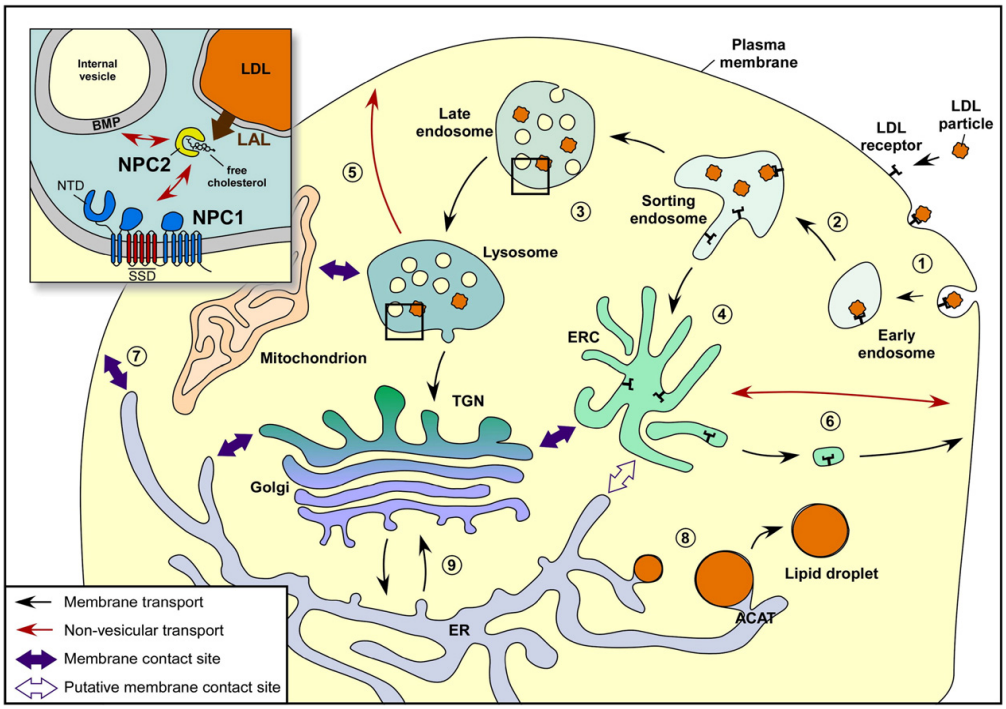

Figure 3.3: Intracellular cholesterol transport. The circulating LDL particles carrying cholesterol and cholesteryl ester are internalized through LDL receptor and transported to sorting endosomes (1, 2). LDL particles are subsequently transported to LE and LY (3), while LDL receptors are recycled via the ERC to the PM (4). Cholesteryl ester hydrolysis by specific lipases such as LAL in LE/LY produces free cholesterol that can efflux from these compartments to other intracellular membranes, such as PM, mostly by non-vesicular transport (5). A precise mechanism for free cholesterol egress from LE/LY is still lacking; however, the membrane-embedded NPC1 and the soluble luminal NPC2 proteins are both required in this process (inset). Cholesterol in the PM can traffic to the ERC by a non-vesicular mechanism; whereas recycling of cholesterol from this compartment back to the PM occurs partly by vesicular and non-vesicular processes (6). Cholesterol translocation from PM to ER allows the homeostatic machinery to be informed about the free cholesterol levels in the cell (7). When it is in excess, the free cholesterol is esterified by ACAT, and fatty acid sterol esters are packed into lipid droplets (8). Newly synthesized cholesterol in the ER is transported mostly to the PM by a non-vesicular process bypassing the Golgi complex, although some of it would follow the secretory pathway, passing through the Golgi complex (9). From (Mesmin and Maxfield, 2009)

3.5 Cholesterol homeostasis in the cell

3.5.1 Cholesterol is synthesized by the mevalonate pathway

Cholesterol is synthesized from acetyl Coenzyme A in a process that requires more than 20 steps. The first committed step in cholesterol synthesis is the production of mevalonate, which arises from the reduction of 3-hydroxy-3-methylglutaryl coenzyme A to mevalonate. The mevalonate pathway is active in all nucleated cells in the body, but is highest in hepatocytes and the brain. Cholesterol can be modified to derivates such as bile acids, vitamin D and steroids. Mevalonate is not only a precursor of cholesterol, but also of non-sterol isoprenoids, geranyl-pyrophosphate and farnesyl pyrophosphate. These products are then further metabolized into a multitude of substances including ubiquinone, haem A, dilichol and prenyl groups that are attached to several proteins (Brown and Goldstein, 1980).

The mevalonate pathway is regulated such that constant production of sterols and non-sterol isoprenoids is assured while guarding against over accumulation of cholesterol. The rate-limiting enzyme in the mevalonate pathway is 3-hydroxy-3-methylglutaryl CoA reductase (HMGCR). As a key enzyme it is regulated via multiple mechanisms: transcription (Edwards et al., 1983), translation (Nakanishi et al., 1988), phosphorylation (Beg et al., 1987) and protein degradation (Goldstein and Brown, 1990). Among these, transcription and degradation have the most dramatic effects. For that reason, I will first describe the transcriptional regulation of the HMGCR followed by a summary about the regulated degradation of HMGCR. Interestingly, both, transcription and degradation of HMGCR require the action of a class of transmembrane proteins, called Insigs that act as anchors and signaling platforms.

3.5.2 Transcriptional control of cholesterol production

Transcriptional control of cholesterol is revolved around the concerted interaction of three membrane-bound proteins: Firstly, Sterol Regulatory Element Binding Protein (SREBP), containing an N-terminal domain that can act as a transcription factor when cleaved in the Golgi complex. Secondly, SREBP cleavage activation protein (Scap), which forms a tight complex with SREBP and either retains SREBP in the ER or escorts its export to the Golgi complex. Thirdly, retention of the SREBP-Scap complex in the ER depends on binding to a third type of proteins, called Insigs.

When cells contain low levels of sterol, genes that are required for cholesterol-, fatty acid-, phospholipid- and triglyceride-synthesis as well as genes required for cholesterol uptake from serum via internalization of LDL are up-regulated. These genes share a DNA promoter region called Sterol Regulatory Element (SRE). The transcription factor binding to SRE is SRE Binding Protein (SREBP). Mammalian cells express three closely related isoforms of SREBP, SREBP-1a, SREBP-1c/ADD1 and SREBP-2. They differ slightly in their transcription targets and expression patterns, but all show a similar orientation and fold in the membrane. Two cytosolic domains are separated by two membrane-spanning helices that flank a short loop that projects into the ER lumen like a hairpin.

The N-terminal domain of SREBP is the part of the protein that can act as a transcription factor for SRE if cleaved off. Newly synthesized SREBP is inserted into the membrane of the ER where the C-terminal domain of SREBP readily binds very tightly to the C-terminus of Scap independently of cholesterols. In sterol-depleted cells, Scap/SREBP is transported to the Golgi complex via a sub-complex of COPII vesicles (Espenshade et al., 2002). Scap most likely binds directly to the recognition complex Sec23/24 via the protein sequence MELADL. This triggers sorting into COPII vesicles via the small GTP binding protein Sar1

and in turn leads to the transport into the Golgi complex (Miller et al., 2003). At the Golgi complex, SREBP is cleaved by two consecutive proteases. Site-1 protease, is a serine protease of the subtilisin family and Site-2 protease, is a Zn2+ metalloprotease (Duncan et al., 1997)(Rawson et al., 1997). The proteases in the Golgi complex are thought to cleave translocated SREBP as soon as it reaches the Golgi complex and are not regulated by cholesterol. In contrast to that, retention of SREBP/Scap in the ER is cholesterol dependent. Scap contains a sterol-sensing domain in its transmembrane helices 2-6 that has been shown to directly bind cholesterol (Radhakrishnan, Sun et al. 2004). Binding of cholesterol to Scap triggers a conformational change that in turn triggers binding to Insig, rendering the MELADL sequence inaccessible to Sec23/24.

Two different genes encoding Insig have been identified in the human genome. They are both highly hydrophobic, containing six transmembrane domains and only short sequences in their C- and N-termini. The major differences between Insig-1 and Insig-2 lie in their cytosolic tails. They both retain Scap/SREBP in the ER and are both degraded when not bound to Scap. However, their transcriptional regulation is different. Insig-2 is constitutively low expressed, but Insig-1 has a SRE in its promoter region and is therefore controlled by SREBP, which was speculated to represent a "damping" mechanism. If Insig-1 is missing, SREBP enters the Golgi complex where the N-Terminus is cleaved off, thus acting as a transcription factor for cholesterol synthesizing proteins and Insig. This mechanism prolongs the time until SREBP is retained in the ER again, thus assuring the production of certain non-cholesterol products of the mevalonate pathway (Engelking et al., 2004).

3.5.3 Regulation of HMGCR stability

All proteins involved in the production of cholesterol have been shown to contain a SRE in their promoter region. Still, the efficiency of transcription is not the same

for all proteins, but vary greatly in respect to each other. One of the proteins that quantities change most dramatically in response to the cholesterol levels is HMGCR. Mammalian HMGCR consists of 887 or 888 amino acids that fold into two distinct domains. The C-terminal domain projects into the cytosol and has been shown to be sufficient to perform the catalytic reaction from 3-hydroxy-3-methylglutaryl coenzyme A to mevalonate (Liscum et al., 1985). The N-terminus contains eight transmembrane spanning helices (Roitelman et al., 1992). Helix two to six show high amino acid similarity to the sterol-sensing domain (SSD) of Scap (Hua et al., 1996). It has been shown that this turnover is regulated through the membrane domain but not by the cytosolic domain of the protein. As both the substrate and the product of enzymatic reaction are water soluble, it has been proposed that the function of the membrane domain of HMGCR is purely regulatory (Gil et al., 1985). In sterol-depleted cells, HMGCR has a half-live of about 12h. When sterols and other isoprenoids accumulate, the half-live is as short as 1h. It was found that this accelerated degradation of HMGCR depends on a series of events including (i) sterol induced binding of HMGCR to Insigs, (ii) ubiquitination of HMGCR by an E3 ligase, called gp-78/AMFR that is attached to a subset of Insigs and (iii) retro-translocation through the ER membrane followed by degradation by the ER associated degradation (ERAD) machinery (Song, Sever et al. 2005).

The first and most crucial step in degradation of HMGCR is its binding to Insigs. As mentioned before, not only HMGCR, but also Scap binds to Insigs and it has been shown that both, HMGCR and Scap even bind the same site on Insigs, as they can abolish each others binding when one or the other is over-expressed (Sever et al., 2003). This sterol mediated binding to Insigs is attributed to the sterol sensing domains (SSD) in the transmembrane helices of the two proteins. The consequences of the binding of HMGCR and Scap to Insigs are very

different, so it is worthwhile to compare these two proteins in more detail. Scap binding to Insigs is mediated by cholesterol. This interaction blocks the binding of COPII proteins to Scap and retains the Scap/SREBP in a stable complex with Insigs in the ER. This prevents all later steps like transport to the Golgi complex, cleavage of SREBP and degradation of Scap. This is fundamentally different compared to HMGCR. HMGCR binds to Insig that is in a complex with a membrane bound E3 ligase, gp-78/AMFR. AMFR binds to another protein, an E2 ubiquitin-conjugating enzyme Ubc7 and to VCP, an ATPase that plays a role in extracting ubiquitinated proteins from membranes. Instead of being more stable when bound to Insigs, HMGCR becomes immediately ubiquitinated on two cytosolic lysine residues by gp78/AMFR (Song et al., 2005b) and consequently degraded through a VCP-dependent mechanism that is similar to ERAD. Interestingly, the ERAD pathway is typically associated with degradation of misfolded or denatured ER proteins and requires ubiquitination and retro-translocation through the ER membrane and degradation in the proteasome (Meusser et al., 2005). It is remarkable because quality control mechanisms must recognize very general patterns in order to function, contrasting the specific regulation of HMGCR. The information provided before has led to speculations on how the differential response of HMGCR and Scap is achieved (Goldstein et al., 2006): Scap could bind to a fraction of Insig that is not attached to gp78/VCP. Scap could also displace or inhibit Insig-bound gp78/VCP. Finally, the membrane domain of HMGCR may be to some extent unfolded, thus triggering the unfolded protein response. This is a very interesting hypothesis as it has been shown in the yeast homolog of HMGCR, Hmg2p (Shearer and Hampton 2005). It must be mentioned though, that yeast Hmg2p is regulated by farnesyl pyrophosphate (FPP) and not by sterols. In addition, HMGCR and Scap are proposed to have different sterol binding specificities, thus HMGCR being regulated by acute accumulation of oxysterols and SREBP/Scap being regulated

by cholesterol levels.

Much research has focused on the triggers for degradation of HMGCR. Already in 1933, Schoenheimer showed that cholesterol biosynthesis is end-product feedback inhibited (Schoenheimer and Breusch, 1933). In the seventies, a set of very basic but elegant experiments showed that cholesterol and mevalonate act synergistically to trigger degradation of HMGCR (Brown et al., 1978). For instance, if the small molecule inhibitor compactin in the presence of cholesterol inhibited HMGCR, HMGCR levels were still significantly higher than in cells with functional HMGCR. If cholesterol was the only regulator of HMGCR, inhibition of HMGCR in the presence of cholesterol should not have had an effect. It was therefore postulated that there was a second feedback via another product of the mevalonate pathway. Different substances have been proposed including geranyl pyrophosphate (Brown and Goldstein, 1980) lanosterol (Song et al., 2005a) and oxidized cholesterols (Saucier et al., 1985). In the last years, oxysterols have received a lot of attention. Among them is lanosterol, a precursor of cholesterol as well as 25-hydroxysterol, a product derived from cholesterol. Both have been shown to cause Scap (Adams, Reitz et al. 2004) and HMGCR (Sever, Yang et al. 2003) to bind Insigs. Both trigger degradation of HMGCR much more potently than cholesterol. Still, 25-hydroxysterol could not be shown to bind to Scap (Radhakrishnan et al., 2004) and the strong differences in hydrophobicity of cholesterol and oxysterols make it hard to compare similarly available amounts. This raises the question about the physiological relevance (Björkhem, 2009) (Gill et al., 2008) how oxidized sterols act on the mevalonate pathway. One teleological reason could be that, as lanosterol is toxic to cells (Xu et al., 2005), HMGCR and Scap/SREBP are fine-tuned such that proteins required to detoxify lanosterol are provided by (oxysterol independent) SREBP but new synthesis of mevalonate is shut down in a oxysterol dependent way (Goldstein et al., 2006).

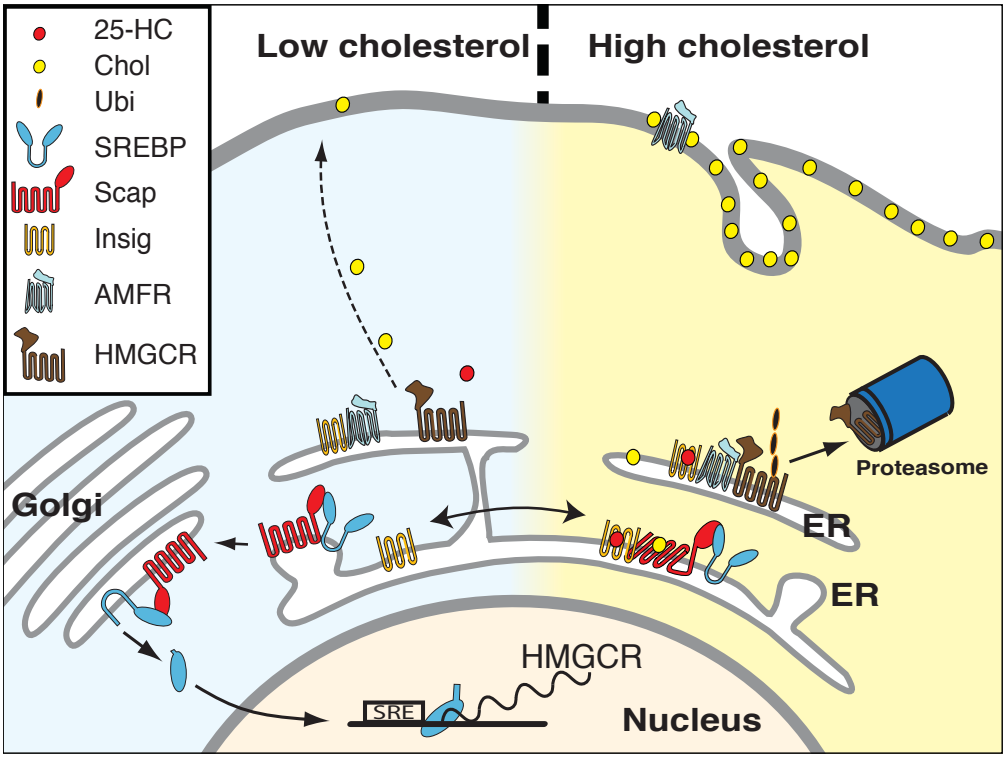

Figure 3.4: Regulation of de novo cholesterol synthesis in the cell. SREBP and Scap form a tight complex. If cholesterol is depleted within the ER, the SREBP/Scap complex is transported to the Golgi complex. In the Golgi complex, the N-terminus of SREBP gets cleaved off and diffuses into the nucleus, where it acts as a transcription factor for cholesterol synthesis genes, among others HMGCR, thus increasing the production of cholesterol. In the ER, HMGCR synthesizes mevalonate. Newly synthesized cholesterol is rapidly transported to and integrated in the plasma membrane by an unknown mechanism. When cellular cholesterol accumulates in the membranes, it induces binding of the SREBP/Scap complex to Insigs, thus rendering SREBP/Scap in the ER. SREBP is not processed anymore, and transcription of cholesterol producing genes stops. HMGCR binds to Insigs and becomes ubiquitinated by Insig-bound AMFR. Ubiquitination of HMGCR leads to its ER associated degradation in the proteasome.

3.6 Bibliography

N Anitschkow. Über die experimentelle atherosklerose der herzklappen. *Virchows Archiv*, Jan 1915. URL http://www.springerlink.com/index/W0224V827584520H.pdf.

A Attie. Abca1: at the nexus of cholesterol, hdl and atherosclerosis. *Trends in biochemical sciences*, Jan 2007. URL http://linkinghub.elsevier.com/retrieve/pii/S0968000407000333.

D Bar-Sagi and J Feramisco. Induction of membrane ruffling and fluid-phase pinocytosis in quiescent fibroblasts by ras proteins. *Science*, Jan 1986. URL http://www.sciencemag.org/cgi/content/abstract/sci;233/4768/1061.

Z Beg, J Stonik, and H Brewer Jr. Modulation of the enzymic activity of 3-hydroxy-3-methylglutaryl coenzyme a reductase by multiple kinase systems involving reversible phosphorylation: a review. *Metabolism*, Jan 1987. URL http://linkinghub.elsevier.com/retrieve/pii/0026049587901016.

S Benesch, S Polo, F Lai, and K Anderson. N-wasp deficiency impairs egf internalization and actin assembly at clathrin-coated pits. *Journal of Cell . . .*, Jan 2005. URL http://jcs.biologists.org/cgi/content/abstract/118/14/3103.

N Benlimame, P Le, and I Nabi. Localization of autocrine motility factor receptor to caveolae and clathrin-independent internalization of its ligand to smooth endoplasmic reticulum. *Mol Biol Cell*, 9(7):1773–86, Jul 1998. URL http://www.ncbi.nlm.nih.gov/entrez/query.fcgi?cmd=Retrieve&db=PubMed&dopt=Citation&list_uids=9658170%20. Journal Article United states.

Ingemar Björkhem. Are side-chain oxidized oxysterols regulators also in vivo? *J Lipid Res*, 50 Suppl:S213–8, Apr 2009. doi: 10.1194/jlr.R800025-JLR200. URL http://www.jlr.org/cgi/content/full/50/Supplement/S213.

E Boucrot, S Saffarian, R Zhang, and T Kirchhausen. Roles of ap-2 in clathrin-mediated endocytosis. *ncbi.nlm.nih.gov*, Jan 2010. URL http://www.ncbi.nlm.nih.gov/pmc/articles/PMC2868873/.

M Bretscher. Surface uptake by fibroblasts and its consequences. *Cold Spring Harbor Symposia on Quantitative ...*, Jan 1982. URL http://symposium.cshlp.org/content/46/707.extract.

M Brown and J Goldstein. Multivalent feedback regulation of hmg coa reductase, a control mechanism coordinating isoprenoid synthesis and cell growth. *The Journal of Lipid Research*, Jan 1980. URL http://www.jlr.org/cgi/content/abstract/21/5/505.

M Brown, J Faust, J Goldstein, I Kaneko, and A Endo. Induction of 3-hydroxy-3-methylglutaryl coenzyme a reductase activity in human fibroblasts incubated with compactin (ml-236b), a competitive inhibitor of the reductase. *J Biol Chem*, 253(4):1121–8, Feb 1978. URL http://www.ncbi.nlm.nih.gov/entrez/query.fcgi?cmd=Retrieve&db=PubMed&dopt=Citation&list_uids=624722.

F Castellano, P Montcourrier, and P Chavrier. Membrane recruitment of rac1 triggers phagocytosis. *Journal of cell science*, 113 (Pt 17):2955–61, Sep 2000. URL http://jcs.biologists.org/cgi/reprint/113/17/2955.

W Castelli, R Garrison, P Wilson, and R Abbott. Incidence of coronary heart disease and lipoprotein cholesterol levels: the framingham study. *Jama*, Jan 1986. URL http://jama.ama-assn.org/cgi/content/abstract/256/20/2835.

T Chang, C Chang, N Ohgami, and Y Yamauchi. Cholesterol sensing, trafficking, and esterification. *Annu Rev Cell Dev Biol*, 22: 129–57, 2006. doi: 10.1146/annurev.cellbio.22.010305.104656. URL http://www.ncbi.nlm.nih.gov/entrez/query.fcgi?cmd=Retrieve&db=PubMed&dopt=Citation&list_uids=16753029.

Z Cheng, R Singh, and D Marks. Membrane microdomains, caveolae, and caveolar endocytosis of sphingolipids (review). *Molecular membrane ...*, Jan 2006. URL http://www.informaworld.com/index/743933919.pdf.

E Damm, L Pelkmans, J Kartenbeck, A Mezzacasa, T Kurzchalia, and A Helenius. Clathrin- and caveolin-1-independent endocytosis: entry of simian virus 40 into cells devoid of caveolae. *J Cell Biol*, 168(3):477–88, Jan 2005. doi: jcb.200407113[pii]10.1083/jcb.200407113. URL http://www.ncbi.nlm.nih.gov/entrez/query.fcgi?cmd=Retrieve&db=PubMed&dopt=Citation&list_uids=15668298.

M Dean, Y Hamon, and G Chimini. The human atp-binding cassette (abc) transporter superfamily. *The Journal of Lipid Research*, Jan 2001. URL http://www.jlr.org/cgi/content/abstract/42/7/1007.

J DiNitto, T Cronin, and D Lambright. Membrane recognition and targeting by lipid-binding domains. *Science's STKE*, Jan 2003. URL http://stke.sciencemag.org/cgi/content/full/OC_sigtrans;2003/213/re16.

Gary J Doherty and Harvey T McMahon. Mechanisms of endocytosis. *Annu Rev Biochem*, 78:857–902, Jan 2009. doi: 10.1146/annurev.biochem.78.081307.110540. URL http://arjournals.annualreviews.org/doi/abs/10.1146/annurev.biochem.78.081307.110540?url_ver=Z39.88-2003&rfr_id=ori:rid:crossref.org&rfr_dat=cr_pub%253dncbi.nlm.nih.gov.

E A Duncan, M S Brown, J L Goldstein, and J Sakai. Cleavage site for sterol-regulated protease localized to a leu-ser bond in the lumenal loop of sterol regulatory element-binding protein-2. *J Biol Chem*, 272(19):12778–85, May 1997.

Edwards, S Lan, R Tanaka, and A Fogelman. Mevalonolactone inhibits the rate of synthesis and enhances the rate of degradation of 3-hydroxy-3-methylglutaryl coenzyme a reductase in rat hepatocytes. *Journal of Biological ...*, Jan 1983. URL `http://www.jbc.org/cgi/content/abstract/258/12/7272`.

L Engelking, H Kuriyama, and R Hammer .... Overexpression of insig-1 in the livers of transgenic mice inhibits srebp processing and reduces insulin-stimulated lipogenesis. *Journal of Clinical ...*, Jan 2004. URL `http://www.jci.org/cgi/content/abstract/113/8/1168`.

Engqvist-Goldstein, K Cunningham, and D Drubin. A hip1r–cortactin complex negatively regulates actin assembly associated with endocytosis. *The EMBO ...*, Jan 2007. URL `http://www.ncbi.nlm.nih.gov/pmc/articles/PMC1817625/`.

P Espenshade, W Li, and D Yabe. Sterols block binding of copii proteins to scap, thereby controlling scap sorting in er. *Proceedings of the ...*, Jan 2002. URL `http://www.pnas.org/cgi/content/abstract/99/18/11694`.

M FR and X Zha. Cholesterol distribution in living cells: Fluorescence imaging using dehydroergosterol as a fluorescent cholesterol analog. *Biophys J*, Jan 1998. URL `http://d.wanfangdata.com.cn/NSTLQK_NSTL_QK2889929.aspx`.

A M Fra, E Williamson, K Simons, and R G Parton. De novo formation of caveolae in lymphocytes by expression of vip21-caveolin. *Proc Natl Acad Sci USA*, 92 (19):8655–9, Sep 1995.

M Frick, N Bright, K Riento, A Bray, and C Merrified. Coassembly of flotillins induces formation of membrane microdomains, membrane curvature, and vesicle budding. *Current Biology*, Jan 2007. URL http://linkinghub.elsevier.com/retrieve/pii/S0960982207015138.

N Friedland, H Liou, and P Lobel. Structure of a cholesterol-binding protein deficient in niemann–pick type c2 disease. *Proceedings of the ...*, Jan 2003. URL http://www.pnas.org/content/100/5/2512.short.

G Gil, J Faust, D Chin, J Goldstein, and M Brown. Membrane-bound domain of hmg coa reductase is required for sterol-enhanced degradation of the enzyme. *Cell*, 41(1):249–58, May 1985. doi: 0092-8674(85)90078-9[pii]. URL http://www.ncbi.nlm.nih.gov/entrez/query.fcgi?cmd=Retrieve&db=PubMed&dopt=Citation&list_uids=3995584.

Saloni Gill, Renee Chow, and Andrew J Brown. Sterol regulators of cholesterol homeostasis and beyond: the oxysterol hypothesis revisited and revised. *Prog Lipid Res*, 47(6):391–404, Nov 2008. doi: 10.1016/j.plipres.2008.04.002. URL http://www.sciencedirect.com/science?_ob=ArticleURL&_udi=B6TBP-4SFG4JD-1&_user=791130&_rdoc=1&_fmt=&_orig=search&_sort=d&_docanchor=&view=c&_acct=C000043379&_version=1&_urlVersion=0&_userid=791130&md5=7d52152371fc6e4c2010cb19778624a3. Very nice! get overview and figure 6!

O Glebov, N Bright, and B Nichols. Flotillin-1 defines a clathrin-independent endocytic pathway in mammalian cells. *Nat Cell Biol*, Jan 2005. URL http://www.nature.com/ncb/journal/vaop/ncurrent/full/ncb1342.html.

J Goldstein and M Brown. Regulation of the mevalonate pathway. *Nature*, Jan

1990. URL http://dolly.biochem.arizona.edu/Bioc462b_Honors_Spring_2009/urdang/Goldstein1990.pdf.

J Goldstein and M Brown. The ldl receptor. *Arteriosclerosis*, Jan 2009. URL http://atvb.ahajournals.org/cgi/content/abstract/29/4/431.

J Goldstein, R DeBose-Boyd, and M Brown. Protein sensors for membrane sterols. *Cell*, Jan 2006. URL http://linkinghub.elsevier.com/retrieve/pii/S0092867405014637.

Hildebrand, Y Wang, G Chimini, and J Kuiper. Combined deletion of macrophage abca1 and abcg1 leads to massive lipid accumulation in tissue macrophages and distinct atherosclerosis at relatively ...., Jan 2008. URL http://atvb.ahajournals.org/cgi/content/full/atvbaha;28/2/258.

David Holowka, Julie A Gosse, Adam T Hammond, Xuemei Han, Prabuddha Sengupta, Norah L Smith, Alice Wagenknecht-Wiesner, Min Wu, Ryan M Young, and Barbara Baird. Lipid segregation and ige receptor signaling: a decade of progress. *Biochim Biophys Acta*, 1746(3):252–9, Dec 2005. doi: 10.1016/j.bbamcr.2005.06.007. URL http://www.sciencedirect.com/science?_ob=ArticleURL&_udi=B6T20-4GKWC10-1&_user=791130&_coverDate=12%252F30%252F2005&_rdoc=1&_fmt=high&_orig=search&_sort=d&_docanchor=&view=c&_acct=C000043379&_version=1&_urlVersion=0&_userid=791130&md5=3b7060fa90543bbedaa29f2092d368f0.

X Hua, A Nohturfft, J Goldstein, and M Brown. Sterol resistance in cho cells traced to point mutation in srebp cleavage-activating protein. *Cell*, Jan 1996. URL http://linkinghub.elsevier.com/retrieve/pii/S0092867400813628.

J Huang and G W Feigenson. A microscopic interaction model of maximum solubility of cholesterol in lipid bilayers. *Biophys J*, 76(4):2142–57, Apr 1999. doi: 10.1016/S0006-3495(99)77369-8.

Hynynen, S Laitinen, R Käkelä, and K Tanhuanpää .... Overexpression of osbp-related protein 2 (orp2) induces changes in cellular cholesterol metabolism and enhances endocytosis. *Biochemical ...*, Jan 2005. URL `http://www.ncbi.nlm.nih.gov/pmc/articles/PMC1184581/`.

Y Im, S Raychaudhuri, W Prinz, and J Hurley. Structural mechanism for sterol sensing and transport by osbp-related proteins. *Nature*, Jan 2005. URL `http://www.nature.com/nature/journal/v437/n7055/abs/nature03923.html`.

R Infante, A Radhakrishnan, and L Abi-Mosleh. Purified npc1 protein: Ii. localization of sterol binding to a 240-amino acid soluble luminal loop. *Journal of Biological ...*, Jan 2008a. URL `http://www.jbc.org/content/283/2/1064.short`.

Rodney E Infante, Michael L Wang, Arun Radhakrishnan, Hyock Joo Kwon, Michael S Brown, and Joseph L Goldstein. Npc2 facilitates bidirectional transfer of cholesterol between npc1 and lipid bilayers, a step in cholesterol egress from lysosomes. *Proc Natl Acad Sci USA*, 105(40):15287–92, Oct 2008b. doi: 10.1073/pnas.0807328105. URL `http://www.pnas.org/content/105/40/15287.long`.

Matthew Kirkham and Robert G Parton. Clathrin-independent endocytosis: new insights into caveolae and non-caveolar lipid raft carriers. *Biochim Biophys Acta*, 1745(3):273–86, Sep 2005. doi: 10.1016/j.bbamcr.2005.06.002. URL `http://www.sciencedirect.com/science?_ob=ArticleURL&_udi=B6T20-4GFV29B-1&_user=791130&_coverDate=09%252F30%252F2005&_rdoc=1&_fmt=high&_orig=search&_sort=d&_docanchor=&view=c&_`

acct=C000043379&_version=1&_urlVersion=0&_userid=791130&md5=b14931ac87e144274a246e3650ff192f.

L Kojic, S Wiseman, F Ghaidi, B Joshi, H Nedev, H Saragovi, and I Nabi. Raft-dependent endocytosis of autocrine motility factor/phosphoglucose isomerase: a potential drug delivery route for tumor cells. *PLoS ONE*, 3(10):e3597, 2008. doi: 10.1371/journal.pone.0003597. URL http://www.ncbi.nlm.nih.gov/entrez/query.fcgi?cmd=Retrieve&db=PubMed&dopt=Citation&list_uids=18974847.

Y Lange, J Ye, and T Steck. How cholesterol homeostasis is regulated by plasma membrane cholesterol in excess of phospholipids. *... of Sciences of the United States ...*, Jan 2004. URL http://www.pnas.org/content/101/32/11664.full.

P Le, G Guay, Y Altschuler, and I Nabi. Caveolin-1 is a negative regulator of caveolae-mediated endocytosis to the endoplasmic reticulum. *J Biol Chem*, 277 (5):3371–9, Feb 2002. URL http://www.ncbi.nlm.nih.gov/entrez/query.fcgi?cmd=Retrieve&db=PubMed&dopt=Citation&list_uids=11724808%20. Journal Article United States.

Y Li and W Prinz. Atp-binding cassette (abc) transporters mediate nonvesicular, raft-modulated sterol movement from the plasma membrane to the endoplasmic reticulum. *Journal of Biological Chemistry*, Jan 2004. URL http://www.jbc.org/content/279/43/45226.short.

L Liscum and N J Munn. Intracellular cholesterol transport. *Biochim Biophys Acta*, 1438(1):19–37, Apr 1999.

L Liscum and S Sturley. Intracellular trafficking of niemann-pick c proteins 1 and 2: obligate components of subcellular lipid transport. *... Acta (BBA)-Molecular*

and Cell Biology of Lipids, Jan 2004. URL http://linkinghub.elsevier.com/retrieve/pii/S1388198104001313.

L Liscum, J Finer-Moore, R Stroud, and K Luskey .... Domain structure of 3-hydroxy-3-methylglutaryl coenzyme a reductase, a glycoprotein of the endoplasmic reticulum. *Journal of Biological ...*, Jan 1985. URL http://www.jbc.org/cgi/content/abstract/260/1/522.

I Lorenzi, L Rohrer, and A von Eckardstein. Lipid efflux by the atp-binding cassette transporters abca1 and abcg1. *... and Cell Biology of Lipids*, Jan 2006. URL http://linkinghub.elsevier.com/retrieve/pii/S1388198106001296.

R Lundmark, G Doherty, M Howes, and K Cortese. The gtpase-activating protein graf1 regulates the clic/geec endocytic pathway. *Current Biology*, Jan 2008. URL http://linkinghub.elsevier.com/retrieve/pii/S0960982208014139.

Lusa, P Somerharju, and C Ehnholm. Dissecting the role of the golgi complex and lipid rafts in biosynthetic transport of cholesterol to the cell surface. *Proceedings of the ...*, Jan 2000. URL http://www.pnas.org/cgi/content/abstract/97/15/8375.

Aldons J Lusis and Päivi Pajukanta. A treasure trove for lipoprotein biology. *Nat Genet*, 40(2):129–30, Feb 2008. doi: 10.1038/ng0208-129. URL http://www.nature.com/ng/journal/v40/n2/abs/ng0208-129.html.

M Marsh and A Helenius. Virus entry: open sesame. *Cell*, 124 (4):729–40, Feb 2006. doi: S0092-8674(06)00182-6[pii]10.1016/j.cell.2006.02.007. URL http://www.ncbi.nlm.nih.gov/entrez/query.fcgi?cmd=Retrieve&db=PubMed&dopt=Citation&list_uids=16497584.

M Marsh and H McMahon. The structural era of endocytosis. *Science*, Jan 1999. URL http://scienceonline.org/cgi/content/abstract/285/5425/215.

M Maurer and J Cooper. The adaptor protein dab2 sorts ldl receptors into coated pits independently of ap-2 and arh. *Journal of cell science*, Jan 2006. URL http://jcs.biologists.org/cgi/content/abstract/119/20/4235.

F Maxfield and A Menon. Intracellular sterol transport and distribution. *Current opinion in cell biology*, Jan 2006. URL http://linkinghub.elsevier.com/retrieve/pii/S0955067406000883.

F Maxfield and M Mondal. Sterol and lipid trafficking in mammalian cells. *Biochemical Society Transactions*, Jan 2006. URL http://www.biochemsoctrans.org/bst/034/0335/bst0340335.htm.

F Maxfield and D Wustner. Intracellular cholesterol transport. *Journal of Clinical Investigation*, Jan 2002. URL http://www.jci.org/cgi/content/full/110/7/891.

Frederick R Maxfield and Ira Tabas. Role of cholesterol and lipid organization in disease. *Nature*, 438(7068):612–21, Dec 2005. doi: 10.1038/nature04399. URL http://www.nature.com/nature/journal/v438/n7068/full/nature04399.html.

L Medina-Kauwe. "alternative" endocytic mechanisms exploited by pathogens: New avenues for therapeutic delivery? *Advanced drug delivery reviews*, Jan 2007. URL http://linkinghub.elsevier.com/retrieve/pii/S0169409X07000993.

G Van Meer, D Voelker, and G Feigenson. Membrane lipids: where they are

and how they behave. *Nature Reviews Molecular ...*, Jan 2008. URL http://www.nature.com/nrm/journal/v9/n2/abs/nrm2330.html.

Jason Mercer and Ari Helenius. Virus entry by macropinocytosis. *Nat Cell Biol*, 11(5):510–20, May 2009. doi: 10.1038/ncb0509-510. URL http://www.nature.com/ncb/journal/v11/n5/abs/ncb0509-510.html.

C Merrifield, D Perrais, and D Zenisek. Coupling between clathrin-coated-pit invagination, cortactin recruitment, and membrane scission observed in live cells. *Cell*, Jan 2005. URL http://linkinghub.elsevier.com/retrieve/pii/S0092867405002874.

Bruno Mesmin and Frederick R Maxfield. Intracellular sterol dynamics. *Biochim Biophys Acta*, 1791(7):636–45, Jul 2009. doi: 10.1016/j.bbalip.2009.03.002. URL http://linkinghub.elsevier.com/retrieve/pii/S1388-1981(09)00073-0.

B Meusser, C Hirsch, E Jarosch, and T Sommer. Erad: the long road to destruction. *Nat Cell Biol*, Jan 2005. URL http://www.nature.com/ncb/journal/v7/n8/abs/ncb0805-766.html.

M Miaczynska, L Pelkmans, and M Zerial. Not just a sink: endosomes in control of signal transduction. *Current opinion in cell biology*, Jan 2004. URL http://linkinghub.elsevier.com/retrieve/pii/S0955067404000742.

E Miller, T Beilharz, P Malkus, and M Lee. Multiple cargo binding sites on the copii subunit sec24p ensure capture of diverse membrane proteins into transport vesicles. *Cell*, Jan 2003. URL http://linkinghub.elsevier.com/retrieve/pii/S0092867403006093.

W Möbius, E Van Donselaar, and Y Ohno-Iwashita. Recycling compartments and the internal vesicles of multivesicular bodies harbor most of the cholesterol found

in the endocytic pathway. *Traffic*, Jan 2003. URL http://www3.interscience.wiley.com/journal/118852849/abstract.

A Motley, N Bright, and M Seaman. Clathrin-mediated endocytosis in ap-2-depleted cells. *Journal of Cell ...*, Jan 2003. URL http://jcb.rupress.org/cgi/content/abstract/162/5/909.

S Mukherjee and F Maxfield. Lipid and cholesterol trafficking in npc. *... (BBA)-Molecular and Cell Biology of Lipids*, Jan 2004. URL http://linkinghub.elsevier.com/retrieve/pii/S1388198104001325.

M Nakanishi, J Goldstein, and M Brown. Multivalent control of 3-hydroxy-3-methylglutaryl coenzyme a reductase. mevalonate-derived product inhibits translation of mrna and accelerates degradation of enzyme. *J Biol Chem*, 263 (18):8929–37, Jun 1988. URL http://www.ncbi.nlm.nih.gov/entrez/query.fcgi?cmd=Retrieve&db=PubMed&dopt=Citation&list_uids=3379053.

Neufeld, J Stonik, S Demosky, and C Knapper. The abca1 transporter modulates late endocytic trafficking. *Journal of Biological ...*, Jan 2004. URL http://www.jbc.org/cgi/content/full/M314160200.

D Park, A Cohen, P Frank, B Razani, and H Lee. Caveolin-1 null (-/-) mice show dramatic reductions in life span. *Biochemistry*, Jan 2003. URL http://www.ncbi.nlm.nih.gov/pubmed/14690422.

R Parton and K Simons. The multiple faces of caveolae. *Nature Reviews Molecular Cell Biology*, Jan 2007. URL http://www.nature.com/nrm/journal/v8/n3/abs/nrm2122.html.

L Pelkmans, J Kartenbeck, and A Helenius. Caveolar endocytosis of simian virus 40 reveals a new two-step vesicular-transport pathway to the er. *Nat Cell Biol*,

3(5):473–83, May 2001. URL http://www.ncbi.nlm.nih.gov/entrez/query.fcgi?cmd=Retrieve&db=PubMed&dopt=Citation&list_uids=11331875%20. Journal Article England.

R Perera, R Zoncu, L Lucast, and P De .... Two synaptojanin 1 isoforms are recruited to clathrin-coated pits at different stages. *Proceedings of the ...*, Jan 2006. URL http://www.pnas.org/content/103/51/19332.abstract.

LM Pierini, P Leopold, P Skiba, and I Tabas. Sphingomyelinase treatment induces atp-independent endocytosis. *Journal of Cell ...*, Jan 1998. URL http://jcb.rupress.org/cgi/content/abstract/140/1/39.

Nina H Pipalia, Mingming Hao, Sushmita Mukherjee, and Frederick R Maxfield. Sterol, protein and lipid trafficking in chinese hamster ovary cells with niemann-pick type c1 defect. *Traffic*, 8(2):130–41, Feb 2007. doi: 10.1111/j.1600-0854.2006.00513.x.

G Praefcke, M Ford, and E Schmid. Evolving nature of the ap2 alpha-appendage hub during clathrin-coated vesicle endocytosis. *The EMBO ...*, Jan 2004. URL http://www.ncbi.nlm.nih.gov/pmc/articles/PMC526462/.

W Prinz. Non-vesicular sterol transport in cells. *Prog Lipid Res*, Jan 2007. URL http://linkinghub.elsevier.com/retrieve/pii/S0163782707000264.

A Radhakrishnan and H McConnell. Condensed complexes of cholesterol and phospholipids. *Biophys J*, Jan 1999. URL http://linkinghub.elsevier.com/retrieve/pii/S0006349599769985.

A Radhakrishnan, L Sun, H Kwon, and M Brown. Direct binding of cholesterol to the purified membrane region of scap:: Mechanism for a sterol-sensing domain.

Molecular cell, Jan 2004. URL http://linkinghub.elsevier.com/retrieve/pii/S1097276504003521.

R B Rawson, N G Zelenski, D Nijhawan, J Ye, J Sakai, M T Hasan, T Y Chang, M S Brown, and J L Goldstein. Complementation cloning of s2p, a gene encoding a putative metalloprotease required for intramembrane cleavage of srebps. *Molecular cell*, 1(1):47–57, Dec 1997.

J Roitelman, E Olender, S Bar-Nun, W Dunn, and R Simoni. Immunological evidence for eight spans in the membrane domain of 3-hydroxy-3-methylglutaryl coenzyme a reductase: implications for enzyme degradation in the endoplasmic reticulum. *J Cell Biol*, 117(5):959–73, Jun 1992. URL http://www.ncbi.nlm.nih.gov/entrez/query.fcgi?cmd=Retrieve&db=PubMed&dopt=Citation&list_uids=1374417.

R Ross. Cell biology of atherosclerosis. *Annu Rev Physiol*, 57:791–804, Jan 1995. doi: 10.1146/annurev.ph.57.030195.004043. URL http://arjournals.annualreviews.org/doi/abs/10.1146/annurev.ph.57.030195.004043?url_ver=Z39.88-2003&rfr_id=ori:rid:crossref.org&rfr_dat=cr_pub%253dncbi.nlm.nih.gov.

K Rothberg, J Heuser, W Donzell, and Y Ying. Caveolin, a protein component of caveolae membrane coats. *Cell*, Jan 1992. URL http://linkinghub.elsevier.com/retrieve/pii/009286749290143Z.

Michael J Rust, Melike Lakadamyali, Feng Zhang, and Xiaowei Zhuang. Assembly of endocytic machinery around individual influenza viruses during viral entry. *Nat Struct Mol Biol*, 11(6):567–73, Jun 2004. doi: 10.1038/nsmb769.

S E Saucier, A A Kandutsch, F R Taylor, T A Spencer, S Phirwa, and A K Gayen. Identification of regulatory oxysterols, 24(s),25-epoxycholesterol and 25-

hydroxycholesterol, in cultured fibroblasts. *J Biol Chem*, 260(27):14571–9, Nov 1985. URL http://www.jbc.org/cgi/reprint/260/27/14571.

R Schoenheimer and F Breusch. Synthesis and destruction of cholesterol in the organism. *Journal of Biological Chemistry*, Jan 1933. URL http://www.jbc.org/content/103/2/439.short.

N Sever, T Yang, M Brown, J Goldstein, and R DeBose-.... Accelerated degradation of hmg coa reductase mediated by binding of insig-1 to its sterol-sensing domain. *Molecular cell*, Jan 2003. URL http://linkinghub.elsevier.com/retrieve/pii/S1097276502008225.

K Simons and E Ikonen. Functional rafts in cell membranes. *Nature*, 387(6633): 569–72, Jun 1997. doi: 10.1038/42408. URL http://www.nature.com/nature/journal/v387/n6633/full/387569a0.html.

K Simons and W Vaz. Model systems, lipid rafts, and cell membranes. *Annu Rev Biophys Biomol Struct*, 33:269–95, 2004. URL http://www.ncbi.nlm.nih.gov/entrez/query.fcgi?cmd=Retrieve&db=PubMed&dopt=Citation&list_uids=15139814%20. Introduction:" Lipid ordering;.

P Skiba, X Zha, F Maxfield, and S Schissel. The distal pathway of lipoprotein-induced cholesterol esterification, but not sphingomyelinase-induced cholesterol esterification, is energy-dependent. *Journal of Biological ...*, Jan 1996. URL http://www.jbc.org/content/271/23/13392.full.

R Soccio, J Breslow, and S Burley. Crystal structure of the mus musculus cholesterol-regulated start protein 4 (stard4) containing a star-related lipid transfer domain. *Proceedings of the ...*, Jan 2002. URL http://www.pnas.org/cgi/content/abstract/99/10/6949.

T Söllner and J Rothman. Neurotransmission: harnessing fusion machinery at the synapse. *Trends in neurosciences*, Jan 1994. URL http://linkinghub.elsevier.com/retrieve/pii/0166223694901783.

B Song, N Javitt, and R Debose-Boyd. Insig-mediated degradation of hmg coa reductase stimulated by lanosterol, an intermediate in the synthesis of cholesterol. *Cell Metabolism*, Jan 2005a. URL http://linkinghub.elsevier.com/retrieve/pii/S1550413105000288.

B Song, N Sever, and R DeBose-Boyd. Gp78, a membrane-anchored ubiquitin ligase, associates with insig-1 and couples sterol-regulated ubiquitination to degradation of hmg coa reductase. *Mol Cell*, 19(6):829–40, Sep 2005b. URL http://www.ncbi.nlm.nih.gov/entrez/query.fcgi?cmd=Retrieve&db=PubMed&dopt=Citation&list_uids=16168377%20.

Theodore L Steck, Jin Ye, and Yvonne Lange. Probing red cell membrane cholesterol movement with cyclodextrin. *Biophys J*, 83(4):2118–25, Oct 2002. doi: 10.1016/S0006-3495(02)73972-6.

D Sullivan, H Ohvo-Rekila, and N Baumann .... Sterol trafficking between the endoplasmic reticulum and plasma membrane in yeast. *Biochemical Society ...*, Jan 2006. URL http://www.biochemsoctrans.org/bst/034/0356/bst0340356.htm.

I Tabas, W J Rosoff, and G C Boykow. Acyl coenzyme a:cholesterol acyl transferase in macrophages utilizes a cellular pool of cholesterol oxidase-accessible cholesterol as substrate. *J Biol Chem*, 263(3):1266–72, Jan 1988.

L Traub and G Lukacs. Decoding ubiquitin sorting signals for clathrin-dependent endocytosis by clasps. *Journal of cell science*, Jan 2007. URL http://jcs.biologists.org/cgi/content/abstract/120/4/543.

Y Tsujishita and J Hurley. Structure and lipid transport mechanism of a star-related domain. *Nature Structural & Molecular Biology*, Jan 2000. URL http://www.nature.com/nsmb/journal/v7/n5/abs/nsb0500_408.html.

E Ungewickell and L Hinrichsen. Endocytosis: clathrin-mediated membrane budding. *Current opinion in cell biology*, Jan 2007. URL http://linkinghub.elsevier.com/retrieve/pii/S0955067407000919.

L Urbani and R D Simoni. Cholesterol and vesicular stomatitis virus g protein take separate routes from the endoplasmic reticulum to the plasma membrane. *J Biol Chem*, 265(4):1919–23, Feb 1990.

Gerrit van Meer. Cellular lipidomics. *EMBO J*, 24(18):3159–65, Sep 2005. doi: 10.1038/sj.emboj.7600798. URL http://www.nature.com/emboj/journal/v24/n18/abs/7600798a.html.

A Vaughan and J Oram. Abca1 redistributes membrane cholesterol independent of apolipoprotein interactions. *The Journal of Lipid Research*, Jan 2003. URL http://www.jlr.org/cgi/content/abstract/44/7/1373.

H Watari, E Blanchette-Mackie, and N Dwyer. Mutations in the leucine zipper motif and sterol-sensing domain inactivate the niemann-pick c1 glycoprotein. *Journal of Biological . . .*, Jan 1999. URL http://www.jbc.org/content/274/31/21861.full.

C Watts and S Amigorena. Phagocytosis and antigen presentation. *Semin Immunol*, 13(6):373–9, Dec 2001. doi: 10.1006/smim.2001.0334. URL http://www.sciencedirect.com/science?_ob=ArticleURL&_udi=B6WX3-45BBXYH-6&_user=10&_coverDate=12%252F31%252F2001&_rdoc=1&_fmt=high&_orig=search&_sort=d&_docanchor=&view=c&_acct=C000050221&_version=1&_urlVersion=0&_userid=10&md5=e09416177bc3505b18130ab23ba3e51e.

P W Wilson, R J Garrison, R D Abbott, and W P Castelli. Factors associated with lipoprotein cholesterol levels. the framingham study. *Arteriosclerosis*, 3(3): 273–81, Jan 1983.

B Wolozin. Cholesterol, statins and dementia. *Current opinion in lipidology*, Jan 2004. URL http://journals.lww.com/co-lipidology/Abstract/2004/12000/Cholesterol,_statins_and_dementia.7.aspx.

B Wolozin, J Manger, and R Bryant. Re-assessing the relationship between cholesterol, statins and alzheimer's disease. *Acta Neurologica ...*, Jan 2006. URL http://www3.interscience.wiley.com/journal/118578445/abstract.

F Xu, S Rychnovsky, and J Belani. Dual roles for cholesterol in mammalian cells. *Proceedings of the ...*, Jan 2005. URL http://www.pnas.org/content/102/41/14551.full.

S Xu, B Benoff, H Liou, P Lobel, and A Stock. Structural basis of sterol binding by npc2, a lysosomal protein deficient in niemann-pick type c2 disease. *Journal of Biological ...*, Jan 2007. URL http://www.jbc.org/content/282/32/23525.short.

Zhi Xu, William Farver, Sarala Kodukula, and Judith Storch. Regulation of sterol transport between membranes and npc2. *Biochemistry*, 47(42):11134–43, Oct 2008. doi: 10.1021/bi801328u.

Yaara Zwang and Yosef Yarden. Systems biology of growth factor-induced receptor endocytosis. *Traffic*, 10(4):349–63, Apr 2009. doi: 10.1111/j.1600-0854.2008.00870.x. URL http://www3.interscience.wiley.com/journal/121569625/abstract?CRETRY=1&SRETRY=0.

4 Aim of the Thesis

From our current knowledge of cholesterol homeostasis, two things become evident:

(I) Cholesterol production is regulated via various feedback loops, of which some are postulated but so far remain elusive. One important hint comes from the fact that most efficient degradation of HMGCR in sterol-depleted cells requires cholesterol and very small amounts of mevalonate. As mevalonate is also an educt for geranyl, a geranylgeranylated protein has been proposed for being involved in the degradation of HMGCR (Goldstein and DeBose-Boyd, 2006). Typically, geranylated proteins are Rab proteins, which are involved in intracellular transport processes.

(II) Cholesterol levels vary dramatically between different membranes in the cell. Remarkably, sites of cholesterol entry like the ER and LE/LY are especially low in sterols, while the plasma membrane is high in cholesterol. Therefore, membrane trafficking or signaling processes between the plasma membrane and the ER must play an important role in controlling de novo cholesterol biosynthesis. This hypothesis is further supported by the fact that up-regulation of HMGCR transcription to activate de novo synthesis of cholesterol is also dependent on membrane trafficking, for example the COPII-dependent shuttling of SREBP/Scap from ER to the Golgi complex.

Taken together, this put forward the hypothesis that mammalian cells have factors that signal the PM cholesterol state to the ER via endocytic membrane trafficking. A very interesting candidate was AMFR because of its dual role: It is the receptor in the endocytosis of AMF but it is also the ubiquitin ligase that

confers ubiquitination and consequently to degradation of HMGCR.

In my PhD project I tried to answer the following questions: Is endocytosis a major control mechanism of HMGCR regulation? If so, which endocytic pathway is involved and which molecular players are required? Finally, I wondered whether either AMFR itself or a factor that was co-internalized with AMFR would change its localization in a cholesterol dependent manner.

Therefore, I first tested whether AMFR changes its localization according to the sterol-state of the cells. Next, I investigated the sensitivity of HMGCR degradation to pharmacological inhibitors. Finally, I generated a bacterial artificial chromosome containing a GFP-tagged version of HMGCR that allows for live, single cell quantification of HMGCR levels. This assay enabled me to identify further mediators of HMGCR using RNAi screening technology and will provide a platform for further RNAi screens in the future.

5 Expression and Degradation of HMG-CoA Reductase is regulated by the endocytic machinery

5.1 Abstract

Cholesterol is an essential constituent of mammalian cell membranes and serves as a signaling molecule as well as a buffer for membrane fluidity. Cholesterol is heterogeneously distributed across different cellular compartments, with the highest concentration at the plasma membrane. For a tight regulation of cholesterol biosynthesis, information about the level of free cholesterol at the plasma membrane may have to be signaled to the production machinery at the endoplasmic reticulum. The existence of such a signaling mechanism is however elusive. Here, we report single-cell analysis of an image-based GFP reporter gene assay of 3-hydroxy-3-methylglutaryl coenzyme A reductase (HMGCR), the rate-limiting enzyme in cholesterol production. We used small molecule inhibitors and RNA interference to reveal novel genes involved in the biosynthesis and degradation of HMGCR. We show the involvement of dynamin and tyrosine kinases in cholesterol-induced degradation of HMGCR and propose that endocytosis is involved to relay information about plasma membrane cholesterol levels to the cholesterol production machinery at the ER.

5.2 Introduction

Cholesterol is an important cause of complex diseases such as arteriosclerosis, heart attack and stroke (Ross, 1995). On the cellular level, changes in the cholesterol concentration alter physical properties of membranes, most notably their fluidity, which is important for membrane ruffling, endocytosis and cell motility. Cholesterol is also believed to contribute to the heterogeneous organization of lipids within the plasma membrane, which may concentrate and segregate certain membrane-spanning and membrane-associated proteins (Brown and London, 1998) (Simons and Vaz, 2004).

Mammalian cells regulate their cholesterol levels by uptake from and disposal to the blood serum or by biosynthesis from acetyl coenzyme A. De novo synthesis of steroids, as well as other non-sterol isoprenoids is concerted by a series of enzymatic reactions known as the mevalonate pathway (Goldstein and Brown, 1990). The rate-limiting enzyme of this pathway is 3-hydroxy-3-methylglutaryl-CoenzymeA-reductase (HMGCR), a transmembrane protein that is located in the smooth endoplasmic reticulum (ER) where it catalyzes the conversion from 3-hydroxy-3-methylglutaryl-coenzyme A to mevalonate. Both transcriptional up-regulation and degradation of HMGCR is centered around cholesterol-mediated binding to ER-residing proteins called Insigs (Espenshade and Hughes, 2007). The transcription factor complex SREBP/Scap is retained in the ER through its cholesterol-mediated association to Insigs and is activated and transported to the Golgi complex only when sterol levels are low. At the Golgi complex, SREBP is cleaved by Site-1 and Site-2 proteases to release the N-terminal, DNA-binding helix-loop-helix leucine zipper domain, which is imported in the nucleus where it acts as a transcription factor for enzymes of the mevalonate pathway and receptors of low density lipoprotein uptake (Goldstein and Brown, 1990) (Hua et al., 1996)(Duncan et al., 1997) (Rawson et al., 1997). Newly synthesized cholesterol is transported by vesicular

and non-vesicular traffic to all membranous compartments of the cell (Ikonen and Jansen, 2008). Its primary site of accumulation is the plasma membrane, where 85% of all unesterified cholesterol is located, with relatively low levels of cholesterol residing in the ER. If sterols are overabundant in the membrane of the ER, HMGCR itself binds via cholesterol to Insigs, where it becomes degraded after being ubiquitinated by an E3 ligase called gp78 or autocrine motility factor receptor (gp78/AMFR). AMFR serves as an E3 ligase in the ER but also acts as a receptor of autocrine motility factor (AMF) when residing in the plasma membrane.

We currently have a very detailed mechanistic understanding of how sterols regulate both the transcription and the degradation of HMGCR (Espenshade and Hughes, 2007), and an RNAi screen of cholesterol localization has recently been performed (Bartz et al., 2009). Furthermore, the existence of additional components of the regulatory machinery has been proposed, but not identified (Goldstein et al., 2006). Cholesterol addition to cells rapidly induces HMGCR degradation via gp78/AMFR, which targets HMGCR for ER-associated degradation.

Here, we report an image-based single-cell reporter gene assay to monitor HMGCR levels in living single cells over time. Using small molecule inhibitors and RNA interference, we have examined the role of genes involved in endocytic membrane trafficking in the expression and degradation of HMGCR in response to serum starvation followed by plasma membrane cholesterol loading. RNAi-mediated knockdown of clathrin heavy chain, adapter protein 2 subunit μ, or dynamin 2 results in impaired up-regulation of HGMCR upon sterol depletion. Cholesterol-triggered degradation of HMGCR is found to be dependent on tyrosine kinases, dynamins and possibly Eps15. This provides the first evidence that endocytosis is involved in the regulation of HMGCR levels upon serum starvation and plasma membrane cholesterol loading.

5.3 Results

Cholesterol-triggered degradation of HMGCR is dynamin- and tyrosine kinase-dependent.

To test if vesicular transport in cholesterol-induced degradation of HMGCR is involved, we examined a number of small molecular inhibitors known to block endocytosis or secretion through the exocytic pathway. We used pharmacological inhibitors that induce a collapse of the Golgi complex into the ER (Brefeldin A), the depolymerization of microtubuli (Nocodazole), the inhibition of dynamin-dependent vesicle fission (Dynasore), or the inhibition of tyrosine kinases (Genistein).

Figure 1a shows the effect of these inhibitors on cholesterol-induced degradation of HMGCR. When sterol-depleted cells were treated for 4h with the drugs, we observed a slight reduction of HMGCR signal in Genistein-treated cells but not in control cells or cells treated with the other drugs. Upon loading free cholesterol onto the plasma membrane of these cells using cholesterol-saturated Methyl-b-Cyclodextrin (Chol-MbCD), Brefeldin A- and Nocodazole-treated cells showed typical, cholesterol-induced HMGCR degradation, similar to control cells. In contrast, Dynasore- and Genistein-treated cells demonstrated a delayed degradation of HMGCR. This indicates that tyrosine kinases and dynamins are involved in cholesterol-triggered degradation of HMGCR.

We decided to focus on the involvement of dynamins. In order to independently confirm an involvement of dynamins in cholesterol-induced degradation of HMGCR, we used two Hela derived cell-lines that were stably transfected with inducible constructs of either a dominant negative or wild type versions of dynamin (Damke et al., 1995). Dominant-negative dynamin (K44A) has been shown to efficiently block dynamin-dependent endocytosis (Damke et al., 1994). Cells

showed efficient and tight induction of the dynamin-wt and dominant-negative constructs (Supplementary Figure 1). Under sterol-depleted conditions, both cell lines demonstrated elevated HMGCR levels. When cholesterol was loaded on the plasma membrane, cells expressing the dominant-negative construct of dynamin showed slower degradation of HMGCR compared to cells expressing the wild-type constructs (Figure 1b). The apparent block of cholesterol-induced HMGCR degradation by dynamin K44A confirms the inhibitory effect of Dynasore in Figure 1a.

BAC-expressed HMGCR-GFP displays similar temporal and spatial expression as endogenous HMGCR.

Cellular biochemical techniques have been extremely powerful in investigating regulation of HMGCR (Espenshade and Hughes, 2007) (Goldstein and Brown, 2009). Nevertheless, these techniques require relatively large amounts of cells, provide only cell population-averaged insights, and do not lend themselves for high-throughput automated screening. To overcome these limitations, we modified a Bacterial Artificial Chromosome (BAC) containing the chromosomal region of HMGCR and added Green Fluorescent Protein (GFP) to the cytosolic C-terminus. Figure 2a schematically shows the manipulated region on the BAC. The BAC contained approximately 140 kb upstream and more than 10 kb downstream of the HMGCR locus (www.mitocheck.org) thus ensuring transcriptional and translational control similar to endogenous HMGCR.

We investigated the GFP intensities in human A431 cells stably transfected with the BAC containing HMGCR-GFP (A431-HMGCR-GFP). GFP intensities were very low in cells grown in medium containing fetal calf serum but these dramatically increased when cells were incubated in serum-free medium containing mevastatin. HMGCR-GFP was rapidly degraded when cholesterol was added to serum-starved cells (see Figure 2b). Using open-source image analysis software (Carpenter

et al., 2006), we quantified and compared the fluorescence intensities of single A431-HMGCR-GFP cells with that of single untransfected A431 cells (Figure 2c). The distributions of single-cell intensities were visualized with boxplots and as density estimates (vertical lines, fitted distributions). In A431-HMGCR-GFP cells, the signals of both HMGCR-GFP and endogenous HMGCR – as visualized with an antibody – correlated with the cholesterol state. The signal distribution of serum-starved cells could easily be distinguished with high confidence ($P < 2.2x10\text{-}16$) from the signal distribution of cells kept in serum or after cholesterol loading. As expected, the antibody signal changed according to the presence of sterols in both A431 and A431-HMGCR-GFP cells, whereas differences in GFP intensities were only detectable in A431-HMGCR-GFP cells. Notably, the antibody signal in A431-HMGCR-GFP cells is higher than in untransfected A431 cells. Apparently, introduction of a third copy of HMGCR into the genome of A431 cells was not compensated by less endogenous HMGCR, but led to higher overall amounts of HMGCR. Furthermore, quantification of a large number of single-cell intensities in the whole population revealed extensive cell-to-cell variability in response to serum starvation, with a subpopulation of cells not responding. Similarly, upon plasma membrane cholesterol loading, we observed a fraction of cells not to respond by down-regulating their levels of HMGCR-GFP. These cells continued to show high levels of HMGCR-GFP. Non-responding cells are visible as outliers in the boxplots. Interestingly the fraction of non-responding cells that kept a high signal after 6h of plasma membrane cholesterol loading was much higher than the fraction of cells that had a high signal under steady-state 10% FCS conditions.

We independently confirmed the change of HGMCR and HGMCR-GFP levels upon starvation and/or plasma membrane cholesterol loading by western blotting (see Figure 2d). Cholesterol depletion of A431-HMGCR-GFP cells revealed an additional immuno-reactive band that migrated with the expected mass of HMGCR-

GFP (˜135 kD). As there is only one copy of HMGCR-GFP in the cells, this band was less pronounced than the signal at 97kD, however it showed similar dynamics compared to the endogenous protein. We also analyzed the subcellular localization of HMGCR-GFP in serum-starved cells. Like endogenous HMGCR in untransfected cells, HMGCR-GFP localizes to a reticular compartment, as well as to specific bright expansions of this network, most likely corresponding to the smooth ER (Figure 2f). Co-localization with the ER-resident chaperone calnexin (CNX) confirmed the localization in the ER (see Figure 2f).

We have been able to create a stable human A431 cell line that expresses a GFP-tagged HMGCR variant under its endogenous promoter system that responds in the same way as endogenous HMGCR to serum starvation and plasma membrane cholesterol loading. It localizes to the right intracellular compartment, and the extensive cell-to-cell variability in responses suggests the presence of currently uncharacterized properties. Thus, although we do not currently know whether HMGCR-GFP can functionally replace endogenous HMGCR, it represents a bona fide reporter system to study dynamics of HMGCR expression and degradation.

An image-based, live degradation assay for HMGCR-GFP using pharmacological inhibitors

Next, we tested the sensitivity of our reporter system in living cells in a 96-well plate setup using an automated microscope that was equipped with a environmental control unit. We imaged app. 1.2 million single serum-starved A431-HMGCR-GFP cells every 45 min over a period of 14 hours during cholesterol loading of the plasma membrane. Cells were either untreated, or treated with one of four inhibitors (BrefeldinA, Nocodazole, Dynasore or Genistein). In non-treated cells, signal intensities were high after starvation, and dropped to background levels during cholesterol loading of the plasma membrane, with the exception of a number

of non-responding cells (Figure 3a and outliers in Figure 3c). Cells that were kept in serum-free medium during the recording maintained high slightly increasing levels of HMGCR-GFP (Fig. 3b, blue line). A similar behavior was observed in BrefeldinA- and Nocodazole-treated cells, indicating that an intact Golgi complex, trafficking between the ER and the Golgi complex, and microtubules are not required to activate the degradation machinery of HMGCR. Notably, in BrefeldinA-treated cells that were kept under starvation conditions (blue line), the levels of HMGCR-GFP slightly dropped, in contrast to control cells or Nocodazole-treated cells, where the signal slightly increased. This reduction in signal might be caused by a block of ER-to-Golgi trafficking of SREBP/Scap that is necessary for the upregulation of HMGCR during starvation (Steck et al., 2002).

Interestingly, treatment of cells with Genistein during starvation resulted in a reduced fluorescence signal (Fig. 3a), confirming our results obtained with western blots (Figure 1a). Furthermore, in both Genistein- and Dynasore-treated cells that were kept under starvation conditions (blue lines), the levels of HMGCR-GFP markedly dropped. Genistein, has been reported to reduce HMGCR up-regulation on various levels (Dreu, Wilcox et al. 2002), to date no reports about Dynasore's influence on HMGCR expression exist. In addition, we observed in both Genistein- and Dynasore-treated cells that during cholesterol loading of the plasma membrane (red lines), the levels of HMGCR-GFP did not deviate from serum-starved cells (blue lines) over time. This indicates that Dynamin and tyrosine kinase signaling are involved in the up-regulation of HMGCR expression during starvation, but also in activating the degradation machinery of HMGCR. The effects are summarized in single-cell boxplots at time-point 800 min of the recordings (Fig. 3c). While BrefeldinA, Dynasore, and in particular Genistein reduced levels of HMGCR-GFP in serum-starved cells over time (red boxplots, compared to control cells), only Dynasore and Genistein blocked degradation of HMGCR-GFP induced by plasma

membrane cholesterol loading (blue and red boxplots are identical). This corresponds to our findings in Figures 1a and 1b.

An image-based live assay of HMGCR-GFP degradation for RNAi screening

A role for dynamin in the regulation of HMGCR expression and degradation suggests a role for endocytosis in these two processes. Because dynamin-dependent endocytosis can be subdivided into several classes of endocytosis, we knocked down various genes involved in endocytosis and membrane trafficking using RNA interference. After three days of gene silencing, cells were serum-starved for 30 hours, fixed, and imaged with automated microscopy. Single-cell intensities were quantified with computerized image analysis. Alternatively, we loaded the plasma membrane with cholesterol for 5 hours after serum starvation, after which cells were fixed, imaged, and quantified. The effect of the knockdown of 18 genes was investigated, tested with 3 independent siRNAs targeting different sites of the mRNA. Of these 18 genes, four are known regulators of HMGCR degradation: gp78/AMFR, the E3 ligase that ubiquitinates HMGCR to target it for ER-associated degradation, VCP, an ATPase that plays a role in extracting ubiquitinated proteins from membranes, and Insig1 and Insig2, which serve as signal-integration scaffolds for both the transcriptional up-regulation and the degradation of cholesterol synthesizing proteins We also silenced the cholesterol transporter NPC1, which is implicated in the lysosomal storage disorder Niemann Pick type C and resides in late endosomes where it plays an important role in cholesterol uptake from endocytosed Low Density Lipoprotein (Mukherjee and Maxfield 2004). The remaining 13 genes are known regulators of membrane trafficking.

Figure 4a shows the effect of RNAi knockdown on HMGCR-GFP expression in serum-starved cells. Knockdown of two genes that are involved in clathrin-

mediated endocytosis most strongly inhibited HMGCR-GFP expression in response to serum starvation. These were clathrin heavy chain (CLTC) and the µ subunit of the adaptor protein complex 2 (AP2M1). Furthermore, knockdown of dynamin 2 also showed a reduction of HMGCR levels, confirming our observation with Dynasore (Figures 1a and 3). The three genes of which knockdown resulted in highest fluorescence levels were the controls AMFR, Insig1 and Insig2. This is in accordance to the current knowledge, as Insig1 and Insig2 are both known to retain the transcription factor precursor Scap/SREBP in the ER, thus preventing HMGCR up-regulation. AMFR is the E3 ligase implicated in degradation of HMGCR; therefore its knockdown should reduce HMGCR degradation. Figure 4b shows a heat-map representation of the HMGCR-GFP intensities shown in Figure 4a.

Next, we set out to investigate the role of the same set of genes in degradation of HMGCR. As siRNA treatments had already influenced the up-regulation of HMGCR-GFP we had to consider this when analyzing the HMGCR-GFP levels after degradation. We postulated that the rate of degradation of HMGCR-GFP is solely depending on the amount of HMGCR-GFP after serum starvation and the protein that is knocked down by the specific siRNA. This allowed us to calculate the remaining signal for each siRNA using the formula (HMGCR-GFPdegraded - background)/(HMGCR-GFPstarved - background)=percent of remaining HMGCR-GFP.

Figure 4c shows the effect of siRNA-mediated knockdown of 18 genes on cholesterol-induced degradation of HMGCR-GFP. VCP, an AAA-ATPase also called p97, that is involved in dislocation of HMGCR in order to get properly degraded (Song et al., 2005), indeed showed to most prominent inhibition of HMGCR-GFP when knocked down. Insig 1 and Insig 2 have been shown to act as signal integration platforms and are also required for efficient degradation of HMGCR (Sever et al., 2003). Interestingly only Eps15, but neither dynamin1 nor dynamin2 showed

slowed degradation of HMGCR-GFP. Figure 4d is a heat-map representation of the results shown in Figure 4c.

5.4 Discussion

We present a reporter gene assay introducing a GFP-cassette into the chromosomal environment of HMGCR on a bacterial artificial chromosome. We demonstrated that the gene-product of this BAC, HMGCR-GFP, is regulated similar to endogenous HMGCR (Figure2). This allows an image-based quantification of HMGCR dynamics in living, single cells. We compared SDS-PAGE and the image-based GFP reporter assay on acute drug treatments and cholesterol-triggered degradation of HMGCR and obtained similar results (Figure 1a and Figure3). An image-based assay provides at least three main advantages: (i) it can be done in living cells, thus reducing experimental noise and allowing paired statistical tests; (ii) it can be automated to a higher degree than SDS page. This allows higher numbers of genes or substances to be tested. (iii) Single cells can be quantified and cell-to-cell variation investigated. It is becoming increasingly apparent that averaging over whole populations can be misleading because cell populations show extensive heterogeneity even under standard cell culture conditions (Snijder et al., 2009). Only single cell quantifications can provide information about the local surrounding of a cell. We provide a proof of principle study about performing and quantifying the effects of a medium number of small molecule inhibitors and siRNAs using automated microscopy in combination with image analysis and statistical analysis. Using a candidate gene approach, we could prove the specificity of the assay in combination with siRNA treatments on known regulators of HGMCR homeostasis.

The current results demonstrate a role of vesicular transport processes in the homeostasis of HGMCR. Cholesterol-induced degradation of HMGCR was blocked by Dynasore, a pharmacological inhibitor of dynamin as well as by over-expression

of a dominant negative dynamin construct (dynamin K44A). Furthermore, using RNAi we were also able to investigate the effect of specific genes for the up-regulation of HMGCR. Surprisingly, siRNA mediated knockdown of three genes involved in dynamin-dependent endocytosis, dynamin 2, clathrin heavy chain, and the µ subunit of adaptor protein complex 2 showed reduced levels of HMGCR-GFP in sterol depleted cells, suggesting an additional role of clathrin and dynamin in the up-regulation of HMGCR levels. This effect was very penetrant for all three siRNAs, making it unlikely to be an off-target effect, however efficient knockdown via RNAi is only achieved after 3 days of siRNA treatment, we cannot rule out secondary or compensatory effects.

Importantly, in the assay monitoring degradation of HGMCR-GFP, Insig1 and Insig2 blocked degradation of HMGCR, but neither dynamin 1 nor dynamin 2 nor AMFR showed an inhibitory effect, as one would have suspected from the previous data. This contradictive result could have several causes. (i) Insufficient knockdown of the targets. It has been reported that dynamins and AMFR have a long half time and are difficult to knock down. (ii) The complexity of the degradation assay. In order to investigate HMGCR without artificial over-expression, siRNA treated cells had to be starved before starting the repletion with cholesterol. The knockdown of regulators of HMGCR already produced a heterogeneous expression profile during serum-starvation; this had to be taken into account during the analysis. (iii) Imprecise assumptions. As mentioned in (ii), we had to compare a broad range of starting levels of HMGCR-GFP. We did not account for a saturation of the degradation machinery on high levels of HMGCR-GFP (Sever et al., 2003). We assumed constant background levels over the whole plate and a constant factor of bleaching; this assumption is less robust on wells with low HMGCR-GFP levels. In contrast to the AP2 complex proteins (µ and β), which accelerate degradation when knocked down, Eps15, a monomeric adapter protein might be required for

degradation of HMGCR, as Eps15 knockdown leads to slowed down degradation of HMGCR that are similar to the controls Insig1 and Insig2.

In this initial study, we have not attempted to dissect the separate effects of cholesterol, oxysterols and non-sterol isoprenoids on HMGCR regulation (Goldstein and Brown, 1990). Furthermore, we did not address the question of cholesterol transport in cells, but looked at a functional readout when blocking transport processes. In regard to cholesterol transport, not only vesicular but also non-vesicular transport would be highly interesting. There, the class of oxysterol binding protein related proteins (ORPs) have been proposed as candidates. In yeast, oxysterol-binding protein homologues (Osh proteins) have been shown to be important for ergosterol and cholesterol transport between membranes (Sullivan et al., 2006) (Raychaudhuri et al., 2006). Furthermore, Genistein treatment showed effects of tyrosine kinases on stability and degradation of HMGCR, making a kinome-wide screen very promising. Finally, although we analyzed single cell intensities, so far we did not investigate the causes of the population heterogeneities we encountered. Using information about the cellular context will provide more specific results beyond collective behavior of cell populations.

As most of unesterified cholesterol resides in the PM, there is the necessity of information flow to the ER, which is the site of cholesterol production. We showed that degradation of HMGCR is dependent on tyrosine kinases (as shown by its sensitivity to Genistein) and dynamin (as shown by its sensitivity to Dynasore and the dominant negative K44A). Interestingly, internalization of AMF-bound AMFR from the PM to the ER is also inhibited by dynamin K44A Genistein (Le and Nabi, 2003) (Kojic et al., 2008). It is therefore very tempting to speculate the transport of AMFR also plays a role in regulating HMGCR. So far internalization of AMFR has been attributed to binding to its ligand AMF. If AMFR would also change its localization depending on the cholesterol levels, this would be an additional regu-

lation of HMGCR stability. AMFR would sit in the PM of sterol-depleted cells. Raising PM sterol levels would trigger AMFR to be internalized via a dynamin and tyrosine kinase dependent pathway, possibly also involving Eps15 (Figure 4c). In the ER, AMFR would act in concert with the ERAD machinery to degrade the Insig-bound HMGCR (Song et al., 2005). Shuttling of AMFR as a result of the cellular cholesterol state should be visible by localization studies of AMFR. In over-expression experiments using pull-downs, AMFR has been reported to constitutively bind to Insigs (Song, Sever et al. 2005). Such over-expression experiment might not reflect physiological conditions and pull-down experiments do not provide information about unbound AMFR. One obvious question then would be how cholesterol levels trigger endocytosis of AMFR in the absence of AMF? Also, if the physiological function of AMFR is to regulate HMGCR levels, what are the consequences of AMF-triggered internalization on HMGCR? Unfortunately we can neither provide localization information of AMFR in a non-overexpression system nor internalization assays of AMF so far. We therefore see our model as a means to provide suggestions for further experiments and conceptual work.

5.5 Material and Methods

5.5.1 Materials

Mevastatin (M2537), Brefeldin A (B7651), Nocodazole (M1404), Amiloride (A7410) Cholesterol powder (C3045) and 25-Hydroxycholesterol (H1015) were bought from Sigma, Germany; Dynasore (BAS 00597512) was bought from Asinex, Russia.

5.5.2 Methods

Generation of a GFP-tagged BAC

The Bacterial Artificial Chromosome (BAC) genomic clone RPCIB753F01654Q, that contains the full genomic sequence of HMGCR including more than 30 kb up- and downstream of the respective start and stop codons, was ordered from ImaGenes, Germany. As this BAC was about 200 kb in size, traditional restriction-and-ligation cloning methods were not applicable. Therefore, a recombination method was used as described in the manual "Gene Bridges K001 Q E BAC Modification Kit-version2.6-2007" and (Cheeseman and Desai 2005). A localization and affinity purification tag (LAP-tag), generously provided by Anthony Hyman (MPI, Dresden, Germany), containing the gene coding for enhanced Green Fluorescence Protein (eGFP), a S-peptide and a Kanamycin/Neomycin resistance cassette was amplified from a parental vector by PCR. The primers were designed such, that they had 75 nucleotide overhangs that would later allow homologous recombination of the LAP-cassette into the C-terminus HMGCR. Forward primer (5'-CGAAGATCAATTTACAAGACCTCCAAGGAGCTTGCACCAAGAAGACAGCCGATTATGATATTCCAACTACTG -3') and reverse primer (5' - GTCCTTTAGAACCCAATGCCCATGTTCCAGTTCAGAACTGTCGGGCTATTTCAGAAGAACTCGTCAAGAAG 3'). In a second step, bacteria containing the BAC were co-transformed with a vector containing the genes performing the recombination and the PCR product described above. Single bacterial colonies were picked and the integrity of the plasmids was confirmed by DNA sequencing of the recombination joints. The generated BAC clone containing the LAP tag at the right position was stably transfected into A431 cells, and its integration was checked by western blot analysis and visible inspection under a fluorescence light microscope.

Cell Culture and Drug treatments

Monolayers of 80-90% confluent A431 cells were maintained in cell culture at 37^{o}C and 5% CO2, and in high glucose Dulbecco's modified Eagle medium (DMEM) supplemented with 10% fetal calf serum (FCS). The medium for A431 with the stably integrated BAC-HMGCR-GFP was additionally supplemented with 500µg/mL G418. Inducible Dynamin 2-dominant negative cells were a generous gift from Sandra Schmid (The Scripps Research Institute, La Jolla,CA) and were cultured as previously reported (500µg/mL G418, 1My/mL Tetracyline) (Damke et al., 1995). For sterol starvation cells were washed three times with PBS and switched to DMEM supplemented with Glutamax and 5mM Mevastatin for 29h. After that, where indicated, cells were pre-incubated with drugs for 45 minutes, before the addition of cholesterol coupled to mβCD to the final amount of 20µg/mL for the indicated amounts of time. Concentrations used for the drug treatments were: Amiloride: 10µM; Brefeldin A 5µg/mL; Dynasore: 6µg/mL; Genistein: 100µM; Nocodazole: 1µM; DMSO was adjusted to a final amount of 0.4%. For live cell imaging, cells were switched from standard DMEM to DMEM without Phenol red and Riboflavin, which was a generous gift from Daniel Gerlich (ETH Zurich, Switzerland), 2h before image acquisition.

Cell Fractionation and Immunoblot Analysis

Cells were harvested by washing twice with ice-cold PBS followed by scraping into 600µL of ice-cold PBS. The suspension was transferred into a micro-centrifuge tube and centrifuged at 103 g for 5 min at 4^{o}C. The pellet was resuspended in 0.4mL Buffer A (10 mM HEPES-KOH [pH 7.4], 10 mM KCl, 1.5 mM MgCl2, 5 mM sodium EDTA, 5 mM sodium EGTA, and 250 mM sucrose) supplemented with Complete Protease Inhibitor Cocktail (Roche). The cell suspension was passed through a 22.5 gauge needle 25 times and centrifuged at 104 g for 7 min at 4°C.

The pellet was resuspended in 0.3mL of Buffer A1 (20 mM HEPES-KOH [pH 7.6], 25% (v/v) glycerol, 0.42 M NaCl, 1.5 mM MgCl2, 1 mM EDTA, 1 mM EGTA, and protease inhibitor cocktail) and rotated for 1h at 4^{o}C followed by centrifugation at 2x104 g for 30 min at 4^{o}C. The supernatant was designated nuclear extract fraction and precipitated over night at -70^{o}C with 1.5mL acetone. The precipitated material was collected by centrifugation for 15 min at 2 x 104 x g at 4^{o}C and solubilized in 100µL Buffer A2 (10 mM Tris-HCl (pH 6.8), 1% (w/v) sodium dodecyl sulfate (SDS), 100 mM NaCl and 1 mM EDTA). Protein concentrations of nuclear extract and membrane fractions were measured using the BCA Kit (Pierce). Protein amounts were adjusted to typically 3.5 µg/µL by adding Buffer A2. Finally, equal amounts of Buffer B (62.5 mM Tris-HCl [pH 6.8], 15% (w/v) SDS, 8 M urea, 10% (v/v) glycerol, and 100 mM DTT) were added together with 6x SDS loading buffer and samples were incubated at 37^{o}C for 30 min prior to SDS-PAGE. After SDS-PAGE on 7.5% gels, proteins were transferred to nylon membranes and incubated with the following antibodies: IgG-A9, a mouse monoclonal antibody against the catalytic domain of human HMG CoA reductase from the culture medium of hybridoma (ATCC Number: CRL-1811), anti-calnexin, a rabbit polyclonal antibody was a generous gift from Ari Helenius (ETH Zürich, Switzerland) and was used as a loading control for ER fractions. Bound antibodies were visualized with peroxidase-conjugated, affinity-purified donkey anti-mouse or anti-rabbit IgG using Immobilon Western HRP Substrate according to the manufacturer's instructions. Pre-stained protein markers were used for molecular weight determination (PageRuler Prestained Protein Ladder plus, Fermentas). Filters were exposed to FUJIFILM Super RX film at room temperature for typically 20 - 300 seconds.

Imaging and Statistical analysis

All live experiments were performed in 96-well plates, and cells were imaged with an ImageXpress Micro automated microscope (Molecular Devices) with 10x magnification at 37^{o}C and 5 % CO2. Single-cell image analysis was performed using CellProfiler (Carpenter et al., 2006). In summary, nuclei were detected using Hoechst 33342 (Sigma, Germany) stain, these regions were expanded to cover the cytoplasm and the total signal intensity per cell was measured. Resulting single cell measurements were exported and analyzed using R (http://www.R-project.org) as described in the figure legends

5.6 Bibliography

F. Bartz, L. Kern, D. Erz, M. Zhu, D. Gilbert, T. Meinhof, U. Wirkner, H. Erfle, M. Muckenthaler, R. Pepperkok, and H. Runz. Identification of cholesterol-regulating genes by targeted rnai screening. *Cell Metab*, 10(1):63–75, Jul 2009. doi: 10.1016/j.cmet.2009.05.009. URL `http://www.ncbi.nlm.nih.gov/sites/entrez?Db=pubmed&Cmd=Retrieve&list_uids=19583955&dopt=abstractplus`.

D. Brown and E. London. Functions of lipid rafts in biological membranes. *Annu Rev Cell Dev Biol*, 14:111–36, 1998. URL `http://www.ncbi.nlm.nih.gov/entrez/query.fcgi?cmd=Retrieve&db=PubMed&dopt=Citation&list_uids=9891780%20`.

A. Carpenter, T. Jones, M. Lamprecht, and C. Clarke. Cellprofiler: image analysis software for identifying and quantifying cell phenotypes. *Genome ...*, Jan 2006. URL `http://www.biomedcentral.com/1465-6906/7/R100/abstract`.

H. Damke, T. Baba, D. Warnock, and S. Schmid. Induction of mutant dynamin specifically blocks endocytic coated vesicle formation. *J Cell Biol*, 127 (4):915–34, Nov 1994. URL http://www.ncbi.nlm.nih.gov/entrez/query.fcgi?cmd=Retrieve&db=PubMed&dopt=Citation&list_uids=7962076.

H. Damke, M. Gossen, S. Freundlieb, H. Bujard, and S. Schmid. Tightly regulated and inducible expression of dominant interfering dynamin mutant in stably transformed hela cells. *Methods Enzymol*, 257:209–20, 1995. URL http://www.ncbi.nlm.nih.gov/entrez/query.fcgi?cmd=Retrieve&db=PubMed&dopt=Citation&list_uids=8583923.

E. A. Duncan, M. S. Brown, J. L. Goldstein, and J. Sakai. Cleavage site for sterol-regulated protease localized to a leu-ser bond in the lumenal loop of sterol regulatory element-binding protein-2. *J Biol Chem*, 272(19):12778–85, May 1997.

P. Espenshade and A. Hughes. Regulation of sterol synthesis in eukaryotes. *Annu Rev Genet*, Jul 2007. URL http://www.ncbi.nlm.nih.gov/entrez/query.fcgi?cmd=Retrieve&db=PubMed&dopt=Citation&list_uids=17666007%20. Journal article.

J. Goldstein and M. Brown. Regulation of the mevalonate pathway. *Nature*, Jan 1990. URL http://dolly.biochem.arizona.edu/Bioc462b_Honors_Spring_2009/urdang/Goldstein1990.pdf.

J. Goldstein and M. Brown. The ldl receptor. *Arteriosclerosis*, Jan 2009. URL http://atvb.ahajournals.org/cgi/content/abstract/29/4/431.

J. Goldstein, R. DeBose-Boyd, and M. Brown. Protein sensors for membrane sterols. *Cell*, Jan 2006. URL http://linkinghub.elsevier.com/retrieve/pii/S0092867405014637.

X. Hua, J. Sakai, M. Brown, and J. Goldstein. Regulated cleavage of sterol regulatory element binding proteins requires sequences on both sides of the endoplasmic reticulum membrane. *Journal of Biological Chemistry*, Jan 1996. URL http://www.jbc.org/content/271/17/10379.short.

E. Ikonen and M. Jansen. Cellular sterol trafficking and metabolism: spotlight on structure. *Curr Opin Cell Biol*, 20(4):371–7, Aug 2008. doi: S0955-0674(08)00058-6[pii]10.1016/j.ceb.2008.03.017. URL http://www.ncbi.nlm.nih.gov/entrez/query.fcgi?cmd=Retrieve&db=PubMed&dopt=Citation&list_uids=18502634.

L. Kojic, S. Wiseman, F. Ghaidi, B. Joshi, H. Nedev, H. Saragovi, and I. Nabi. Raft-dependent endocytosis of autocrine motility factor/phosphoglucose isomerase: a potential drug delivery route for tumor cells. *PLoS ONE*, 3(10):e3597, 2008. doi: 10.1371/journal.pone.0003597. URL http://www.ncbi.nlm.nih.gov/entrez/query.fcgi?cmd=Retrieve&db=PubMed&dopt=Citation&list_uids=18974847.

P. Le and I. Nabi. Distinct caveolae-mediated endocytic pathways target the golgi apparatus and the endoplasmic reticulum. *J Cell Sci*, 116(Pt 6):1059–71, Mar 2003. URL http://www.ncbi.nlm.nih.gov/entrez/query.fcgi?cmd=Retrieve&db=PubMed&dopt=Citation&list_uids=12584249.

R. B. Rawson, N. G. Zelenski, D. Nijhawan, J. Ye, J. Sakai, M. T. Hasan, T. Y. Chang, M. S. Brown, and J. L. Goldstein. Complementation cloning of s2p, a gene encoding a putative metalloprotease required for intramembrane cleavage of srebps. *Molecular cell*, 1(1):47–57, Dec 1997.

S. Raychaudhuri, Y. Im, and J. Hurley. Nonvesicular sterol movement from plasma membrane to er requires oxysterol-binding protein $# x02013; related proteins

and phosphoinositides. ... *Journal of Cell Biology*, Jan 2006. URL http://ukpmc.ac.uk/articlerender.cgi?artid=1153171.

R. Ross. Cell biology of atherosclerosis. *Annu Rev Physiol*, 57:791–804, Jan 1995. doi: 10.1146/annurev.ph.57.030195.004043. URL http://arjournals.annualreviews.org/doi/abs/10.1146/annurev.ph.57.030195.004043?url_ver=Z39.88-2003&rfr_id=ori:rid:crossref.org&rfr_dat=cr_pub%253dncbi.nlm.nih.gov.

N. Sever, T. Yang, M. Brown, J. Goldstein, and R. DeBose-.... Accelerated degradation of hmg coa reductase mediated by binding of insig-1 to its sterol-sensing domain. *Molecular cell*, Jan 2003. URL http://linkinghub.elsevier.com/retrieve/pii/S1097276502008225.

K. Simons and W. Vaz. Model systems, lipid rafts, and cell membranes. *Annu Rev Biophys Biomol Struct*, 33:269–95, 2004. URL http://www.ncbi.nlm.nih.gov/entrez/query.fcgi?cmd=Retrieve&db=PubMed&dopt=Citation&list_uids=15139814%20. Introduction:" Lipid ordering;.

B. Snijder, R. Sacher, P. Rämö, E.-M. Damm, P. Liberali, and L. Pelkmans. Population context determines cell-to-cell variability in endocytosis and virus infection. *Nature*, 461(7263):520–3, Sep 2009. doi: 10.1038/nature08282. URL http://www.nature.com/nature/journal/v461/n7263/full/nature08282.html.

B. Song, N. Sever, and R. DeBose-Boyd. Gp78, a membrane-anchored ubiquitin ligase, associates with insig-1 and couples sterol-regulated ubiquitination to degradation of hmg coa reductase. *Mol Cell*, 19(6):829–40, Sep 2005. URL http://www.ncbi.nlm.nih.gov/entrez/query.fcgi?cmd=Retrieve&db=PubMed&dopt=Citation&list_uids=16168377%20.

T. L. Steck, J. Ye, and Y. Lange. Probing red cell membrane cholesterol movement with cyclodextrin. *Biophys J*, 83(4):2118–25, Oct 2002. doi: 10.1016/S0006-3495(02)73972-6.

D. Sullivan, H. Ohvo-Rekila, and N. B. . . . . Sterol trafficking between the endoplasmic reticulum and plasma membrane in yeast. *Biochemical Society . . .* , Jan 2006. URL `http://www.biochemsoctrans.org/bst/034/0356/bst0340356.htm`.

5.7 Figure Legends

Figure 1: Tyrosine kinases and Dynamin family members are implicated in cholesterol-induced degradation of HMGCR

(a) A431 cells were cultured in serum free medium containing 25µM Mevastatin for 29 h to induce HMGCR expression. After that, cells were pre-incubated with the indicated drugs for 45 min and degradation of HMGCR was triggered by addition of 20µg/mL cholesterol (final) for 3h. Cells were harvested and subjected to SDS-PAGE using a monoclonal HMGCR antibody to detect HMGCR and a polyclonal Antibody against calnexin as a loading control. (b) HeLa cells either carrying an inducible wild type or dominant negative Dynamin 2 construct (Damke94), were seeded in tetracycline-containing medium. Cells were switched to serum free medium containing 25µM Mevastatin without tetracycline, to allow both induction of HMGCR and Dynamin expression. After 30h, degradation of HMGCR was triggered by addition of 20µg/mL cholesterol for two or four hours. Cells were harvested and subjected to SDS-PAGE using a monoclonal HMGCR antibody to detect HMGCR and calnexin as a loading control. (FCS: fetal calf serum containing DMEM; BFA: Brefeldin A; Noc: Nocodazole; Dyn: Dynasore; Gen: Genistein)

Figure 2: An HMGCR-GFP transgene is regulated in a cholesterol dependent manner similar to endogenous HMGCR

(a) Schematic representation of the engineered bacterial artificial chromosome (BAC) containing the full genomic sequence of HMGCR plus an eGFP cassette fused to the C-terminus. (b) Image-based analysis showing cholesterol induced expression and degradation of HMGCR-GFP in A431 cells stably transfected with this BAC. Cells were seeded in 96-well, microclear plates and either switched to serum free medium containing 25µM Mevastatin or kept in 10% FCS. After 30h, half of the starved wells were supplemented with 20µg/mL cholesterol (final) whereas the other wells were kept in serum free medium, for an additional 5h. Representative images of fixed cells are shown. HMGCR-GFP in green; nuclei in blue (c) Boxplots and estimated density distributions of the total single cell fluorescence in the background cell line A431 and A431 cells stably carrying the BAC. HMGCR signal was compared by juxtaposing GFP fluorescence to indirect fluorescence of a monoclonal antibody against endogenous HMGCR. red boxplots and lines: antibody signal; green boxplots and lines GFP signal. (d) Western blot analysis showing the cholesterol-dependent expression and degradation of HMGCR-GFP compared the endogenous HMGCR in the background A431 cell line and the newly generated A431 cell line carrying the stably integrated BAC (e) HMGCR-GFP resides in calnexin positive ER. Triple-color, high-resolution immune fluorescence of HMGCR-GFP and calnexin in a serum-starved cell, containing the stably integrated BAC. (f) High resolution image of endogenous HMGCR in a starved A431 cell not containing the HMGCR-GFP BAC. (FCS: Fetal calf serum; IRES: internal ribosome entry site promoter; neo: Neomycin resistance gene;. P: PreScission cleavage site; S: S-peptide; T, TEV cleavage site)

Figure3: Image-based fluorescent reporter assay of living cells confirms the involvement of Dynamin family members and tyrosine kinases in cholesterol-triggered degradation of HMGCR

(a) A431-HMGCR-GFP cells were seeded in a 96well microclear plate and switched to serum free medium containing 25µM Mevastatin. Then, cells were pre-incubated with the indicated drugs for 45 min, and either kept in serum free medium or treated with addition of 20µg/mL cholesterol (final). Cells were imaged at 37°C in a humidified atmosphere every 45 min for a total period of 800 min. Representative images of imaged wells are shown. HMGCR-GFP in green, nuclei in blue. (b) Time-course of single cell fluorescence. Dots represent measured median single cell values, lines are regressions. Blue and red lines represent cells with or without cholesterol add-back respectively. (c) Boxplots representing the whole population of single cell fluorescence of the treatments in Figure 3b at the final time point of image acquisition.

Figure 4: A candidate based siRNA screen reveals the involvement of components of the clathrin-mediated endocytosis machinery in the regulation of HMGCR levels.

(a) Genes regulating the starvation-induced up-regulation of HMGCR. Cells seeded in 96-well plate were treated with one of three different siRNAs targeting genes either involved in endocytosis or in the regulation of HMGCR. After three days, cells were starved for 30h and imaging was performed as described in Figure 3. Single cell intensities from each of three independent experiments were Z-score normalized, resulting in an estimation of the experimental variation (indicated as the variance of the thin, colored boxplots). The median value of the three replicas was considered the siRNA value. The combination of the three siRNA values per gene resulted in the gene value, indicated by the light grey boxplots, and their

variance is the discrepancy of different siRNA targeting the same gene. Genes were ranked according to the mean value of the three siRNA values per gene. (b) Heat-map of the siRNA values from (a). (c) Genes involved in cholesterol-induced degradation of HMGCR-GFP. Cells were treated as in (a) but cholesterol was added after 30h of starvation and living cells were imaged every 45 min during a time course of 600 min. After removing background intensities, the fraction of remaining signal of each replicate before and after degradation was calculated. Z-scores, Replicate variation, siRNA and gene values were calculated as in (a). Genes were ranked according to the mean value of each normalized siRNA value. (d) Heat-map of the siRNA values from (c).(green, yellow and red boxplots indicate siRNA1, siRNA2, siRNA3 of each gene respectively)

Figure 5: Hypothesis how cells sense their overall cholesterol content by cholesterol-induced endocytosis of AMFR

In cholesterol-depleted cells, AMFR is transported into the PM. When cholesterol accumulates in the PM, an unknown cue triggers AMFR to be internalized in a dynamin-dependent route from the PM to the ER. There, AMFR ubiquitinates HMGCR and targets it to ER associated degradation.

Supplementary Figure 1: Efficient and tight induction of the dynamin-wt and dominant-negative constructs of Hela cell lines in cholesterol depletion medium

Hela Cell lines, carrying either a dominant negative or wild-type constructs of dynamin 2 –HA were grown in medium containing 10% FCS and tetracycline. After 18h, cells were switched to serum free medium supplemented with 25µM Mevastatin and either cultured in the presence or the absence of tetracycline. After additional 24 hours, cells were harvested and subjected to SDS-PAGE.

Supplementary Figure 2: AMFR does not change its localization upon sterol depletion

A431 cells were transfected with AMFR-GFP (Figure 2a-b) or AMFR-myc (Figure 2c-f), switched to either serum free medium containing 25µM Mevastatin or kept in 10% FCS. After 30h, cells were fixed and AMFR-myc cells were antibody-stained. Some AMFR-myc transfected cells were additionally stained with a monoclonal antibody targeting endogenous AMFR (Figure 2e-f). Cells were mounted on cover slides and imaged using a confocal microscope.

5.8 Figures

Figure 1

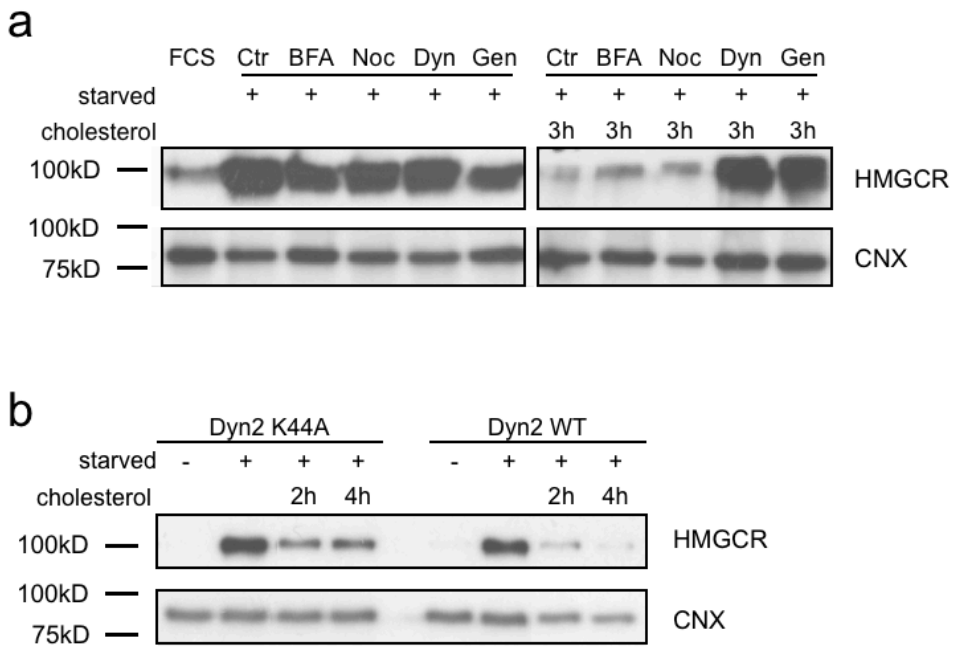

Figure 5.1:

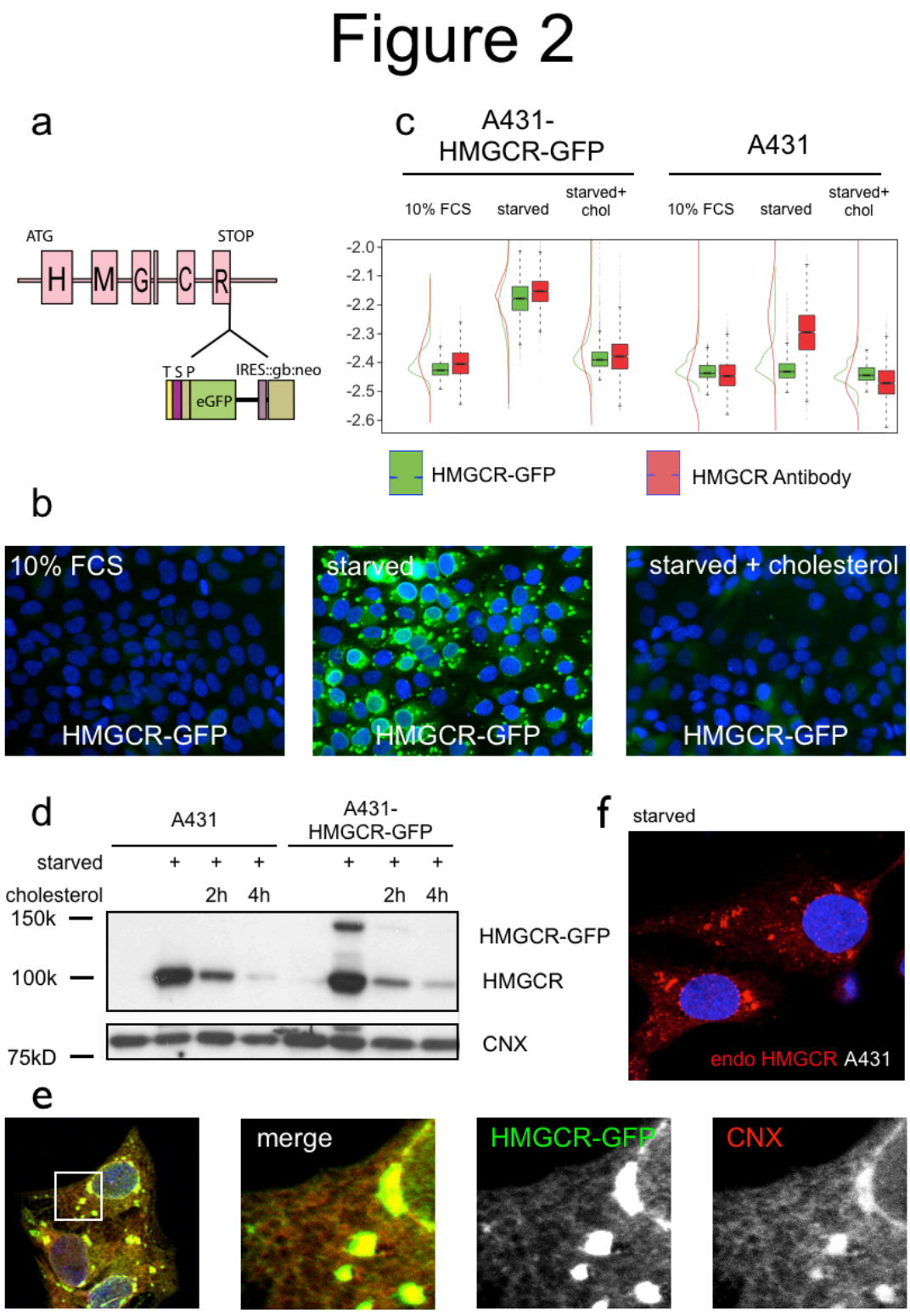
Figure 2
a
ATG
STOP
H
M
G
C
R
T S P
IRES::gb:neo
eGFP
c
A431-
HMGCR-GFP
A431
10% FCS
starved
starved+
chol
10% FCS
starved
starved+
chol
-2.0
-2.1
-2.2
-2.3
-2.4
-2.5
-2.6
HMGCR-GFP
HMGCR Antibody
b
10% FCS
HMGCR-GFP
starved
HMGCR-GFP
starved + cholesterol
HMGCR-GFP
d
A431
A431-
HMGCR-GFP
starved
+ + + + + +
cholesterol
2h 4h 2h 4h
150k
100k
75kD
HMGCR-GFP
HMGCR
CNX
f
starved
endo HMGCR A431
e
merge
HMGCR-GFP
CNX

Figure 5.2:

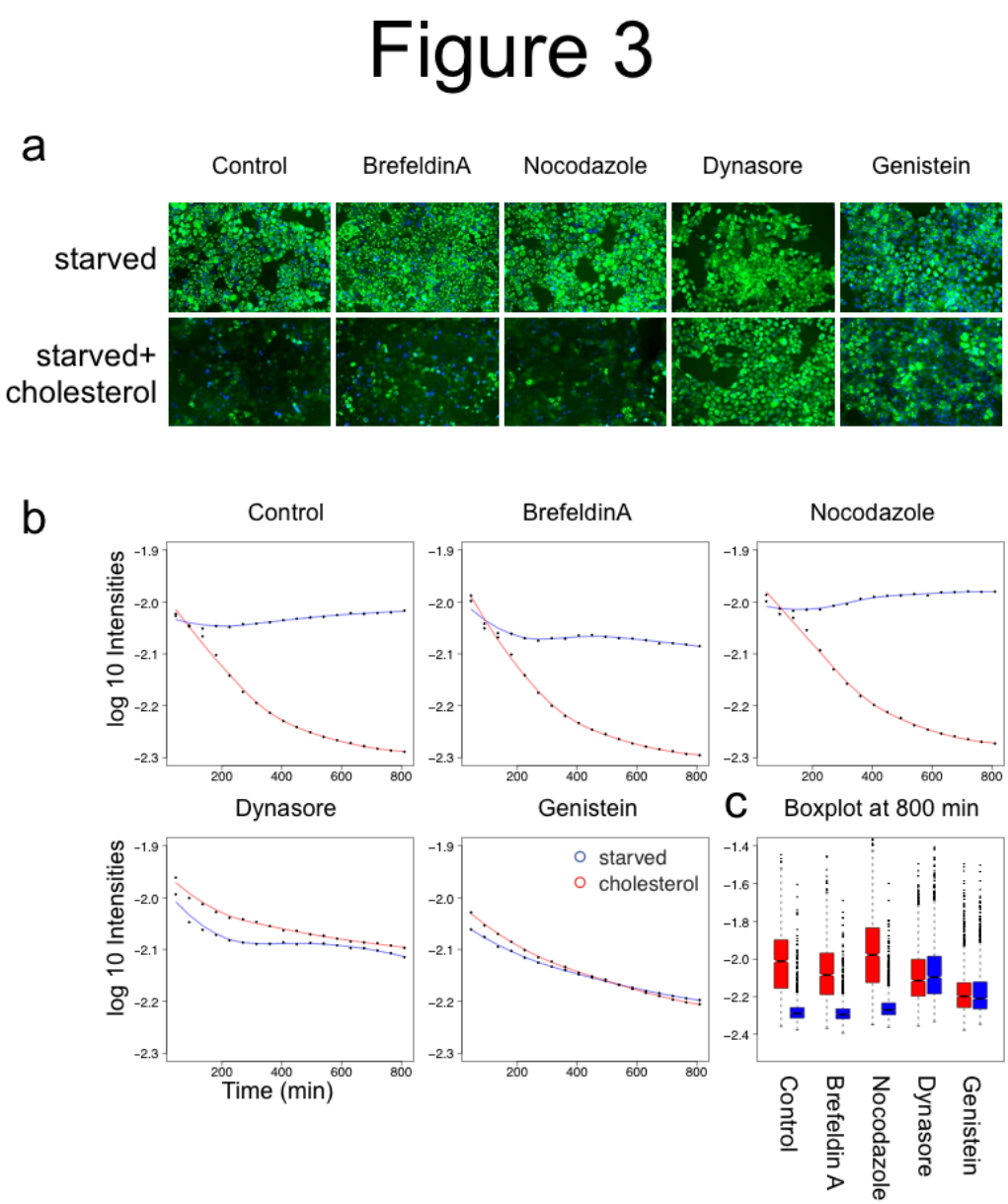
Figure 3
a
Control
BrefeldinA
Nocodazole
Dynasore
Genistein
starved
starved+
cholesterol
b
Control
BrefeldinA
Nocodazole
Dynasore
Genistein
log 10 Intensities
Time (min)
starved
cholesterol
c
Boxplot at 800 min
Control
Brefeldin A
Nocodazole
Dynasore
Genistein

Figure 5.3:

Figure 4

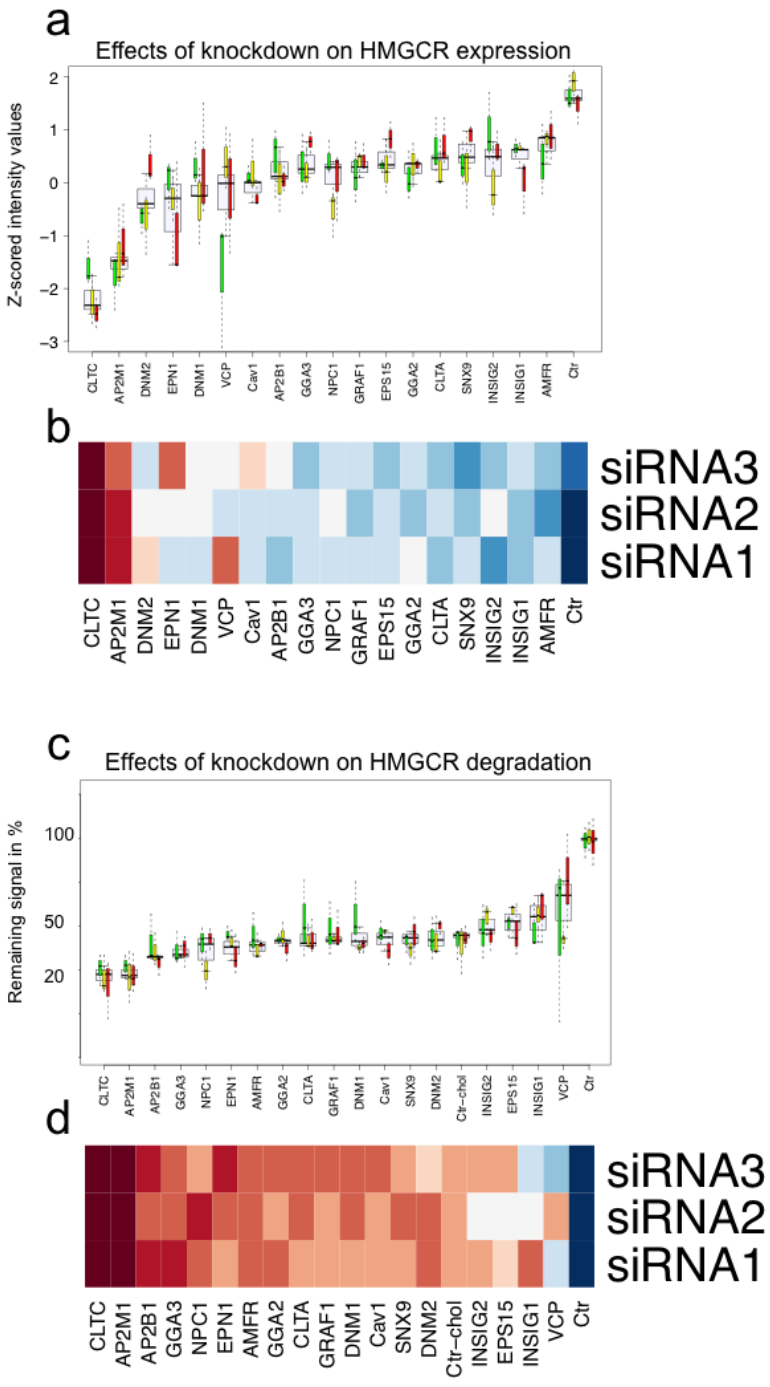

Figure 5.4:

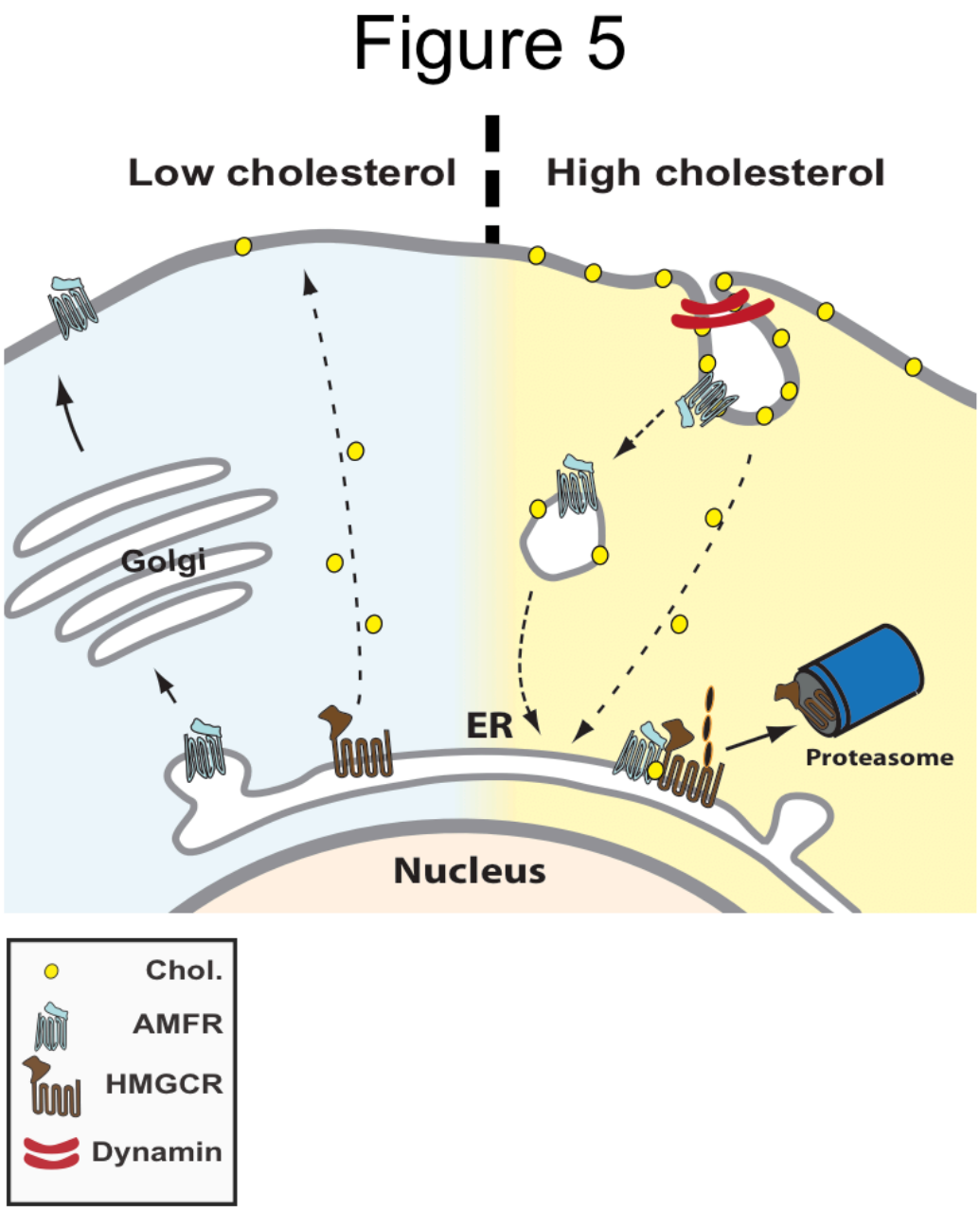
Figure 5
Low cholesterol
High cholesterol
Golgi
ER
Proteasome
Nucleus
Chol.
AMFR
HMGCR
Dynamin

Figure 5.5:

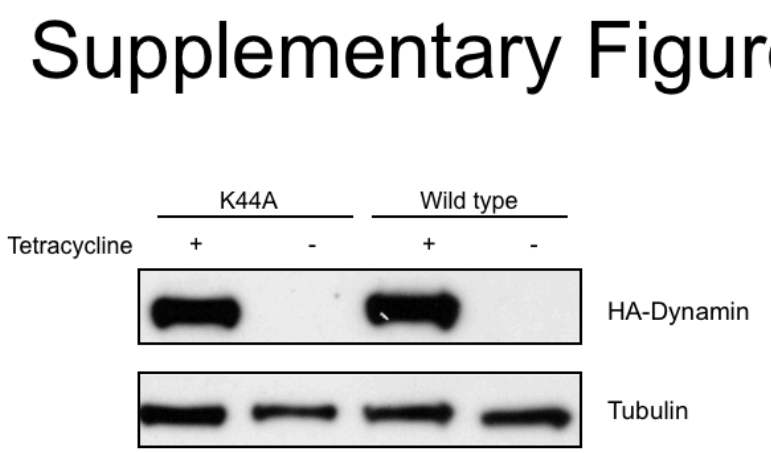
Supplementary Figure 1
K44A
Wild type
Tetracycline
+
-
+
-
HA-Dynamin
Tubulin

Figure 5.6:

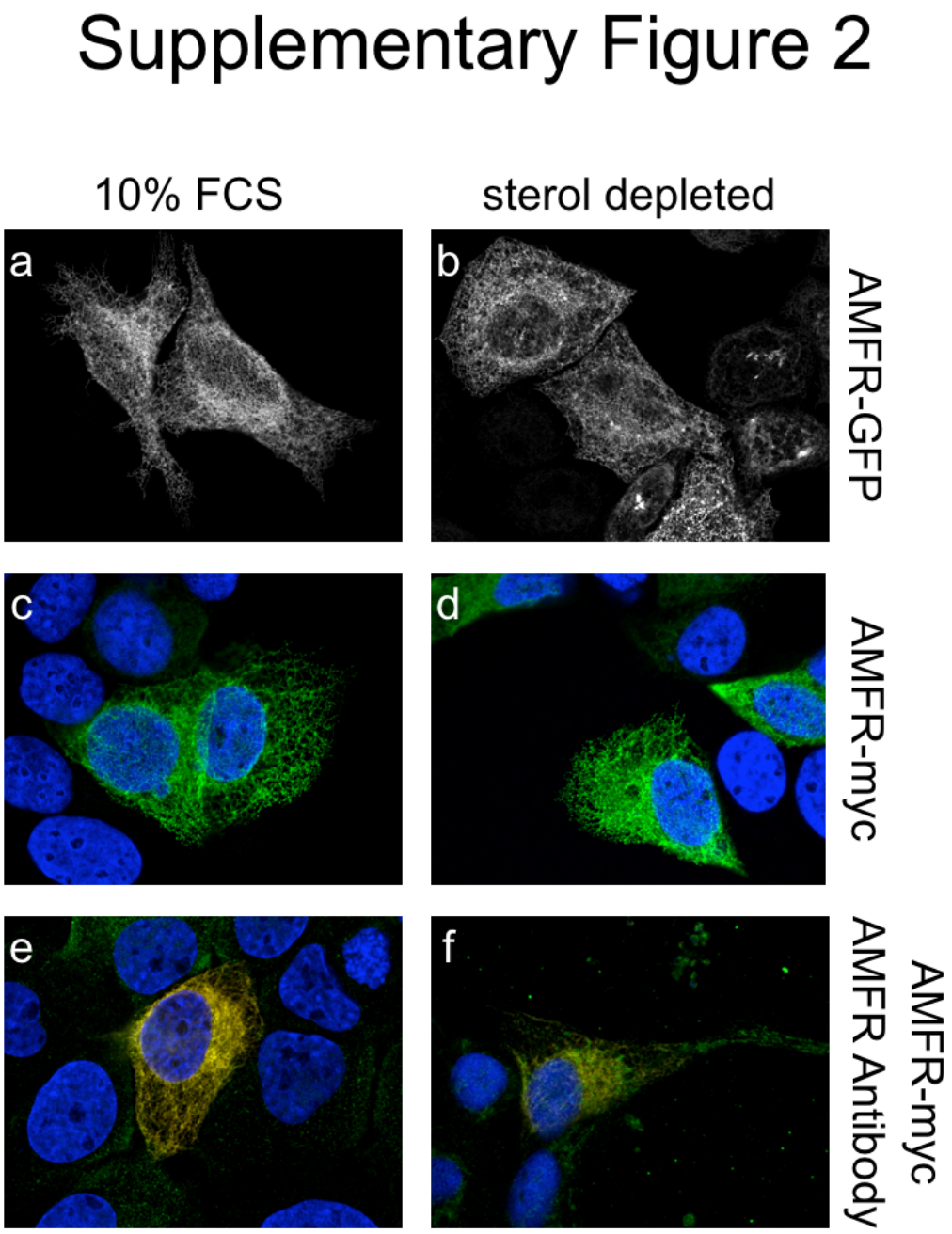
Supplementary Figure 2
10% FCS
sterol depleted
a
b
c
d
e
f
AMFR-GFP
AMFR-myc
AMFR-myc
AMFR Antibody

Figure 5.7:

6 Discussion

6.1 Definition of the question and formulation of the hypothesis

Excess of cholesterol is an important cause of complex diseases such as arteriosclerosis, heart attack and stroke. In physiological amounts, cholesterol is an essential constituent of mammalian cell membranes, which changes the fluidity of membranes and serves as a signaling molecule. Changes in the cholesterol concentration of cell membranes have important consequences for membrane ruffling, endocytosis and cellular motility.

The rate-limiting enzyme of cholesterol production is the 3-hydroxy-3-methylglutaryl-CoenzymeA-reductase (HMGCR), which is located in the membrane of the smooth endoplasmic reticulum (ER). Newly synthesized cholesterol leaves the ER rapidly via vesicular and non-vesicular traffic to all membranous compartments of the cell, leaving relatively low levels of cholesterol in the ER. Its primary site of accumulation is the plasma membrane (PM), where 85% of all unesterified cholesterol is stored. On the beginning of my thesis was a question: How can a cell "know" its overall cholesterol content and adjust its cholesterol production according to it?

We postulated an information relay from the PM, where cholesterol levels are highest, to the ER, where cholesterol is produced. We speculated that this information relay is achieved by vesicular transport of either a yet to be identified cue, or cholesterol itself. Our hypothesis was backed-up by two facts: Cholesterol-

dependent vesicular transport has been shown to play an important role in transcriptional control of cholesterol homeostasis: Up-regulation of HMGCR is dependent on the COP-II mediated vesicular transport of the SREBP/Scap complex from the ER to the Golgi (Goldstein et al., 2006). The second fact that backed-up our hypothesis was the dual role of AMFR. AMFR acts as a receptor of AMF that is internalized via a clathrin-independent, dynamin-dependent pathway (Benlimame et al., 1998) (Kojic et al., 2007)(Kojic et al., 2008). In addition, AMFR acts as an E3 ligase that targets HMGCR for degradation in a cholesterol dependent manner.

We therefore asked ourselves: Is endocytosis a major control mechanism of HMGCR regulation? If so, which endocytic pathway is involved and which molecular players are required? Finally, we wondered whether either AMFR itself or a factor that was co-internalized with AMFR could be involved in cholesterol sensing?

Is endocytosis a means to regulate HMGCR degradation?

In order to investigate HMGCR dynamics, cells were grown in the presence of an inhibitor of de novo cholesterol synthesis (mevastatin) without external cholesterol, thus inducing HMGCR levels to be elevated drastically. When cholesterol was added to the medium, HMGCR levels dropped rapidly.

Small molecule inhibitors

The most straightforward tool to test the involvement of general mechanisms was the use of small molecule inhibitors. We induced a collapse of the Golgi complex into the ER (Brefeldin A), the depolymerization of microtubuli (Nocodazole), the inhibition of dynamin-dependent vesicle fission (Dynasore), or the inhibition of tyrosine kinases (Genistein). Depolymerization of microtubuli did not influence HMGCR levels when compared to control treatment. Brefeldin A, Dynasore and Genistein induced different degrees of cholesterol-independent degradation of

HMGCR. It is known that the Golgi (Brefeldin A) is required for processing the transcription factor of HMGCR - and all other genes required for cholesterol production; a collapsed Golgi would therefore inhibit transcription of new HMGCR and explain the effect of Brefeldin A. Genistein, a tyrosine kinase inhibitor, reduced HMGCR levels in cholesterol-depleted cells even stronger than Brefeldin A. This is in accordance to reports that HMGCR is degraded and inhibited in various ways upon Genistein treatment (Dreu et al., 2002). Dynasore, a inhibitor of dynamin, enhanced cholesterol-independent degradation of HMGCR to a similar extent as Brefeldin A. This result suggests that dynamin-dependent processes are also involved in stabilizing HMGCR.

In cells treated with Brefeldin A, Nocodazole and in controls, addition of cholesterol triggered a rapid degradation of HMGCR. However, in Dynasore and Genistein treated cells, HMGCR degradation could not be further enhanced by addition of cholesterol. This means that even though these drugs induced a reduction of HMGCR signal, cholesterol-induced degradation of HMGCR was blocked in these cells. Interestingly, Brefeldin A did not block cholesterol-induced degradation and might be solely involved in the transcriptional control of HMGCR. The effect of Genistein on cholesterol-triggered degradation of HMGCR has not been reported before, probably because of an overshadowing effect of Genistein on the stability of HMGCR. As there are about 90 tyrosine kinases in the human genome, it is very well possible that the double effect of Genistein of both triggering cholesterol-independent degradation and blocking cholesterol induced degradation results from blocking different tyrosine kinases. The inhibition of cholesterol-triggered degradation of HMGCR by Dynasore is the most striking hint that dynamin-dependent endocytosis is required for HMGCR degradation.

We also tested the drugs chlorpromazine and MG132. Chlorpromazine is an inhibitor of clathrin-mediated endocytosis, but is highly toxic and was therefore

not suited to rather long incubation times. MG132 is a proteasome inhibitor and showed similar results as Dynasore.

Therefore, we concluded that dynamin-dependent endocytosis is a regulator of cholesterol-induced degradation of HMGCR. We further concluded that this process is tyrosine kinases dependent, but independent of the Golgi apparatus and microtubuli.

6.1.1 Define the endocytic pathway that regulates HMGCR degradation

Dominant negative dynamin

Next, we wanted to verify that the block the cholesterol-induced degradation of HMGCR by Dynasore resulted from its inhibition of dynamins. For that, we used a stable cell line that carried an inducible, dominant negative construct of dynamin 2 that has been shown to block dynamin-dependent endocytosis of transferrin and EGF receptor (Damke et al., 1994). dynamin 2 (K44A) showed a slower degradation compared to dynamin 2 (wild type), which was consistent with the results obtained from Dynasore.

SV40 infection

We hypothesized that cholesterol addition to the medium was triggering endocytosis and thereby bringing a HMGCR degradation cue from the PM to the ER. If this would be the case, triggering endocytosis to the ER by other means than cholesterol should also transport components of the cholesterol regulation system to the ER and thereby trigger degradation of HMGCR in starved cells.

We decided to infect cholesterol-depleted cells with SV40 virus. We did so for several reasons: First of all, SV40 is internalized via caveolae/raft dependent endocytosis, that is eventually dependent on the earlier identified dynamin. Secondly, the target of SV40's vesicular journey through the cell is the ER (Pelkmans et al.,

2001). Thirdly, viruses are highly dependent on the host's machinery, and are therefore excellent tools to study cellular functions. So far, no physiological role for the uptake route of SV40 has been postulated, so we wondered if SV40 hijacks an uptake mechanism for measuring the overall cholesterol content of a cell. However, when we infected cholesterol-depleted CV1 cells with purified SV40, we could not see a degradation of HMGCR.

There are several problems related to this experiment: (i) We had to use purified SV40 particles because the serum in SV40 stock would have otherwise triggered degradation. This led to (ii) reduced infection in CV-1 cells from virtually 100% to 70-80% (iii) it is not clear if the membrane turnover that is induced by SV40 is enough to trigger HMGCR degradation to an extent that is not compensated by HMGCR synthesis. (iv) it is known that internalized cargo undergoes massive sorting events; therefore the lipid composition of SV40 might change such that eventual degradation triggers are lost.

Taken together, the result obtained by the SV40 transfection suggests that caveolae dependent endocytosis is not strongly controlling the HMGCR levels. However, due the above listed caveats of our experiments, a more rigorous test should be applied, e.g. influence of knock down of components important for caveolae dependent endocytosis on the dynamics of HMGCR levels.

6.1.2 Identify molecular players of HMGCR regulation

In order to genetically identify genes involved in HMGCR degradation, we performed RNAi-mediated knockdown of 18 genes that were either known regulators of HMGCR or involved in endocytosis and membrane trafficking. Four genes showed a decreased cholesterol-induced degradation of HMGCR. Out of these four genes, three were positive controls (VCP, Insig 1 & 2) and one was a monomeric adapter protein of clathrin-mediated endocytosis (Eps15). VCP is an ATPase

that plays a role in extracting ubiquitinated HMGCR from membranes during ER associated degradation. Insig1 and 2 are proteins that bind both AMFR and HMGCR thus acting as scaffold proteins for the ubiquitination of HMGCR. Eps 15 is involved in the internalization of several cargos of clathrin mediated endocytosis, notably, it has been suggested to mediate clathrin-dependent uptake of LDL even in the absence of adapter protein 2 (Motley et al., 2003).

Importantly, neither the positive control AMFR - the E3 ligase required to target HMGCR for degradation - nor the candidates dynamin 1 and 2 showed an inhibitory effect of HMGCR degradation. AMFR has been shown to be the E3 ligase for HMGCR in several reports, but RNAi against AMFR is inefficient (Roger Geiger, personal communication) and ubiquitination of HMGCR might not be the rate-limiting factor. Why did neither dynamin1 nor dynamin2 show an inhibitory effect? Besides the possibility that the experiments using dominant-negative dynamin 2 and Dynasore both produced artifacts and dynamin does not play a role in HMGCR degradation, there are also other explanations for this effect. Again, gene knockdown might have been inefficient, but yet another methodological concern was that siRNA treated cells showed different expression levels of HMGCR after sterol depletion. In order to compare the effects between different siRNAs, it was necessary to consider the HMGCR levels before cholesterol add-back, background fluorescence levels and bleaching during the experiment. Normalization to values that are close to background always emphasize technical noise and thus put more uncertainty to such results. Starting levels of HMGCR were lowest upon RNAi against clathrin heavy chain and adapter protein 2 subunit µ. And indeed, also epsin 1, dynamin 1 and dynamin 2 showed reduced levels of HMGCR already before cholesterol addition, which complicated the analysis considerable.

6.1.3 Is AMFR transported in a cholesterol dependent manner?

Already from a very early point in the project, AMFR was a prime candidate as a marker for endocytosis events in the regulation of HMGCR levels. AMFR was an attractive candidate for at least two reasons: (i) It is endocytosed from the PM to the ER. (ii) It acts as the E3 ligase that ubiquitinates HMGCR.

Therefore, we tested the localization of AMFR in different cholesterol conditions. We stained against endogenous AMFR with a monoclonal antibody showing that endogenous levels of AMFR are very low in A431 and Hela cells. So, we over-expressed AMFR-GFP and AMFR-myc, which resulted in an exclusive localization of AMFR in the ER independently of the cholesterol state of the cells. There are in principle three interpretations possible: Either overexpression of AMFR led to artificial localization, or this shuttling mechanism is only present in specific cell lines, or AMFR does not substantially change its localization upon cholesterol-depletion.

Overexpression is known to produce artifacts. It has been shown that overexpression of HMGCR led to a saturation of the degradation machinery. Only when Insig and HMGCR were co-expressed, HMGCR could be efficiently degraded. Similarly, a factor that facilitates the transport of AMFR could be saturated in AMFR over-expressing cells and thus lead to the retention of AMFR in the ER.

What about the possibility that AMFR is only shuttled in certain cell types? It has been reported that expression of AMF and AMFR is highest in certain metastatic cancer cell lines stimulating cell motility and metastasis. Blocking of AMF internalization has been shown to inhibit motile behavior (Watanabe et al., 1996) and injection of an antibody that competes with AMF for AMFR binding stimulates cell motility has been shown to promote metastasis in rodents (Nabi et al., 1990). This autocrine motility loop of AMF excretion and uptake via AMFR has even been proposed as a delivery route for cancer drugs because it is boosted

specifically in malignant cells (Kojic et al., 2008). This specificity to malignant cells is in conflict with the fact that basically all nucleated cells show elevated HMGCR levels upon cholesterol-depletion and makes it rather unlikely that both phenomena are regulated by the same mechanism.

The most likely explanation is that AMFR does not change its localization in a cholesterol-dependent manner. In pull down experiments, AMFR has been shown to bind to Insigs using pull down experiments (Song et al., 2005). Even though a pull-down experiment cannot quantify how much of a certain protein is bound and cannot tell anything about the non-bound pool of protein, it showed that a certain pool always resided in the ER. There is also a report that a truncated version of AMFR that did not contain the proposed receptor domain could still ubiquitinate another transmembrane protein, KAI1 (Tsai et al., 2007). It is therefore likely, that AMFR does not require its receptor domain in order to degrade HMGCR, which in turn would argue against the model of a localization loop.

Therefore, we reasoned that AMFR does not shuttle between the ER and the PM in a cholesterol-dependent manner.

6.2 Conclusion and Outlook

How does a cell sense its overall cholesterol levels? We have gathered evidence that it uses a vesicular mechanism that is dynamin - and possibly Eps 15 - dependent. It seems unlikely, that AMFR shuttles between the PM and the ER in a cholesterol dependent manner. We also were not able to trigger degradation of HMGCR when we infected CV1 cells with SV40 and therefore propose that HMGCR level regulation is caveolin independent. Therefore, a molecular mechanism for HMGCR regulation via endocytosis is still to be shown. In the future it will be interesting to (i) further define the endocytic pathway downstream of dynamin that regulates HMGCR (ii) decipher the function of the different domains of AMFR, (iii) to

identify the tyrosine kinases that regulate HMGCR.

Eps 15 and other dominant negative constructs

Dominant negative dynamin 2 could confirm dynamin as being involved in cholesterol-triggered HMGCR degradation, recapitulating a result that was at first obtained by the small molecule inhibitor Dynasore. RNAi data suggest an effect of Eps15, a protein that is involved in clathrin-mediated dynamin-dependent endocytosis. Expression of dominant negative Eps15 therefore suggests itself as a means to confirm the RNAi data.

We have earlier tried to transiently over-expressed GFP-tagged dominant negative constructs in an image-based format. The rationale behind was that we would identify the transfected cells by their GFP fluorescence and would then measure HMGCR intensity using a monoclonal antibody against HMGCR. Similar experiments are frequently used in the endocytosis field. However, when we transfected A431 cells with an "empty" GFP vector and switched the cells to serum-free medium supplemented with mevastatin, the GFP expression dropped drastically. This effect is not surprising, because inhibition of cholesterol - and isoprenyl - synthesis will reduce the metabolism in the cells. This effect was even more pronounced for the dominant negative constructs. The reason for this is that dominant negative constructs often show a cytotoxic effect; therefore cholesterol depletion put a double selection on the cells. As a consequence, cholesterol depletion in transiently transfected cells resulted in a small number of GFP expressing cells that contained strongly reduced levels of HMGCR. This setup did not allow for further analysis.

It might therefore be necessary to generate a cell line bearing an inducible Eps15 (Y850F). This approach was already successfully applied for dynamin 2. In a cell line, virtually 100% of the cells express the construct of interest; this allows bulk

measurements like SDS PAGE, which can detect small amounts of protein with higher sensitivity than indirect fluorescence of an antibody stain.

6.2.1 Dissect the role of AMFR

As mentioned earlier, AMFR has been reported to fulfill at least two roles: (i) AMFR is the receptor of AMF, and expression of both AMF and AMFR are associated with higher motility in cultured cells and bad survival prognosis and metastasis in patients. AMF is a cytokine with several functions in embryonic development and metastasis (Fairbank et al., 2009). Incubation with a monoclonal antibody against AMFR could trigger metastatic behavior of F16-F1 cells in rodents. (ii) AMFR has a E3 ligase activity. AMFR has been reported to be involved in the degradation of several proteins like the metastasis suppressor KAI1 (Tsai et al., 2007), the cystic fibrosis transmembrane regulator CFTRDeltaF508 (Morito et al., 2008), HMGCR and Insig1.

The most evident thing to do would be to dissect which domain of AMFR is required for its various functions. So far, we did not have sufficient siRNA knockdown to see a block in HMGCR degradation. This is also a prerequisite for rescue studies, and ideally we would even use a knockout cell line. Fortunately, there is a conditional knockout ES cell line available that would allow expression of different domains of AMFR in order to investigate its single parts. It has been shown that a truncated version AMFR that lacked its receptor domain was still able to ubiquitinate the metastasis suppressor KAI1. It would be very interesting if this truncated version can also degrade HMGCR. Also, it is not known if binding of AMFR to Insigs is required to ubiquitinate HMGCR. Expression of a binding-deficient version of AMFR could answer this question.

6.2.2 Identify the molecular players of the Genistein phenotype

Genistein is a tyrosine kinase inhibitor reported to decrease cholesterol synthesis and esterification but increase expression of the LDL-receptor (Dreu et al., 2002). In this study, we also found that Genistein decreased degradation of HMGCR. However, the tyrosine kinases that lead to these effects are not known.

We have manipulated a Bacterial Artificial Chromosome (BAC) containing 140kb upstream and 10kb downstream of HMGCR and engineered a GFP to the C-terminus of the protein-product. A stable cell line bearing this BAC served as a reporter of HMGCR levels because HMGCR-GFP was expressed and degraded like endogenous HMGCR. This made it possible to monitor HMGCR levels in living, single cells.

Using this modified BAC, we would propose to assay Genistein's effect on HMGCR expression. For this we propose the knockdown of all tyrosine kinases followed by cholesterol depletion in A431-HMGCR-GFP cells. Knockdown of tyrosine kinases that are important for HMGCR expression will result in lower levels of HMGCR-GFP in reporter cells. A screen for HMGCR expression involves less handling steps. It is therefore faster and less error-prone. As a consequence it will be easier to interpret than a screen for HMGCR degradation.

In a second step extent our analysis to a assay to measure the degradation of HMGCR. Finally, we would screen for a larger gene set.

Comparative siRNA screens

When A431-HMGCR-GFP cells are cholesterol depleted, HMGCR-GFP expression depends not only on cholesterol-specific processes, but also on many general processes. These general processes are transcription, RNA processing, RNA maturation, RNA export, mRNA stability, translation, folding and protein stability to name a few. One possibility to enrich for specific hits and identify general mechanisms of protein expression is to perform a comparative screen for the expression

of a non-cholesterol related gene.

For simplicity, this control screen would express GFP with an inducible promoter that is independent on SRE. Using the SRE-independent expression, the cell number in the well and the strength of expression of the control-GFP reporter of every siRNA could be compared to the cell number and HMGCR-GFP signal of the same siRNA. Thus, the knockdown of a gene that influences general protein expression would result in reduced GFP levels of both HMGCR-GFP cells but also in GFP cells. However, knockdown of a gene that specifically regulates HMGCR will only reduce the fluorescence HMGCR-GFP cells but not in (control) GFP cells. For the quest of finding regulators of HMGCR, only those genes that result in high GFP and low HMGCR-GFP expressing cells will be considered.

Eventually, one could also think of adding a construct containing mCherry behind a SRE promoter into the A431-HMGCR-GFP cells as a transcriptional reporter. This would allow distinguishing between HMGCR stability and HMGCR transcription. We think a comparative GFP-reporter screen is the basis for an interpretation for cholesterol triggered HMGCR degradation.

Yet another comparative screen would certainly be interesting: In our screens, we added cholesterol into the medium; this is thought to resemble cholesterol that is newly synthesized and rapidly inserted directly into the membranes. In contrast to that, cholesterol from the serum is taken-up via LDL particles and known to require clathrin-dependent endocytosis and leave late endosomes/ lysosomes via NPC 1&2. It would therefore be interesting which genes are shared by both regulation mechanisms and which other genes are specific for the respective cholesterol sources.

Image analysis

It is worthwhile to think more carefully about possible directions of an image-based analysis. In our lab, there are several projects that focus on the influence of

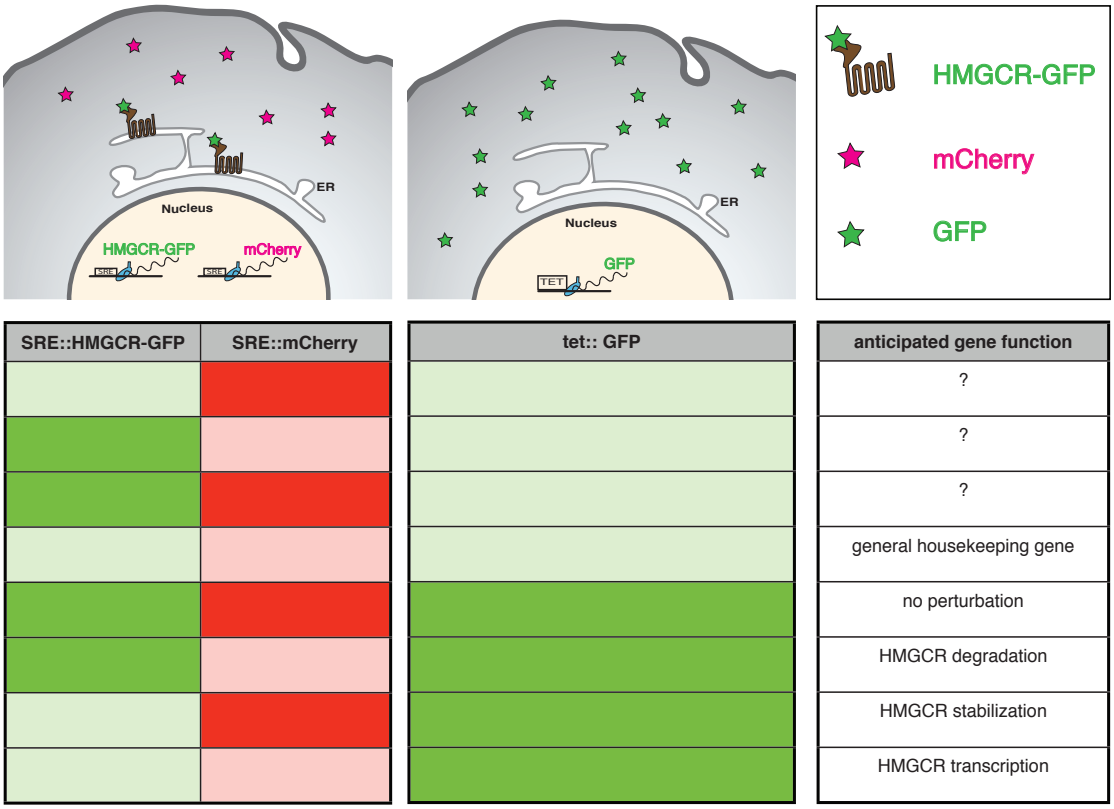

Figure 6.1: A comparative screen requires two cell-lines to be screened. One cell line contains a GFP reporter under an inducible promoter (tet). The other cell line bears HMGCR-GFP and mCherry under its endogenous promoter (SRE). Knockdown of a gene that is required for general protein expression will result in low GFP expression levels of all three reporters. Knockdown of a gene involved in HMGCR up-regulation will results in lower HMGCR-GFP levels and lower mCherry levels. Knockdown of a gene involved in HMGCR degradation will result in high HMGCR levels, but low mCherry levels. Knockdown of a gene involved in the stabilizing HMGCR will result in low HMGCR-GFP levels but high mCherry levels.

cellular context on single cell reaction e.g. (Snijder et al., 2009). To date, we have not investigated the influence of factors like local cell density, or cell-cycle state on HMGCR-GFP signal. These will certainly influence our understanding of the effect of a specific siRNA on our readout.

HMGCR-GFP has some specifics in respect to the signal, because HMGCR-GFP is not uniformly distributed throughout the cell, but localizes into the ER and is enriched in punctuate structures within the ER. We did not investigate on the properties of the subdomain of punctae, but we suggest that the dynamics of the punctae might be different from the HMGCR-GFP in the rest of the ER. Also, analysis of the size and number of punctae might provide additional information, especially for the interpretation of different RNAi phenotypes. In order to reduce false positives and false negatives and enrich for specific hits in a screen with a large number of genes, it will be of vital importance to investigate the local cell environment and the influence of the punctate structures of HMGCR on the quantification.

Suggestions for an up-scaled screen

In order to perform a screen with a larger number of siRNAs, a number of improvements should be made.

It is imperative to use 384 well plates instead of 96 well plates. The advantages are severalfold: There is a certain degree of variation between different plates independent of the number of wells; using 384 well plates is cheaper and requires less space.

One impression that we had is that the position of a well on plate has an influence on the signal intensities; therefore it might be necessary to randomize the different siRNA targeting one gene to different positions on the plates.

In order to quantify signals with a high reliability, we think it would be beneficial to add a “signal standard” in every well. Fluorescent particles with known size

and known quantum yield would provide an in-well calibration of signals and thus compensate for uneven illumination and for fluctuations of the light source.

Finally, up to now, we did all washing steps by hand. This was a minor problem in 96 well plates, but for 384 well plates, we would suggest the find an automated solution.

Taken together, I strongly believe that we are on the verge for a new era that will allow the identification of main molecular players in HMGCR regulation. Using high-throughput methods in combination with careful comparative analysis like the improvements I mentioned above might allow us to enter these horizons.

6.3 Bibliography

N. Benlimame, P. Le, and I. Nabi. Localization of autocrine motility factor receptor to caveolae and clathrin-independent internalization of its ligand to smooth endoplasmic reticulum. *Mol Biol Cell*, 9(7):1773–86, Jul 1998. URL http://www.ncbi.nlm.nih.gov/entrez/query.fcgi?cmd=Retrieve&db=PubMed&dopt=Citation&list_uids=9658170%20. Journal Article United states.

H. Damke, T. Baba, D. Warnock, and S. Schmid. Induction of mutant dynamin specifically blocks endocytic coated vesicle formation. *J Cell Biol*, 127 (4):915–34, Nov 1994. URL http://www.ncbi.nlm.nih.gov/entrez/query.fcgi?cmd=Retrieve&db=PubMed&dopt=Citation&list_uids=7962076.

L. D. Dreu, L. Wilcox, J. Edwards, and M. Huff. Soya phytoestrogens, genistein and daidzein, decrease apolipoprotein b secretion from hepg2 cells through multiple mechanisms. *Biochemical ...*, Jan 2002. URL http://www.ncbi.nlm.nih.gov/pmc/articles/PMC1222800/.

M. Fairbank, P. St-Pierre, and I. R. Nabi. The complex biology of autocrine motility factor/phosphoglucose isomerase (amf/pgi) and its receptor, the gp78/amfr e3 ubiquitin ligase. *Mol Biosyst*, 5(8):793–801, Aug 2009. doi: 10.1039/b820820b. URL http://www.rsc.org/publishing/journals/MB/article.asp?doi=b820820b.

J. Goldstein, R. DeBose-Boyd, and M. Brown. Protein sensors for membrane sterols. *Cell*, Jan 2006. URL http://linkinghub.elsevier.com/retrieve/pii/S0092867405014637.

L. Kojic, B. Joshi, P. Lajoie, P. Le, M. Cox, D. Turbin, S. Wiseman, and I. Nabi. Raft-dependent endocytosis of autocrine motility factor is phosphatidylinositol 3-kinase-dependent in breast carcinoma cells. *J Biol Chem*, 282(40):29305–13, Oct 2007. URL `http://www.ncbi.nlm.nih.gov/entrez/query.fcgi?cmd=Retrieve&db=PubMed&dopt=Citation&list_uids=17690101%20`.

L. Kojic, S. Wiseman, F. Ghaidi, B. Joshi, H. Nedev, H. Saragovi, and I. Nabi. Raft-dependent endocytosis of autocrine motility factor/phosphoglucose isomerase: a potential drug delivery route for tumor cells. *PLoS ONE*, 3(10):e3597, 2008. doi: 10.1371/journal.pone.0003597. URL `http://www.ncbi.nlm.nih.gov/entrez/query.fcgi?cmd=Retrieve&db=PubMed&dopt=Citation&list_uids=18974847`.

D. Morito, K. Hirao, Y. Oda, N. Hosokawa, F. Tokunaga, D. M. Cyr, K. Tanaka, K. Iwai, and K. Nagata. Gp78 cooperates with rma1 in endoplasmic reticulum-associated degradation of cftrdeltaf508. *Mol Biol Cell*, 19(4):1328–36, Apr 2008. doi: 10.1091/mbc.E07-06-0601. URL `http://www.molbiolcell.org/cgi/content/full/19/4/1328`.

A. Motley, N. Bright, and M. Seaman. Clathrin-mediated endocytosis in ap-2-depleted cells. *Journal of Cell ...*, Jan 2003. URL `http://jcb.rupress.org/cgi/content/abstract/162/5/909`.

I. R. Nabi, H. Watanabe, and A. Raz. Identification of b16-f1 melanoma autocrine motility-like factor receptor. *Cancer Res*, 50(2):409–14, Jan 1990.

L. Pelkmans, J. Kartenbeck, and A. Helenius. Caveolar endocytosis of simian virus 40 reveals a new two-step vesicular-transport pathway to the er. *Nat Cell Biol*, 3(5):473–83, May 2001. URL `http://www.ncbi.nlm.nih.gov/entrez/query.`

fcgi?cmd=Retrieve&db=PubMed&dopt=Citation&list_uids=11331875%20. Journal Article England.

B. Snijder, R. Sacher, P. Rämö, E.-M. Damm, P. Liberali, and L. Pelkmans. Population context determines cell-to-cell variability in endocytosis and virus infection. *Nature*, 461(7263):520–3, Sep 2009. doi: 10.1038/nature08282. URL http://www.nature.com/nature/journal/v461/n7263/full/nature08282.html.

B. Song, N. Sever, and R. DeBose-Boyd. Gp78, a membrane-anchored ubiquitin ligase, associates with insig-1 and couples sterol-regulated ubiquitination to degradation of hmg coa reductase. *Mol Cell*, 19(6):829–40, Sep 2005. URL http://www.ncbi.nlm.nih.gov/entrez/query.fcgi?cmd=Retrieve&db=PubMed&dopt=Citation&list_uids=16168377%20.

Y. C. Tsai, A. Mendoza, J. M. Mariano, M. Zhou, Z. Kostova, B. Chen, T. Veenstra, S. M. Hewitt, L. J. Helman, C. Khanna, and A. M. Weissman. The ubiquitin ligase gp78 promotes sarcoma metastasis by targeting kai1 for degradation. *Nat Med*, 13(12):1504–9, Dec 2007. doi: 10.1038/nm1686. URL http://www.nature.com/nm/journal/v13/n12/abs/nm1686.html.

H. Watanabe, K. Takehana, M. Date, T. Shinozaki, and A. Raz. Tumor cell autocrine motility factor is the neuroleukin/phosphohexose isomerase polypeptide. *Cancer Res*, 56(13):2960–3, Jul 1996. URL http://cancerres.aacrjournals.org/content/56/13/2960.long.

7 Material and methods

7.1 Materials

Gifts

Many materials were generous gifts from various people. Most of those gifts were donations within the institute and although they were mostly everyday materials and equipment, they have been indispensable for this project. Some crucial gifts are mentioned here as pars pro toto.

Calnexin antibody was a kind gift from Ari Helenius (ETH, Zurich). 3F3A Antibody was a generous gift from Ivan Nabi (University of British Columbia, Canada). Imaging-DMEM without Riboflavin and Phenolred was provided by Daniel Gerlich (ETH, Zurich). Hela cells bearing inducible dynamin 2 wild type or dynamin K44A dominant negative were a gift from Sandra Schmid (The Scripps Research Institute, USA). The LAP-cassette was provided by Ina Poser (Max Planck Institute for Molecular Cell Biology and Genetics, Germany)

Table 7.1: Antibodies

Antibody	Donor species	Supplyer	Cat. No
A9 HMGCR	mouse, monoclonal IgG	ATCC	CRL-1811
HMGCR	rabbit, polyclonal	upstate	07-572
AMFR-, C-Terminal	rabbit, polyclonal	Abgent	AP2162b
gp78/ AMFR	rat, monoclonal IgM	Nabi lab	3F3A
beta-tubulin	rabbit, polyclonal	abcam	ab6046
Anti c-Myc (A-14)	mouse	Santa Cruz	sc-789
HA-probe (Y-11)	rabbit, polyclonal	Santa Cruz	sc-805
Caveolin N20	rabbit, polyclonal	Santa Cruz	sc-894
calnexin	rabbit, polyclonal	Helenius lab	-

Table 7.2: Chemicals

Substance	Producer	Cat. No.
Immobilon Western HRP Substrate	millipore	WBKLS0500
PageRuler Prestained Protein Ladder plus	Fermentas	SM 1811
Geneticin	Gibco	11811-031
Complete Protease Inhibitor Cocktail	Roche	11 873 580 001
Mevastatin	Sigma	M2537
Brefeldin A	Sigma	B7651
Nocodazole	Sigma	M1404-2MG
Dynasore	Asinex	BAS 00597512
Amiloride	Sigma	A7410
MG132	Sigma	C2211
Cholesterol powder	Sigma	C3045
25-Hydroxycholesterol	Sigma	H1015
Hoechst 33342	Sigma	14533-100MG
QuantiTect Rev. Transcription Kit	Qiagen	205311
Precisor High-Fidelity DANN Polymerase	BioCat	1706-250-BL
L-Arabinose	Sigma	A3256-100G
Lipofectamine 2000	Invitrogen	11668019
DMEM	Gibco	41965
DMEM w/o Riboflavin w/oPhenol red	Gibco	costume composition: 041-96205M
Hygromycin	Invitrogen	10687010

Table 7.3: siRNAs used for candidate screen

Gene Symbol	Full Gene Name	RefSeq Number (Oligo1)	RefSeq Number (Oligo2)	RefSeq Number (Oligo3)
AMFR	autocrine motility actor receptor	NM_001144	NM_001144	NM_001144
AP2B1 AP2B1	adaptor-related protein complex 2, beta 1 subunit	NM_001030006	NM_001030006	NM_001030006
AP2M1 AP2M1	adaptor-related protein complex 2, mu 1 subunit	NM_001025205 NM_001025205	NM_001025205 NM_001025205	NM_001025205 NM_001025205
CLTA	clathrin, light chain (Lca)	NM_001076677	NM_001076677	NM_001076677
CLTC	clathrin, heavy chain (Hc)	NM_004859	NM_004859	NM_004859
DNM2	dynamin 2	NM_004945	NM_004945	NM_004945
EPN1	epsin 1	NM_013333	NM_013333	NM_013333
EPS15	epidermal growth factor receptor pathway substrate 15	NM_001981	NM_001981	NM_001981
GGA2	golgi associated, gamma adaptin ear containing, ARF binding protein 2	NM_015044	NM_015044	NM_015044
GGA3	golgi associated, gamma adaptin ear containing, ARF binding protein 3	NM_138619	NM_138619	NM_138619
INSIG1	insulin induced gene 1	NM_198337	NM_198337	NM_198337

INSIG2	insulin induced gene 2	NM_016133	NM_016133	NM_016133
NPC1	Niemann-Pick disease, type C1	NM_000271	NM_000271	NM_000271
SNX9	sorting nexin 9	NM_016224	NM_016224	NM_016224
VCP	valosin-containing protein	NM_007126	NM_007126	NM_007126
GRAF1				
DMN1				

Table 7.4: Primers for ABCA1

BAC ABCA1	clone: RPCIB753H0332Q (imaGenes)
ABCA1_FLAP_ forward_N-Term:	GCCTTCCAGGGCTCCCGAGCCACACGCTGGG GGTGCTGGCTGAGGGAACATGGTGTCCAAGGGCGAGGAACTG
ABCA1_FLAP_ reverse_N-Term:	AAAGTGAGGTTCTTCCACAGCAGCAACCTCAGCTGA GGCCAACAAGCCATGGCCCTGGGCAGGTCGTCGGTCAG
seq 5' of stop	CATATCCGGACCACACAGTC
seq 3' of stop	CGTAGCTCCTAGCCTGCTGT
ABCA1_FLAP_ forward_CTerm	CAGTTCTCACATCTTTTCTACAGGATGAGAAA GTGAAAGAAAGCTATGTAGATTATGATATTCCAACTACTG
ABCA1_FLAP_ reverse_CTerm	GAAAGTCTAGTTCCTCTTTACTTTCAG CCACCCCGTATGAACAGGATTCTTCAGAAGAACTCGTCAAGAAG
seq 5' of ATG	GCCAAGGACCAAAGTGATGATG
seq 3' of ATG	TGGCTCTTTTCTCCACAACA

Table 7.5: Primers for HMGCR

BAC HMGCR	clone: RPCIB753F01654Q (imagenes)
ABCA1_FLAP_ forward_N-Term:	GCCTTCCAGGGCTCCCGAGCCACACGCTG GGGGTGCTGGCTGAGGGAACATGGTGTCCAAGGGCGAGGAACTG
ABCA1_FLAP_ reverse_N-Term:	AAAGTGAGGTTCTTCCACAGCAGCAACCTCAG CTGAGGCCAACAAGCCATGGCCCTGGGCAGGTCGTCGGTCAG
seq 5' of stop	CATATCCGGACCACACAGTC
seq 3' of stop	CGTAGCTCCTAGCCTGCTGT
ABCA1_FLAP_ forward_CTerm	CAGTTCTCACATCTTTTCTACAGGATGAGAAAG TGAAAGAAAGCTATGTAGATTATGATATTCCAACTACTG
ABCA1_FLAP_ reverse_CTerm	GAAAGTCTAGTTCCTCTTTACTTTCAGCCACCCCG TATGAACAGGATTCTTCAGAAGAACTCGTCAAGAAG
seq 5' of ATG	GCCAAGGACCAAAGTGATGATG
seq 3' of ATG	TGGCTCTTTTCTCCACAACA

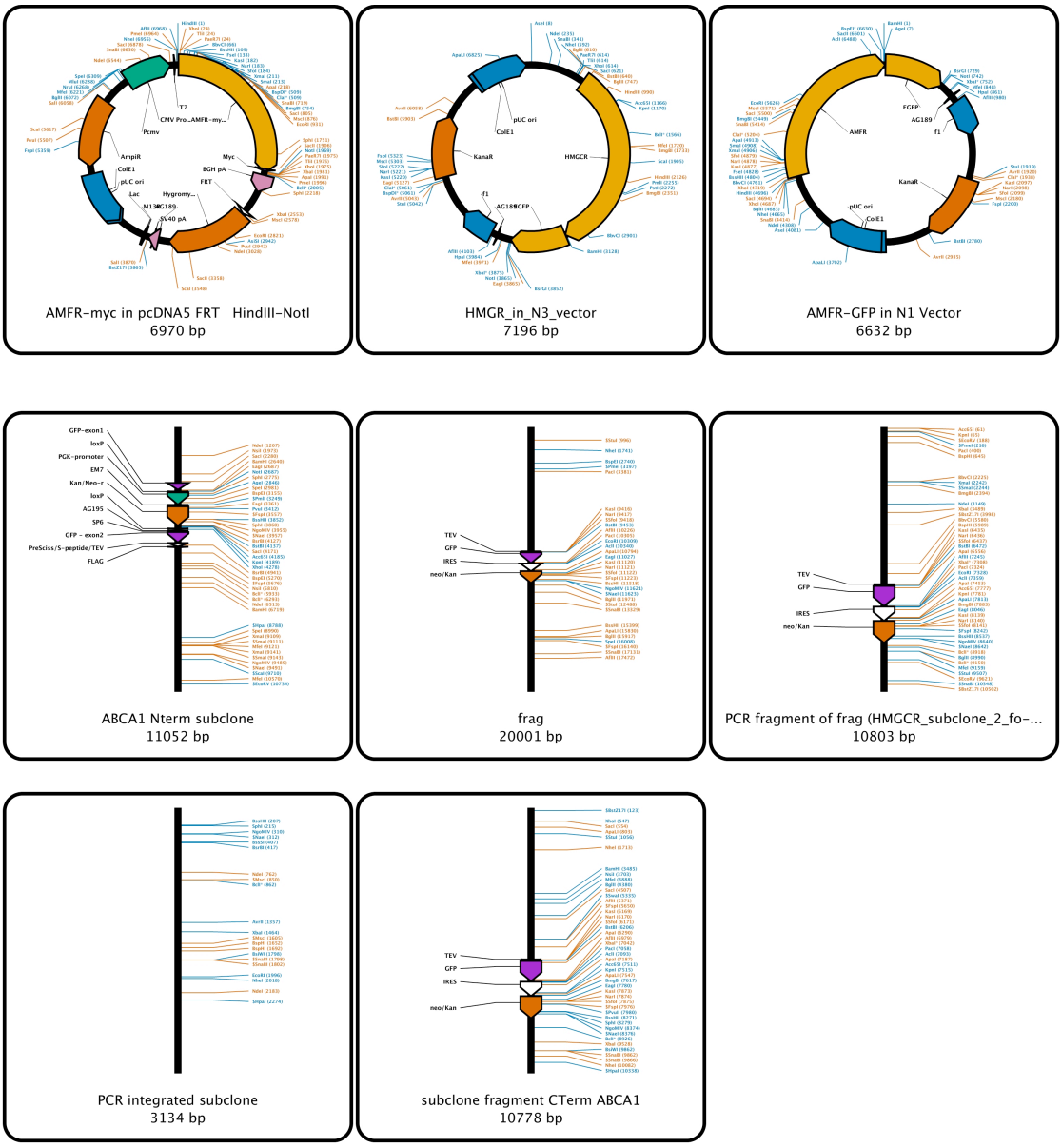

Figure 7.1: Vectormaps of generated constructs

7.2 Methods

7.2.1 Cloning of HMGCR-GPF, AMFR-GFP and AMFR-myc

AMFR, also called gp78, cDNA was bought from imaGenes GmbH. A myc tagged version of AMFR in a pcDNA5 Vector, was constructed as follows. A primer pair with a forward primer, having an additional HindIII restriction site at the 5' end of AMFR ("HindIII_Myc-AMFR_forw" AAGCTTATGGAGCAGAAAC-TCATCTCTGAAGAGGATCTGATGCCGCTGCTCTTCCTCGAGCGC) and a reverse primer containing the sequence for myc and a Not1 restriction site ("AMFR-stop_myc_NotI" GCGGCCGCCAGATCCTCTTCAGAGATGAGTTTCTGCT-CGGAGGTCTGCTGCTTCTGAAGC) was used to amplify DNA from the cDNA plasmid. The resulting PCR product was ligated into the vector using the introduced NotI and HindIII sites. AMFR-GFP was cloned utilizing a N1 vector from Clonetech. Following primers were used: "AMFR_forw_HindIII" ATAAA-GCTTCG ATGCCGCTGCTCTTCCTCGAGC and "AMFR_rev-STP_BamHI" GGATCCGGAGG TCTGCTGCTTCTGAA

HMGCR cDNA was bought from imaGenes GmbH. HMGCR-GFP containing a GFP-tag at the C-terminal of HMGCR was constructed using a Clonetech N3 Vector as follows. A primer pair amplifying HMGCR from a cDNA plasmid was designed such that the forward primer for the 5' contained an additional Sca1 restriction site and the 3' primer did not contain a STOP but an in-frame BamH1 restriction site. ("Sca1-HMGR for" GAGCTCATGTTGTCAAGACTTTTTCGA-ATG; "HMGR rev. -STOP BamH1": GGATCCGGCTGTCTTCTTGGTGCA-A). DNA was amplified and cloned in the target vector using the given restriction sites and standard cloning procedures.

7.2.2 Insertion of a LAP cassette into HMGCR on a BAC

The Bacterial Artificial Chromosome (BAC) genomic clones for ABCA1 and HMGCR, containing the full genomic sequences of the respective genes including more than 30 kb up- and downstream of the respective start and stop codons were ordered from ImaGenes. As these BACs were more than 200 kb in size, traditional restriction-and-ligation cloning methods were not applicable. Therefore, a recombination method as described in (Poser, Sarov et al. 2008) using a "localization and affinity purification"-tag (LAP-tag) (Cheeseman and Desai 2005) was employed. Procedures were done according to the manual "Gene Bridges K001 Q E BAC Modification Kit-version2.6-2007".

The LAP-tag cassette contains the gene coding for enhanced Green Fluorescence Protein (eGFP), a S-peptide and a Kanamycin/Neomycin resistance. This cassette was PCR amplified with primers that had 75 nucleotide overhangs, which would later allow homologous recombination of the LAP-cassette into the C-terminus or N-terminus of HMGCR and ABCA1, respectively. The PCR was done using Precisor High-Fidelity DANN Polymerase utilizing the supplied GC buffer for difficult reactions. The thermo-cycling machine was programmed as follows: 2min 98^{o}C; 5x[30 sec 98^{o}C; 40 sec 57^{o}C; 60 sec 72^{o}C]; 30x [30 sec 98^{o}C; 40 sec 65^{o}C; 60 sec 72^{o}C]; leave at 4^{o}C.

Bacteria containing the BAC were co-transformed with the Red/ET vector (Gene Bridges BAC Modification Kit), which contained the genes required for performing the recombination reaction following the supplier's manual. Then, expression of the recombination genes was turned on by a temperature switch and addition of L-arabinose followed by electroporation to transform the bacteria with the PCR product explained before. Single bacteria colonies were picked and DNA sequencing of recombination joints confirmed successful recombination. The verified BAC containing the LAP tag was stably transfected into A431 cells, its inte-

gration was checked by colony PCR, western blot analysis and visible inspection under a fluorescence light microscope.

7.2.3 Cell Culture

Monolayers of 80-90% confluent A431 and HeLa cells were maintained in cell culture at 37^{o}C and 5% CO2, and in high glucose Dulbecco's modified Eagle medium (DMEM) (Gibco) supplemented with 10% fetal calf serum (FCS) and 2% Glutamax (Invitrogen). The medium for A431 with the stably integrated BAC-HMGCR-GFP was additionally supplemented with 500µg/mL G418 (Gibco). Inducible dynamin 2 (dominant negative and wild type) cells were cultured as previously reported (500µg/mL G418, 1µg/mL Tetracycline) (Damke, Gossen et al. 1995).

FAK -/- mouse fibroblasts were cultured in Dulbecco's modified Eagle medium (DMEM) (Gibco) supplemented with 10% fetal calf serum (FCS), non-essential amino acids for MEM (Invitrogen) and 2% Glutamax (Invitrogen) as reported in (Sieg, Hauck et al. 1999). FAK rescue cells were kept in Dulbecco's modified Eagle medium (DMEM) supplemented with 10% fetal calf serum (FCS), non-essential amino acids for MEM and 2% Glutamax (Invitrogen) supplemented with Hygromycin B (Invitrogen) (1:300).

7.2.4 Drug Treatments

Cells were washed three times with PBS and switched to DMEM supplemented with Glutamax (Invitrogen) and 25µM mevastatin for 29h. After that cells were pre-incubated with drugs for 45 minutes, before the addition of cholesterol coupled to MβCD (20µg/mL). Concentrations used for the drug treatments were: Amiloride: 10µM; Brefeldin A 5µg/mL; Dynasore: 6µg/mL; Genistein: 100µM; Nocodazole: 1µM; DMSO was adjusted to a final amount of 0.4%. Analysis was either performed using cell fractionation and immunoblot analysis, or image-based

analysis. For details about "Image-based Assays" and "Cell Fractionation and Immunoblot Analysis" see their respective chapters.

7.2.5 Image-based Assays

BAC-HMGCR-GFP based drug assay

20.000 A431 cells that were stably transfected with the BAC-HMGCR-GFP ("A431-HMGCR-GFP cells") were seeded in each well of a 96 well plate. After 24h row B to H was washed 3 times with PBS and switched to DMEM supplemented with Glutamax (Invitrogen) and 25µM mevastatin (final concentration). Cells were switched from standard DMEM to DMEM without Phenolred and without Riboflavin, 2h before image acquisition. After a total of 29h of serum starvation, cells of three wells were incubated with Brefeldin A, Amiloride, MG132, Genistein, Nocodazole and Dynasore for 45 min as described in the section "Drug Treatments". MβCD-Cholesterol was added containing Hoechst 33342 (Sigma) stain (100ng/mL final concentration) and the plate was imaged every 45 minutes using an ImageXpress Micro automated microscope (Molecular Devices) with 10x magnification at 37^{o}C and 5 % CO2. Illumination for the GFP channel was set to 500 milliseconds per image and 9 images were acquired per well.

Antibody based drug assay

20.000 A431 cells were seeded in each well of a 96 well plate. After 24h row B to H was washed 3 times with PBS and switched to DMEM with Glutamax (Invitrogen) supplemented with 25µM mevastatin (final concentration). After 29h of serum starvation, cells of two wells were treated with Brefeldin A, Amiloride, MG132, Genistein, Nocodazole and Dynasore for 45 min. MβCD-Cholesterol was added and cells were fixed every 0.5 hours. Cells were permeabilized and stained with 30µL of pure A9 hybridoma supernatant over night at 4^{o}C. Next day, cells

were washed 3 times with PBS. Secondary goat anti-mouse antibody was diluted 1:400 and cells were incubated for 45 min at room temperature. Finally nuclei were stained with DAPI (1:1000) and plates were scanned on a 20x CellworX automated microscope (Applied Precision). Illumination for the HMGCR channel was set to 1.5 seconds per image and 9 images were acquired per well.

7.2.6 Cell Fractionation and Immunoblot Analysis

Cells were harvested by washing twice with ice-cold PBS followed by scraping into 600µL of ice-cold PBS. The suspension was transferred into a micro-centrifuge tube and centrifuged at 103 x g for 5 min at 4ºC. The pellet was resuspended in 0.4mL Buffer A (10 mM HEPES-KOH [pH 7.4], 10 mM KCl, 1.5 mM MgCl2, 5 mM sodium EDTA, 5 mM sodium EGTA, and 250 mM sucrose) supplemented with Complete Protease Inhibitor Cocktail (Roche). The cell suspension was passed through a 22.5 gauge needle 25 times and centrifuged at 104 x g for 7 min at 4°C. The pellet was resuspended in 0.3mL of Buffer A1 (20 mM HEPES-KOH [pH 7.6], 25% (v/v) glycerol, 0.42 M NaCl, 1.5 mM MgCl2, 1 mM EDTA, 1 mM EGTA, and protease inhibitor cocktail) and rotated for 1h at 4ºC followed by centrifugation at 2x104 x g for 30 min at 4ºC. The supernatant was designated nuclear extract fraction and precipitated over night at -70ºC with 1.5mL acetone. The precipitated material was collected by centrifugation at 2 x 104 x g for 15 min at 4ºC and solubilized in 100µL Buffer A2 (10 mM Tris-HCl [pH 6.8], 1% (w/v) sodium dodecyl sulfate (SDS), 100 mM NaCl and 1 mM EDTA). Protein concentrations of nuclear extract and membrane fractions were measured using the BCA Kit (Pierce). Protein amounts were adjusted to typically 3.5 µg/µL by adding Buffer A2. Finally, equal amounts of Buffer B (62.5 mM Tris-HCl [pH 6.8], 15% (w/v) SDS, 8 M urea, 10% (v/v) glycerol, and 100 mM DTT) and samples were mixed together and supplemented with 6x SDS loading buffer. Samples were incubated for 30 min

at 37°C prior to SDS-PAGE. After SDS-PAGE on 7.5% gels, proteins were transferred to nylon membranes and incubated with the following antibodies: IgG-A9, a mouse monoclonal antibody against the catalytic domain of human HMG CoA reductase from the culture medium of hybridoma (ATCC Number: CRL-1811) and anti-calnexin, a rabbit polyclonal antibody, which was used as a loading control for ER fractions. Bound antibodies were visualized with peroxidase-conjugated, affinity-purified donkey anti-mouse or anti-rabbit IgG using Immobilon Western HRP Substrate according to the manufacturer's instructions. Pre-stained protein markers were used for molecular weight determination (PageRuler Prestained Protein Ladder plus, Fermentas). Filters were exposed to FUJIFILM Super RX film at room temperature for typically 20 - 300 seconds.

7.2.7 siRNA treatment of A431-HMGCR-GFP cells

For siRNA assays, 9.9µL OptiMem (Gibco) were mixed with 0.1µL Lipofectamin 2000 (Invitrogen) and incubated for 15 min. At the same time 5µL of siRNA (1µM) were mixed with 5µL of OptiMem and incubated for 10 min. 10µL of transfection-mix was pipetted onto a 96 well plate (Greiner) containing 10µL of the diluted siRNAs and incubated for 15-20 min. After this, 3700 A431-HMGCR-GFP cells were seeded onto a 96 well plate containing the complexed siRNAs. 18h after the transfection, cells were washed with PBS and DMEM supplemented with 10% FCS was added. After 3 days, cells were washed 4 times with PBS and switched to DMEM supplemented with Glutamax (Invitrogen) and 25µM mevastatin (final concentration). After 30h of serum starvation, cells were switched from standard DMEM to DMEM without Phenolred and Riboflavin. MβCD-Cholesterol solution that was supplemented with Hoechst 33342 (100ng/mL final concentration) was added. Cells were imaged using an ImageXpress Micro automated microscope (Molecular Devices) with 10x magnification at 37°C and 5 % CO2. Illumination

for the GFP channel was set to 500 milliseconds, 9 images were takes per well.

7.2.8 qrtPCR of ABCA1, AMFR and VCP

RNA extraction using Invitrogen TRIZOL Reagent

Cells were grown to 90% confluence in a 3.5 cm dish. 1mL of TRIZOL was added and cells were lysed by pipetting up and down several times using a 1mL pipette tip. After that, the lysate was transferred to a falcon tube and samples were incubated for 5 to 15min at room temperature. 0.2 mL of chloroform was added, tubes were shaken by hand for 15 seconds and incubated for another 2 to 3 min at room temperature. Finally, tubes were centrifuged at 12,000 $\times$ g for 15 minutes at 4^{o}C. The aqueous phase containing the RNA was transferred to a fresh tube and 0.5 mL of isopropanol was added. Samples were incubated at room temperature for 10 min and centrifuged at 12,000 $\times$ g for 10min at 4^{o}C. The supernatant was removed and the RNA pellet was washed with 1 mL 75% ethanol by vortexing and centrifugation at 7500 x g for 5 min at 4^{o}C. The supernatant was removed; the RNA pellet was tried for 5 to 10 min and dissolved in RNase-free water. After measuring the A260/A280 ratio, samples were stored at -20^{o}C.

Reverse Transcription (QuantiTect Reverse Transcription)

Template RNA was thawed on ice. Genomic DNA was eliminated using 2µL gDNA Wipeout Buffer for 1µg RNA in a total volume of 14µL. RNA wipeout buffer was incubated for 2min at 42^{o}C and immediately put on ice. The reverse transcription was set up using all 14µL of wipeout RNA from before, plus 1 µL of Quantiscript Reverse Transcriptase (Qiagen), 5µL of RT Buffer and 1µL of RT Primer Mix, which summed up to 20µL. This mix was incubated for 15-20min at 42^{o}C followed by heat inactivation of the Quantiscript Reverse Transcriptase at 95^{o}C for 3 min. Samples were stored on -20^{o}C.

Quantitative PCR (Invitrogen)

The final mix for the qrtPCR contained 2µL of 10x Buffer (final concentration: 2mM dNTPs, 100mM Tris [pH 8.5], 500mM KCl, 20mM MgCl2 and 1.5% Triton), 0.4 µL Jump Start Taq (Sigma), 0.1 µL SYBR Green, 6µL Trehalose(2M), 0.5µL Formamide 0.2µL primers (final concentration: 250nM) and 3 µL of cDNA template summing up to 20µL. The thermal cycler was programmed as follows. 10min 95°C; 40x[60sec 95°C; 30sec 57°C; 30sec 72ºC] Results were saved in a comma separated file and analyzed with an R script that I developed for this. This script is available on the DVD in the appendix

7.2.9 Image analysis and statistical analysis

Single-cell image analysis was performed using CellProfiler (Carpenter, Jones et al. 2006). The pipeline used for analyzing A431-HMGCR-GFP-cells is in the appendix DVD. In summary, nuclei were detected using their Hoechst 33342 or DAPI signals, these regions were expanded to cover the cytoplasmic area and the integrated signal intensity per cell was measured. Image analysis was done on the Brutus cluster of ETH using the image analysis platform iBRAIN developed in our lab.

Resulting single cell intensity measurements were exported from CellProfiler output via Matlab to the csv format and imported to R (http://www.R-project.org). Data transformation and representation is described in the "Results" section. Scripts developed for the analysis can also be found on the appendix DVD.

8 Focal adhesion kinase establishes lipid rafts on the cell surface by controlling transcription of the cholesterol transporter ABCA1.

Eva-Maria Damm[1], Berend Snijder[1,2,4], Lilli Stergiou[1,4], Xue Li Guan[3], Herbert Polzhofer[1,2], David Lamparter[1], Markus R. Wenk[3], Lucas Pelkmans[1]

[1]Institute of Molecular Systems Biology, ETH Zurich, 8093 Zürich, Switzerland.

[2]Zürich PhD program in Molecular Life Sciences.

[3]Yong Loo Lin School of Medicine, Department of Biochemistry and Department of Biological Sciences, National University of Singapore, Singapore 117456.

[4]These authors contributed equally to this work.

* Correspondence should be addressed to L.P. (pelkmans@imsb.biol.ethz.ch)

Cells adapt their membrane lipid composition to local cell density and relative position within a population [1]. It is however unclear how this is established and if it is used to adjust the cell's physiology to its microenvironment. Here we report a new regulatory system by which Focal Adhesion Kinase (FAK) controls, in a population context-dependent manner, cell surface levels of cholesterol and sphingolipids via the ABC transporter A1 (ABCA1). We show that FAK suppresses *ABCA1* transcription via the Phosphoinositide 3-kinase – Akt pathway and the transcription factor FoxO. High levels of ABCA1 result in lower levels of cholesterol and sphingolipids, lower membrane lipid ordering,

lysosomal targeting of sphingolipids and sphingolipid-binding ligands, and defects in signalling to growth in size and to spreading. Our results have uncovered the mechanism by which cells regulate their membrane lipid composition as a function of their microenvironment to control a variety of processes, including endocytosis, signalling, and cell spreading.

The extensive cell-to-cell variability in endocytosis and membrane lipid composition in a population of adherent monoclonal human cells is strongly determined by the population context [1]. When cells are growing in sparse regions, they have higher levels of the sphingolipid GM1 on their cell surface and contain higher levels of active (i.e. phosphorylated) Focal Adhesion Kinase (FAK) [1]. FAK (a.k.a. PTK2) is an extensively studied tyrosine kinase that plays important roles in cell growth and intracellular signal transduction in response to interactions with the extracellular matrix [2-7]. However, despite the wealth of information on cell adhesion signalling, the mechanism by which it controls membrane lipid composition has remained elusive.

GM1 and FAK synergize in determining successful infection by Simian Virus 40 (SV40) [1], a non-enveloped virus that binds to GM1 and hijacks clathrin-independent endocytosis for infectious entry [8-10]. When cells are exogenously loaded with GM1, FAK phosphorylation increases in sparsely growing cells [1]. In return, FAK may determine the levels of GM1 on the cell surface [11]. Similarly, activation of b1-integrin, which signals to FAK [6], depends on sphingolipids [12], and depletion of b1-integrin may lead to a loss of sphingolipids on the cell surface [13,14]. This indicates the existence of an interdependent relationship between plasma membrane levels of sphingolipids and FAK signalling, but it is unclear how that relationship is established and how it impacts cellular activities within a population.

To study cell-to-cell variability in the endocytic itinerary of fluorescent Cholera

Toxin B (ChTxB), a pentavalent GM1-binding ligand, we applied unbiased computerized image analysis, and quantified in large populations of single monoclonal adherent human cells the enrichment of internalized ChTxB in the Golgi complex (GM130), phosphorylation of FAK (pFAK), and local cell density (Supplementary Methods). This demonstrated that ChTxB enrichment in the Golgi complex displays large population context-determined cell-to-cell variability. In cells growing sparsely that have high levels of active FAK, cells do not only bind more ChTxB [1], but also target internalized ChTxB 3-fold more efficiently to the Golgi complex than in densely growing cells (Fig. 1A). This suggests that active FAK is not only important for high levels of GM1 on the cell surface, but also for targeting a GM1-binding ligand to the Golgi complex.

To examine this, we compared cells from a FAK knockout mouse (FAK-ko cells), with FAK-ko cells in which FAK was stably re-expressed (FAK-rescue) [15], and with cells from a wild-type mouse (FAK-wt). Stable FAK re-expression reverted the loss-of-FAK phenotype to that observed in FAK-wt cells (see below), and we refer to both cell lines as FAK-expressing cells. FAK-ko cells had dramatically reduced levels of GM1 compared to FAK-expressing cells, which was mainly localized to intracellular organelles (Fig. 1B). Furthermore, in FAK-ko cells the little ChTxB that could bind was rapidly endocytosed to late endosomes and lysosomes (Fig. 1C) via the canonical endocytic pathway (Supplementary Fig. 1), and did not accumulate in the Golgi complex (Supplementary Fig. 1G). In FAK-expressing cells, ChTxB was retained on the cell surface or endocytosed to the Golgi complex (Fig. 1C), but did not accumulate in late endosomes and lysosomes (Supplementary Fig. 1J).

We also observed that SV40 was unable to infect FAK-ko cells (Fig. 1D), confirming the RNAi phenotype of FAK [1,16]. In addition, we could not rescue SV40 infection by exogenously loading GM1 sphingolipids onto the cell surface of FAK-

ko cells (Fig. 1D). That the loading protocol was efficient and led to functional integration of GM1 sphingolipids into the membrane was confirmed with fluorescent lipid analogs and with a mutant melanoma mouse cell line, GM95, which lacks all glucose-based glycolipids [17] (Supplementary Fig. 2). Because supplementing GM1 restores SV40 infection in GM95 cells [10], a lack of sphingolipids on the cell surface could not be the only reason for a block in virus infection in cells lacking FAK.

When we followed the exogenously surface-loaded sphingolipids, we observed that they were rapidly targeted to late endosomes and lysosomes in FAK-ko cells (Supplementary Fig. 3), reminiscent of the endocytic itinerary of ChTxB in these cells (see Fig. 1D and Supplementary Fig. 1). In FAK-expressing cells, surface-loaded sphingolipids were mainly retained on the cell surface similar to GM95 cells (Supplementary Fig. 3), and numerous other cell lines tested (not shown). Furthermore, we noticed that the amount of the caveolar coat component caveolin-1 (Cav-1) on the cell surface was reduced, and mainly displayed a perinuclear accumulation (Fig. 1E).

To explain these observations, we looked for RNAi phenotypes in our ongoing RNAi screens that allow SV40 to infect densely growing cells (Supplementary Methods), which SV40 normally does not infect [1]. Such a population context-specific effect would imply the existence of molecular machinery that suppresses SV40 infection in densely growing cells when FAK is not active. Remarkably, we found that the silencing of the cholesterol transporter *ABCA1* led to an increase of SV40 infection in HeLa cells, and more strongly in the densely growing subpopulation (Fig. 2A).

To test whether a functional interaction exists between FAK and ABCA1, we compared the mRNA levels of *ABCA1* between FAK-ko and FAK-expressing cells. Strikingly, *ABCA1* mRNA levels were on average 18-fold higher in FAK-ko cells

than in FAK-expressing cells (fig. 2B). Furthermore, FAK-expressing cells demonstrate a cell density-dependent regulation of *ABCA1* transcription, with high *ABCA1* transcription in densely growing cells and no detectable *ABCA1* transcription in sparsely growing cells (Fig. 2C). FAK-ko cells had lost the ability to control *ABCA1* transcription as a function of cell density (Fig. 2C).

To unravel how FAK suppresses *ABCA1* transcription, we looked for potential transcription factors that had a cell density-dependent RNAi phenotype in SV40 infection similar to *ABCA1*. The best-characterized transcription factor of *ABCA1* is Liver X receptor (LXR), a nuclear receptor that is activated by oxysterols [18,19]. Although we found that silencing LXRa (*NR1H2*) led to an increase of SV40 infection (Supplementary Fig. 4), consistent with the RNAi phenotype of *ABCA1*, it did not do so specifically in densely growing cells (Supplementary Fig. 4). Furthermore, canonical LXR signalling, as well as cholesterol sensing, was not perturbed in FAK-ko cells (Supplementary Fig. 4). Although *ABCA1* mRNA levels were consistently higher in FAK-ko cells compared to FAK-expressing cells, they still responded to serum starvation and cholesterol loading, which is mediated by LXR signalling [19]. Thus, FAK seemed to control *ABCA1* transcription via a population context-specific mechanism that works in parallel with LXR.

Interestingly, we found that silencing the transcription factor FoxO3 did affect SV40 infection in a population context-specific manner, increasing infection most strongly in densely growing cells (Fig. 2D). A sequence analysis of the promoter region of both human and mouse *ABCA1* revealed numerous FoxO response elements (Supplementary Fig. 5). When we silenced FoxO3 to app 40% in FAK-ko cells (more efficient knockdown was not achieved, Supplementary Fig. 5), *ABCA1* transcription was also reduced by app. 40% (Fig. 2E). In FAK-expressing cells, no effect was observed. Thus, FoxO3 is a transcription factor of *ABCA1*, which acts specifically in densely growing cells that do not have active FAK.

FoxO transcription factors shuttle between the nucleus and the cytosol in a phosphorylation-dependent manner [20,21]. When phosphorylated, they accumulate in the cytosol and are therefore unable to promote transcription in the nucleus. In FAK-ko cells, about half of FoxO was present in the nucleus, while in FAK-expressing cells, FoxO accumulated in the cytosol (Fig. 2F). FoxO transcription factors are phosphorylated by the Ser/Thr kinase Akt [21], which is activated downstream of Class I Phosphoinositide 3-kinase (PI3K) [22,23]. Furthermore, activated FAK binds PI3K [24].

To study whether FAK suppresses FoxO activity and thus *ABCA1* transcription via PI3K-Akt signalling, we analyzed levels of active Akt. Strikingly, FAK-ko cells did not contain any phosphorylated Akt, in strong contrast to FAK-expressing cells, which contain large amounts of phosphorylated Akt (Fig. 2G). Furthermore, when we inhibited PI3K with LY294002 in FAK-expressing cells, we observed an increase in *ABCA1* transcription to the level observed in untreated FAK-ko cells (Fig. 2H). In FAK-ko cells, only a slight increase in ABCA1 transcription was observed upon inhibiting PI3K. In addition, we found that RNAi-mediated silencing of specific isoforms of Akt and Class I PI3K reduced SV40 infection (Fig. 2I). These results are consistent with a pathway by which FAK suppresses transcription of *ABCA1* via the PI3K-Akt pathway and the transcription factor FoxO3. This pathway works in a cell density-dependent manner. *ABCA1* transcription is suppressed in sparsely growing cells in which FAK is active and is induced in densely growing cells when FAK is inactive. High levels of ABCA1 in turn inhibit SV40 to infect densely growing cells.

ABCA1 mediates cholesterol efflux [19,25]. Since SV40 infection depends on cholesterol [26], ABCA1 might inhibit SV40 infection by reducing cholesterol levels. Such a mechanism could also explain the intracellular accumulation of Cav-1 and the targeting of sphingolipids to the lysosome in FAK-ko cells, which occurs when

cellular cholesterol levels are perturbed [27-29]. Lipid mass spectrometry revealed that FAK-ko cells were depleted in their cholesterol-ester stores (Fig. 3A), and fluorescence-activated cell sorting of filipin-stained cells, which fluoresces when it binds to free cholesterol, demonstrated that FAK-ko cells also have reduced levels of free cholesterol (Fig. 3B). Furthermore, mass spectrometry confirmed that FAK-ko cells have lower levels of GM3, a precursor in the biosynthetic pathway of GM1, and revealed strikingly elevated levels of ceramide, the backbone of sphingolipids (Fig 3C).

If lower levels of both cholesterol and sphingolipids are the reason for reduced SV40 infection in FAK-ko cells, then a combined add back of cholesterol and sphingolipids should rescue SV40 infection in these cells. Strikingly, while add-back of GM1 alone did not rescue SV40 infection (see Fig. 1D), including free cholesterol in the add-back experiment did restore SV40 infection in FAK-ko cells (fig. 4A). Pharmacological inhibition of ABCA1 with Glyburide [30] or RNAi-mediated silencing of *ABCA1* also restored SV40 infection in FAK-ko cells (Fig. 4A). Filipin staining showed that these treatments restored free cholesterol levels in FAK-ko cells to those observed in FAK-expressing cells (not shown).

In addition, we observed that either cholesterol add back, or inhibition of ABCA1 restored the capacity of FAK-ko cells to retain GM1 on the cell surface (Fig. 4B). Note that when solely GM1 is added to FAK-ko cells it accumulates in lysosomes (Supplementary Fig. 3). Both treatments also switched back the endocytic itinerary of ChTxB from the lysosome to the Golgi complex (Fig. 4C), and restored Cav-1 localization to the cell surface (Fig. 4D). Furthermore, both treatments restored membrane lipid ordering to the extent observed in FAK-expressing cells (Fig. 4E), as measured with the fluorescent lipid ordering sensor Laurdan [31]. Similar observations were made with a detergent resistance assay (not shown). Thus, FAK controls endocytosis of sphingolipids and their ligands, subcellular localization of

Cav-1, and membrane lipid ordering by modulating levels of cholesterol through ABCA1. This is corroborated by the observation that artificial over-expression of ABCA1 decreases detergent resistance of the plasma membrane and interferes with caveolae formation [32].

Activation of both the RhoGTPase Rac1, which is important for cell spreading, and Akt, which induces growth in cell size, can occur downstream of activated FAK and PI3K [23,24,33-35] (see also Fig. 2G). Their activation has also been reported to depend on sphingolipids and/or cholesterol [36,37]. Strikingly, either cholesterol add back, or inhibition of ABCA1 partially restored activation of Rac1 (Fig. 4F, top), phosphorylation of Akt (Fig. 4F, middle), and cytosolic accumulation of FoxO (Fig. 4F, bottom) in the absence of FAK. Consistent with restored Rac1 and Akt signalling, we observed that upon both treatments, FAK-ko cells regained their ability to spread on the extracellular matrix (Fig. 4G, top) and to grow in size (Fig. 4G, bottom). Thus, FAK controls Rac1- and Akt-mediated signalling to cell spreading and growth in cell size, in part by modulating membrane lipid composition through ABCA1.

By unravelling how population context determines cell-to-cell variability in membrane lipid composition, SV40 infection and ChTxB endocytosis, we have revealed a new regulatory system by which cells couple their microenvironment to cellular physiology through modulation of the levels of cholesterol and sphingolipids. This system affects membrane lipid ordering, the endocytic itinerary of sphingolipid-binding ligands, cellular signalling, cell spreading and size, as well as infectious virus entry.

A minimal model that fits our experimental observations (Fig. 4H) shows a mechanism involving the activation of FAK in sparsely growing cells, which leads to the suppression of *ABCA1* transcription via the PI3K-Akt pathway and the transcription factor FoxO. Suppression of *ABCA1* leads to higher levels of free

cholesterol and sphingolipids, which are now retained on the cell surface. This leads to increased membrane lipid ordering, the ability of ChTxB to trigger endocytosis to the Golgi complex, activation of Akt and Rac1, and increased cell size and spreading. The fact that the level of phosphorylated Akt is increased when ABCA1 is inhibited, and exogenous loading of GM1 on the cell surface induces activation of FAK [1,12] indicates the existence of positive feedback loops in this system. Indeed, activated integrins, which signal to FAK, are enriched in regions of the plasma membrane with high lipid ordering [13], which increases when ABCA1 is suppressed (see Fig. 4E).

While the basic core of this new regulatory system has now been revealed, many details of its circuitry and how it affects cellular physiology will need to be further studied. For instance, how does ABCA1 activity impact on levels and retention of GM1 on the cell surface? Is that caused by the suggested ability of ABCA1 to scramble the cholesterol-dependent ordering of certain lipids [32], by the intracellular accumulation of the sphingolipid- and cholesterol-scaffolding protein Cav-1 (see Fig. 4D), or because sphingolipid biosynthesis downstream of ceramide senses levels of cholesterol [38-40] and stops when cholesterol levels drop? The high levels of free ceramide in FAK-ko cells (see Fig. 3C) indicate that sphingolipid biosynthesis is indeed perturbed. In addition, loss of sphingolipids might be the result of increased targeting to and degradation in the lysosome when FAK is inactive and levels of cholesterol decrease (Supplementary Fig. 6).

What is also needed is to better understand how these lipids control endocytic machinery that dictates traffic to and from lysosomes or the Golgi complex [41-43]. Interestingly, FAK-ko cells have a higher rate of clathrin-mediated endocytosis (Supplementary Fig. 7), which is consistent with observations that this endocytic pathway is more active in densely growing cells [1]. We also need to understand better how activation of Rac1 and phosphorylation of Akt is regulated by mem-

brane lipid composition [36,37], and how that relates to lipid composition-dependent activation of integrins [12,13].

Continuing efforts to understand the integrated complexity of cell adhesion signalling [44] should now decouple the cell's response that is a consequence of direct regulation via protein-protein interactions from what is downstream of changes in membrane lipid composition and ordering, established by the FAK-ABCA1 system. We expect that by analyzing which defects in cell adhesion act through defects in membrane lipid composition, further insights will be made.

Acknowledgements:

We thank Karin Mench for excellent experimental support throughout this work, Christoph Hauck for FAK-rescue cells, and the Light Microscopy Centre of the ETH Zürich for technical support. EMD was supported by The Roche Research Foundation, Oncosuisse, and the Sassella Stiftung, LS by the Bonnizi-Theler Foundation, LP by the Swiss National Science Foundation, the SystemsX.ch RTD projects PhosphoNetX and LipidX, the ETH Zürich, and the European Union, and MRW by the Singapore National Research Foundation (CRP Award No. 2007-04), the Biomedical Research Council of Singapore (R-183-000-211-305) and the National Medical Research Council (R-183-000-224-213).

Author Contributions:

LP supervised the project. EMD, LS, HP and DL performed experiments, BS performed all computational image analysis, XLG performed the lipid mass spectrometry in the laboratory of MRW. LP, EMD, and BS made figures and wrote the manuscript.

Author Information:

The authors declare no competing financial interests. Correspondence and requests for materials should be addressed to L.P.

References:

1. Snijder, B. et al. Population context determines cell-to-cell variability in endocytosis and virus infection. *Nature* **461**, 520-523 (2009).

2. Guan, J. L. & Shalloway, D. Regulation of focal adhesion-associated protein tyrosine kinase by both cellular adhesion and oncogenic transformation. *Nature* **358**, 690-692 (1992).

3. Schaller, M. D. et al. pp125FAK a structurally distinctive protein-tyrosine kinase associated with focal adhesions. *Proc Natl Acad Sci U S A* **89**, 5192-5196 (1992).

4. Lipfert, L. et al. Integrin-dependent phosphorylation and activation of the protein tyrosine kinase pp125FAK in platelets. *J Cell Biol* **119**, 905-912 (1992).

5. Renshaw, M. W., Price, L. S. & Schwartz, M. A. Focal adhesion kinase mediates the integrin signaling requirement for growth factor activation of MAP kinase. *J Cell Biol* **147**, 611-618 (1999).

6. Mitra, S. K. & Schlaepfer, D. D. Integrin-regulated FAK-Src signaling in normal and cancer cells. *Curr Opin Cell Biol* **18**, 516-523 (2006).

7. Geiger, B., Spatz, J. P. & Bershadsky, A. D. Environmental sensing through focal adhesions. *Nat Rev Mol Cell Biol* **10**, 21-33 (2009).

8. Pelkmans, L., Kartenbeck, J. & Helenius, A. Caveolar endocytosis of simian virus 40 reveals a new two-step vesicular-transport pathway to the ER. *Nat Cell Biol* **3**, 473-483 (2001).

9. Damm, E. M. et al. Clathrin- and caveolin-1-independent endocytosis: entry of simian virus 40 into cells devoid of caveolae. *J Cell Biol* **168**, 477-488 (2005).

10. Ewers, H. et al. GM1 structure determines SV40-induced membrane invagination and infection. *Nat Cell Biol* **12**, 11-8; sup pp 1-12 (2010).

11. Palazzo, A. F., Eng, C. H., Schlaepfer, D. D., Marcantonio, E. E. & Gundersen, G. G. Localized stabilization of microtubules by integrin- and FAK-facilitated

Rho signaling. *Science* **303**, 836-839 (2004).

12. Sharma, D. K. et al. The glycosphingolipid, lactosylceramide, regulates beta1-integrin clustering and endocytosis. *Cancer Res* **65**, 8233-8241 (2005).

13. Gaus, K., Le Lay, S., Balasubramanian, N. & Schwartz, M. A. Integrin-mediated adhesion regulates membrane order. *J Cell Biol* **174**, 725-734 (2006).

14. Singh, R. D. et al. Gangliosides and beta1-Integrin Are Required for Caveolae and Membrane Domains. *Traffic* (2009).

15. Sieg, D. J., Hauck, C. R. & Schlaepfer, D. D. Required role of focal adhesion kinase (FAK) for integrin-stimulated cell migration. *J Cell Sci* **112**, 2677-2691 (1999).

16. Pelkmans, L. et al. Genome-wide analysis of human kinases in clathrin- and caveolae/raft-mediated endocytosis. *Nature* **436**, 78-86 (2005).

17. Ichikawa, S., Nakajo, N., Sakiyama, H. & Hirabayashi, Y. A mouse B16 melanoma mutant deficient in glycolipids. *Proc Natl Acad Sci U S A* **91**, 2703-2707 (1994).

18. Edwards, P. A., Kast, H. R. & Anisfeld, A. M. BAREing it all: the adoption of LXR and FXR and their roles in lipid homeostasis. *J Lipid Res* **43**, 2-12 (2002).

19. Schmitz, G. & Langmann, T. Transcriptional regulatory networks in lipid metabolism control ABCA1 expression. *Biochim Biophys Acta* **1735**, 1-19 (2005).

20. Biggs, W. H. r., Meisenhelder, J., Hunter, T., Cavenee, W. K. & Arden, K. C. Protein kinase B/Akt-mediated phosphorylation promotes nuclear exclusion of the winged helix transcription factor FKHR1. *Proc Natl Acad Sci U S A* **96**, 7421-7426 (1999).

21. Carlsson, P. & Mahlapuu, M. Forkhead transcription factors: key players in development and metabolism. *Dev Biol* **250**, 1-23 (2002).

22. Leevers, S. J., Vanhaesebroeck, B. & Waterfield, M. D. Signalling through phosphoinositide 3-kinases: the lipids take centre stage. *Curr Opin Cell Biol* **11**,

219-225 (1999).

23. Alessi, D. R. et al. Characterization of a 3-phosphoinositide-dependent protein kinase which phosphorylates and activates protein kinase Balpha. *Curr Biol* **7**, 261-269 (1997).

24. Chen, H. C., Appeddu, P. A., Isoda, H. & Guan, J. L. Phosphorylation of tyrosine 397 in focal adhesion kinase is required for binding phosphatidylinositol 3-kinase. *J Biol Chem* **271**, 26329-26334 (1996).

25. Tam, S. P., Mok, L., Chimini, G., Vasa, M. & Deeley, R. G. ABCA1 mediates high-affinity uptake of 25-hydroxycholesterol by membrane vesicles and rapid efflux of oxysterol by intact cells. *Am J Physiol Cell Physiol* **291**, C490-502 (2006).

26. Pelkmans, L., Puntener, D. & Helenius, A. Local actin polymerization and dynamin recruitment in SV40-induced internalization of caveolae. *Science* **296**, 535-539 (2002).

27. Hayer, A., Stoeber, M., Bissig, C. & Helenius, A. Biogenesis of Caveolae: Stepwise Assembly of Large Caveolin and Cavin Complexes. *Traffic* (2009).

28. Hortsch, R. et al. Glycolipid Trafficking in Drosophila Undergoes Pathway Switching in Response to Aberrant Cholesterol Levels. *Mol Biol Cell* (2010).

29. Schulze, H., Kolter, T. & Sandhoff, K. Principles of lysosomal membrane degradation: Cellular topology and biochemistry of lysosomal lipid degradation. *Biochim Biophys Acta* **1793**, 674-683 (2009).

30. Nieland, T. J. et al. Cross-inhibition of SR-BI- and ABCA1-mediated cholesterol transport by the small molecules BLT-4 and glyburide. *J Lipid Res* **45**, 1256-1265 (2004).

31. Gaus, K., Zech, T. & Harder, T. Visualizing membrane microdomains by Laurdan 2-photon microscopy. *Mol Membr Biol* **23**, 41-48 (2006).

32. Landry, Y. D. et al. ATP-binding cassette transporter A1 expression dis-

rupts raft membrane microdomains through its ATPase-related functions. *J Biol Chem* **281**, 36091-36101 (2006).

33. Vuori, K., Hirai, H., Aizawa, S. & Ruoslahti, E. Introduction of p130cas signaling complex formation upon integrin-mediated cell adhesion: a role for Src family kinases. *Mol Cell Biol* **16**, 2606-2613 (1996).

34. Brugnera, E. et al. Unconventional Rac-GEF activity is mediated through the Dock180-ELMO complex. *Nat Cell Biol* **4**, 574-582 (2002).

35. Burridge, K. & Wennerberg, K. Rho and Rac take center stage. *Cell* **116**, 167-179 (2004).

36. del Pozo, M. A. et al. Integrins regulate Rac targeting by internalization of membrane domains. *Science* **303**, 839-842 (2004).

37. Lasserre, R. et al. Raft nanodomains contribute to Akt/PKB plasma membrane recruitment and activation. *Nat Chem Biol* **4**, 538-547 (2008).

38. Scheek, S., Brown, M. S. & Goldstein, J. L. Sphingomyelin depletion in cultured cells blocks proteolysis of sterol regulatory element binding proteins at site 1. *Proc Natl Acad Sci U S A* **94**, 11179-11183 (1997).

39. D'Angelo, G. et al. Glycosphingolipid synthesis requires FAPP2 transfer of glucosylceramide. *Nature* **449**, 62-67 (2007).

40. Guan, X. L. et al. Functional interactions between sphingolipids and sterols in biological membranes regulating cell physiology. *Mol Biol Cell* **20**, 2083-2095 (2009).

41. Olkkonen, V. M. et al. The OSBP-related proteins (ORPs): global sterol sensors for co-ordination of cellular lipid metabolism, membrane trafficking and signalling processes? *Biochem Soc Trans* **34**, 389-391 (2006).

42. Mayor, S. & Pagano, R. E. Pathways of clathrin-independent endocytosis. *Nat Rev Mol Cell Biol* **8**, 603-612 (2007).

43. Linder, M. D. et al. Rab8-dependent recycling promotes endosomal choles-

terol removal in normal and sphingolipidosis cells. *Mol Biol Cell* **18**, 47-56 (2007).

44. Zaidel-Bar, R., Itzkovitz, S., Ma'ayan, A., Iyengar, R. & Geiger, B. Functional atlas of the integrin adhesome. *Nat Cell Biol* **9**, 858-867 (2007).

8.1 Figure legends

Figure 1 | Cell-to-cell variability and loss-of-FAK phenotype in ChTxB endocytic itinerary, SV40 infection, and Cav-1 localization.

a. Single-cell enrichment (Supplementary methods) of internalized ChTxB in the Golgi complex as a function of increasing cell density (left) or increasing levels of pFAK (right). 2,634 single cells were quantified. Cells that grow at low local cell density have a three-fold higher enrichment ($P<0.001$) of ChTxB in the Golgi complex than cells growing at high local cell density (reference). Similarly, internalized ChTxB is targeted at least 2-fold more efficiently ($P<0.001$) to the Golgi complex in cells with high levels of pFAK than in cells with low levels of pFAK (reference). Grey areas indicate the 25^{th} and 75^{th} percentile areas of the single-cell measurements. **b.** Total levels of GM1 in FAK-ko and FAK-expressing cells determined with ChTxB after cell fixation. In FAK-ko cells, GM1 levels are dramatically lower, and GM1 localizes to intracellular perinuclear organelles. Scalebars: 20 µm. Boxplots indicate the $\log_{10}$ mean ChTxB intensity of 4,531 (FAK-ko) and 638 (FAK-rescue) single cells. **c.** After 60 min of uptake, ChTxB accumulates in Lysotracker-positive organelles in FAK-ko cells (arrowheads), while it is present in GM130-positive structures in FAK-expressing cells. Scalebars: 5 µm (FAK-ko) and 20 µm (FAK-wt and -rescue). **d.** SV40 does not infect FAK-ko cells, nor after GM1 addback, while it efficiently infects FAK-expressing cells. Infection index (mean ± s.d.; n=3) represents the fraction of SV40-infected (T antigen-positive) cells in each cell population (19 - 50 x 10^3 single cells). **e.** FAK-ko and FAK-expressing cells transiently expressing Cav1-GFP. In FAK-ko cells, the majority of

Cav1-GFP accumulates in a perinuclear area, while in FAK-expressing cells Cav1-GFP is present on the cell surface in a characteristic spot-like pattern. Scalebars: 20 µm.

Figure 2 | FAK suppresses ABCA1 transcription via the PI3K-Akt pathway and FoxO

a. RNAi of *ABCA1* in HeLa cells increases SV40 infection (mean ± s.d.; n=2) with app. 1.5 fold (validated with 2 independent siRNAs). Analysis of the RNAi phenotype in 6250 single cells at different local cell densities (1-8 [low], 8-12 [medium], and 12-20 [high] cells per $6.5x10^3$ μm^2) (Supplementary methods) demonstrates that the highest increase in infection is in cells growing at high local cell density (for example images, see Supplementary Fig. 4D). The relative infection index (left) is the infection index of SV40 in each condition relative to control (scrambled siRNA). The Log_2 relative infection index (right) (mean ± s.d.; n=3) is the Log_2-transformed fraction of infected cells in each of the three density groups divided by the fraction of infected cells in the same density groups in control cells. A value of 0 indicates no change in infection compared to control, while a value of 1.0 represents a 2-fold increase of infection compared to control. **b.** Quantitative real-time PCR (Supplementary methods) demonstrates that *ABCA1* mRNA levels (mean ± s.d; n=9) are 18-fold higher in FAK-ko cells than in FAK-expressing cells. **c.** ABCA1 mRNA levels are controlled by local cell density in a FAK-dependent manner. In FAK-ko cells, ABCA1 mRNA levels are high irrespective of the density of cells, while in FAK-expressing cells, ABCA1 mRNA levels are barely detectable in cells at low cell density. **d.** RNAi of *FOXO3* in HeLa cells increases SV40 infection, especially in densely growing cells (for example images, see Supplementary Fig. 4D). Infection index was quantified from 6154 single cells (mean ± s.d.; n=2). **e.** *FOXO3* RNAi (maximum silencing efficiency achieved was 40%, see Supplementary Fig. 5) leads to a 43% reduction ($P<0.05$)

of ABCA1 mRNA levels in FAK-ko cells, while it does not effect ABCA1 mRNA levels in FAK-wt cells (mean ± s.d.; n=4). **f.** Western blots of cytosol and nucleus extracts of FAK-ko and FAK-expressing cells demonstrate cytosolic accumulation of FoxO only in FAK-expressing cells. Amount of cytosolic FoxO compared to the nucleus is 3-fold higher ($P<0.05$) in FAK-expressing cells (mean ± s.d.; n=4). The nucleus marker Lamin B and the cytosol marker GAPDH show that the extracts were clean. **g.** Western blot of S473-phosphorylated Akt demonstrates that FAK-ko cells have no detectable phosphorylated Akt, while FAK-expressing cells have high levels of phosphorylated Akt. **h.** Treatment of FAK-wt cells with the PI3K inhibitor LY294002 strongly increases *ABCA1* transcription ($P<0.01$) to a level comparable with untreated FAK-ko cells. LY294002 treatment slightly increases *ABCA1* transcription in FAK-ko cells. Bars are mean values ± s.d.; n=3) **i.** RNAi of *AKT3* and *PIK3CD* reduce SV40 infection (mean ± s.d.; n=2) (validated with 2 independent siRNAs).

Figure 3 | Loss-of-FAK leads to reduced cellular cholesterol levels and sphingolipids, while levels of free ceramide increase.

a. Mass spectrometry of lipid extracts from protein-normalized cell lysates (Supplementary methods) of FAK-ko and FAK-expressing cells reveals that FAK-expressing cells contain higher levels of cholesterol esters than FAK-ko cells (*$P<0.05$; **$P<0.01$). Bars are mean values ± s.d.; n=4. **b.** FACS-based single-cell analysis of filipin staining (Supplementary methods) in FAK-ko and FAK-expressing cells reveals that FAK-ko cells have reduced levels of free cholesterol compared to FAK-expressing cells ($P<0.05$). Bars are means of the mean intensities of at least 34 x 10^3 single cells ± s.d.; n=3. **c.** Mass spectrometry reveals that FAK-expressing cells have much higher levels of the sphingolipid GM3 than FAK-ko cells. Conversely, FAK-ko cells have elevated levels of free ceramide compared to FAK-expressing cells ($P<0.01$). Bars are mean values ± s.d.; n=4.

Figure 4 | FAK controls cell surface levels of GM1, SV40 infection, Cav1 localization, and Rac1- and Akt-dependent signalling to cell spreading and growth in size, via ABCA1.

a. SV40 infection is rescued in FAK-ko cells when cholesterol is included in add-back experiments (GM1/Chol), when ABCA1 is inhibited with Glyburide (Gly), or when ABCA1 is silenced (RNAi *ABCA1*) (**P<0.01; ***P<0.001). Infection index (from at least 805 single cells) are mean values ± s.d.; n=3. **b.** Including cholesterol in add-back experiments (GM1/Chol) and inhibition of ABCA1 (Gly) restores the capability of FAK-ko cells to retain GM1 on their cell surface (P<0.001). Bars are mean values ± s.d.; n=15) Scalebars: 20 µm. **c.** Including cholesterol in add-back experiments (GM1/Chol), or inhibition of ABCA1 (Gly) restores the capability of FAK-ko cells to target endocytosed ChTxB to the Golgi complex. Scalebars: 10 µm. **d.** Inclusion of cholesterol in add-back experiments (GM1/Chol), or inhibition of ABCA1 (Gly) restores the capability of FAK-ko cells to localize Cav1-GFP to the cell surface (**P<0.01; ***P<0.001). Bars are mean values ± s.d.; n=5-6. Scalebars: 15 µm. **e.** GP score distributions of Laurdan (left) (Supplementary methods). Blue lines and points represent measurements, red lines represent fitted two-component Gaussian mixture models, of which each component is depicted by black lines (left Gaussian for GP scores of a non-ordered lipid environment and the right Gaussian for GP scores of an ordered lipid environment). Fits are shown for FAK-ko cells (ERF=$0.7\text{x}10^{-3}$) and FAK-ko cells treated with Glyburide (ERF=$1.1\text{x}10^{-3}$). Comparing GP score distributions demonstrates that FAK-ko cells have low membrane lipid ordering compared to FAK-expressing cells. Including cholesterol in add-back experiments (GM1/Chol) and inhibition of ABCA1 (Gly) restores the membrane lipid ordering of FAK-ko cells to that observed in FAK-expressing cells (**P<0.01; ***P<0.001). Bars are mean values of 30-100 single cells ± s.d.; n=6-10. Scalebars: 50 µm. **f.** The amount of activated

Rac1 (top), determined by binding to the RBD domain of PAK1 (Supplementary methods) is lower in cell lysates of FAK-ko cells than in FAK-expressing cells ($P<0.001$). Bars are mean values ± s.d.; n=3. Including cholesterol in add-back experiments (GM1/Chol) and inhibition of ABCA1 (Gly) restores levels of activated Rac1 ($P<0.001$) (top), phosphorylation of Akt at S473 (middle), and FoxO accumulation in the cytosol (bottom) in FAK-ko cells. **g.** Including cholesterol in add-back experiments (GM1/Chol) and inhibition of ABCA1 (Gly) increases cell spreading ($P<0.001$) (mean of 12-50 single-cell areas ± s.d.) and nucleus size in FAK-ko cells (boxplots of averages of at least 585 single cells; n=3). Nucleus size is a faithful readout of cell size (see Ref. 1). **h.** Minimal model that fits the experimental findings. When cells grow at low local cell density, FAK becomes activated, leading to the suppression of *ABCA1* transcription via the PI3K-Akt pathway and FoxO3. High expression of ABCA1 decreases the levels of cholesterol and sphingolipids, which affects membrane lipid ordering, Cav1 localization at the cell surface, ChTxB endocytosis to the Golgi complex, and SV40 infection. This also affects activation of Rac1 and cell spreading, and feeds back on FAK and Akt signalling, which is responsible for cell spreading and growth in cell size.

8.2 Figures

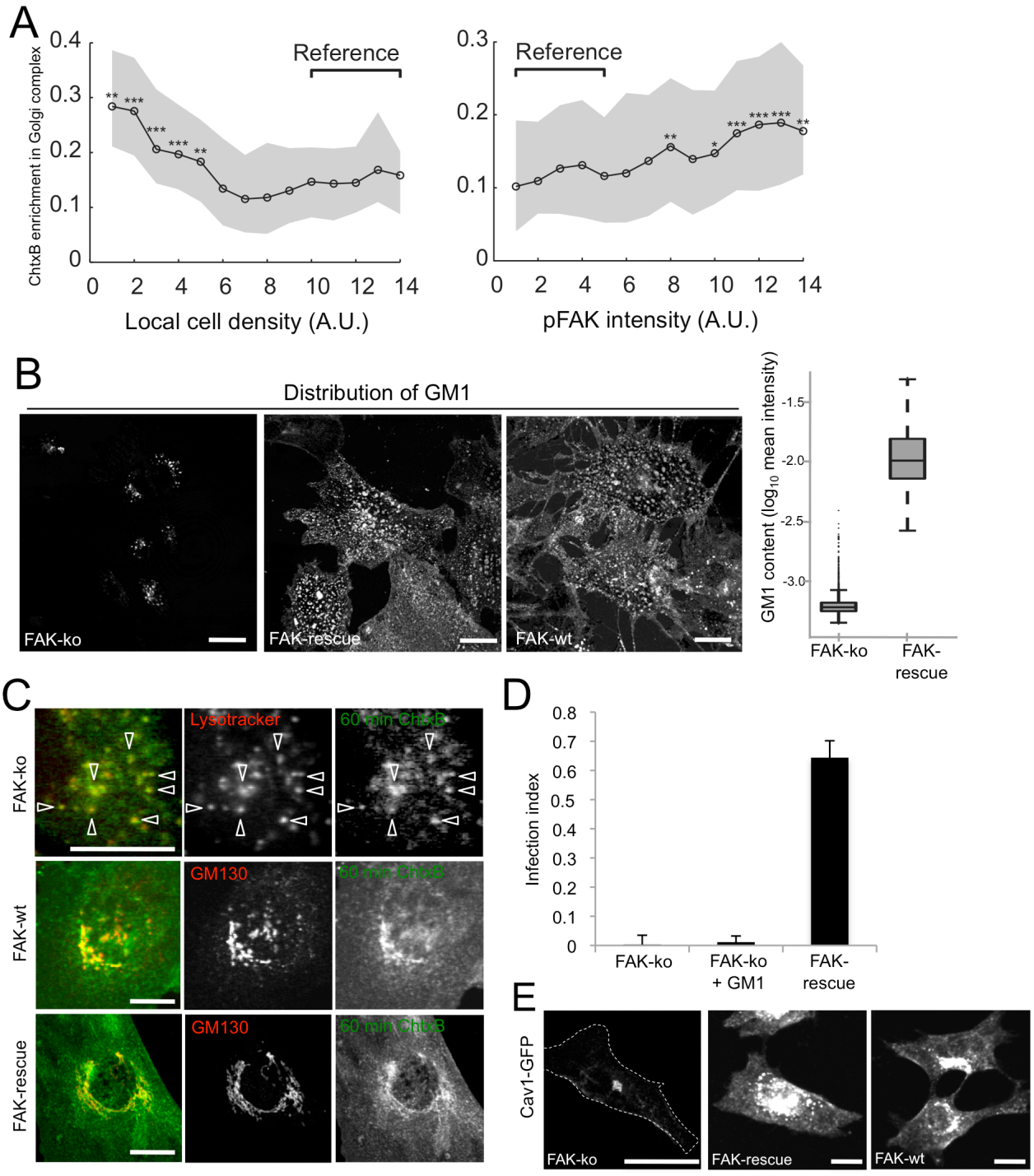
A
ChtxB enrichment in Golgi complex
Reference
Local cell density (A.U.)
pFAK intensity (A.U.)
B
Distribution of GM1
FAK-ko
FAK-rescue
FAK-wt
GM1 content (log10 mean intensity)
C
LysoTracker
60 min ChtxB
GM130
D
Infection index
FAK-ko
FAK-ko + GM1
FAK-rescue
E
Cav1-GFP

Figure 1

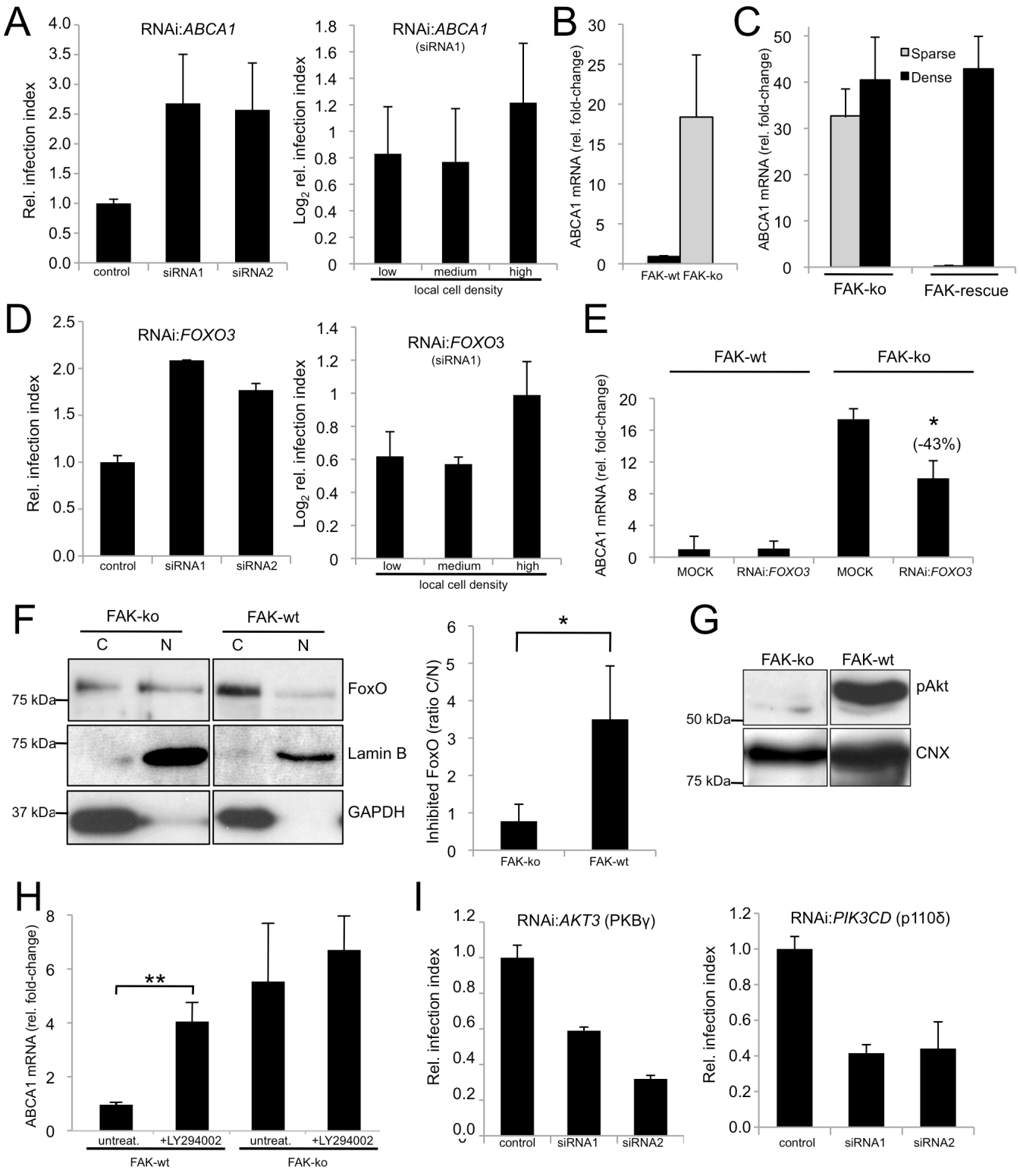
A
RNAi:ABCA1
Rel. infection index
control
siRNA1
siRNA2
RNAi:ABCA1
(siRNA1)
Log2 rel. infection index
low
medium
high
local cell density
B
ABCA1 mRNA (rel. fold-change)
FAK-wt FAK-ko
C
Sparse
Dense
ABCA1 mRNA (rel. fold-change)
FAK-ko
FAK-rescue
D
RNAi:FOXO3
Rel. infection index
control
siRNA1
siRNA2
RNAi:FOXO3
(siRNA1)
Log2 rel. infection index
low
medium
high
local cell density
E
FAK-wt
FAK-ko
ABCA1 mRNA (rel. fold-change)
*
(-43%)
MOCK
RNAi:FOXO3
MOCK
RNAi:FOXO3
F
FAK-ko
FAK-wt
C
N
C
N
75 kDa
FoxO
75 kDa
Lamin B
37 kDa
GAPDH
Inhibited FoxO (ratio C/N)
*
FAK-ko
FAK-wt
G
FAK-ko
FAK-wt
50 kDa
pAkt
75 kDa
CNX
H
ABCA1 mRNA (rel. fold-change)
**
untreat.
+LY294002
untreat.
+LY294002
FAK-wt
FAK-ko
I
RNAi:AKT3 (PKBγ)
Rel. infection index
control
siRNA1
siRNA2
RNAi:PIK3CD (p110δ)
Rel. infection index
control
siRNA1
siRNA2

Figure 2

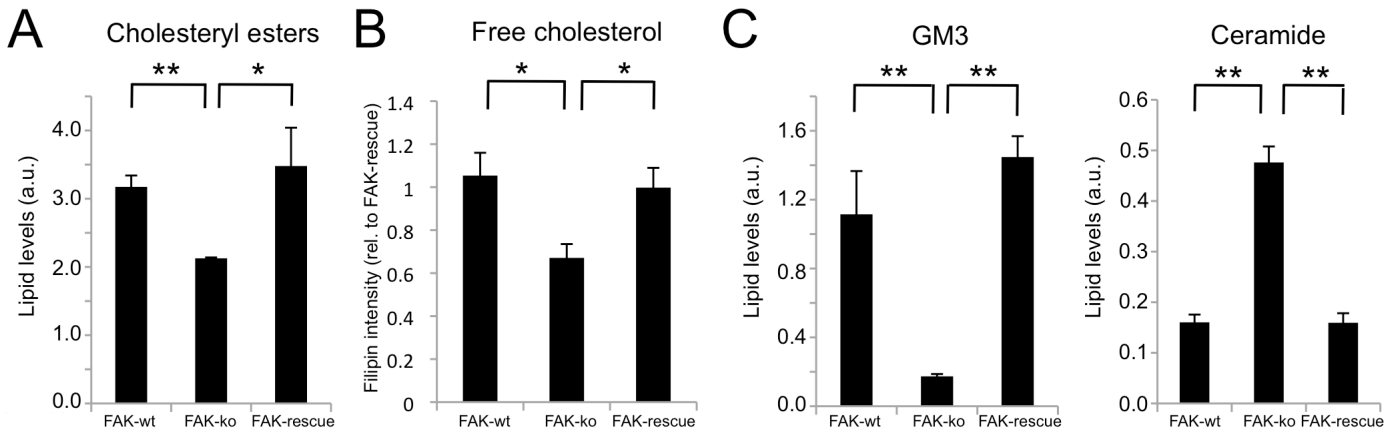
A
Cholesteryl esters
**
*
Lipid levels (a.u.)
4.0
3.0
2.0
1.0
0.0
FAK-wt
FAK-ko
FAK-rescue
B
Free cholesterol
*
*
Filipin intensity (rel. to FAK-rescue)
1.4
1.2
1
0.8
0.6
0.4
0.2
0
FAK-wt
FAK-ko
FAK-rescue
C
GM3
**
**
Lipid levels (a.u.)
1.6
1.2
0.8
0.4
0.0
FAK-wt
FAK-ko
FAK-rescue
Ceramide
**
**
Lipid levels (a.u.)
0.6
0.5
0.4
0.3
0.2
0.1
0.0
FAK-wt
FAK-ko
FAK-rescue

Figure 3

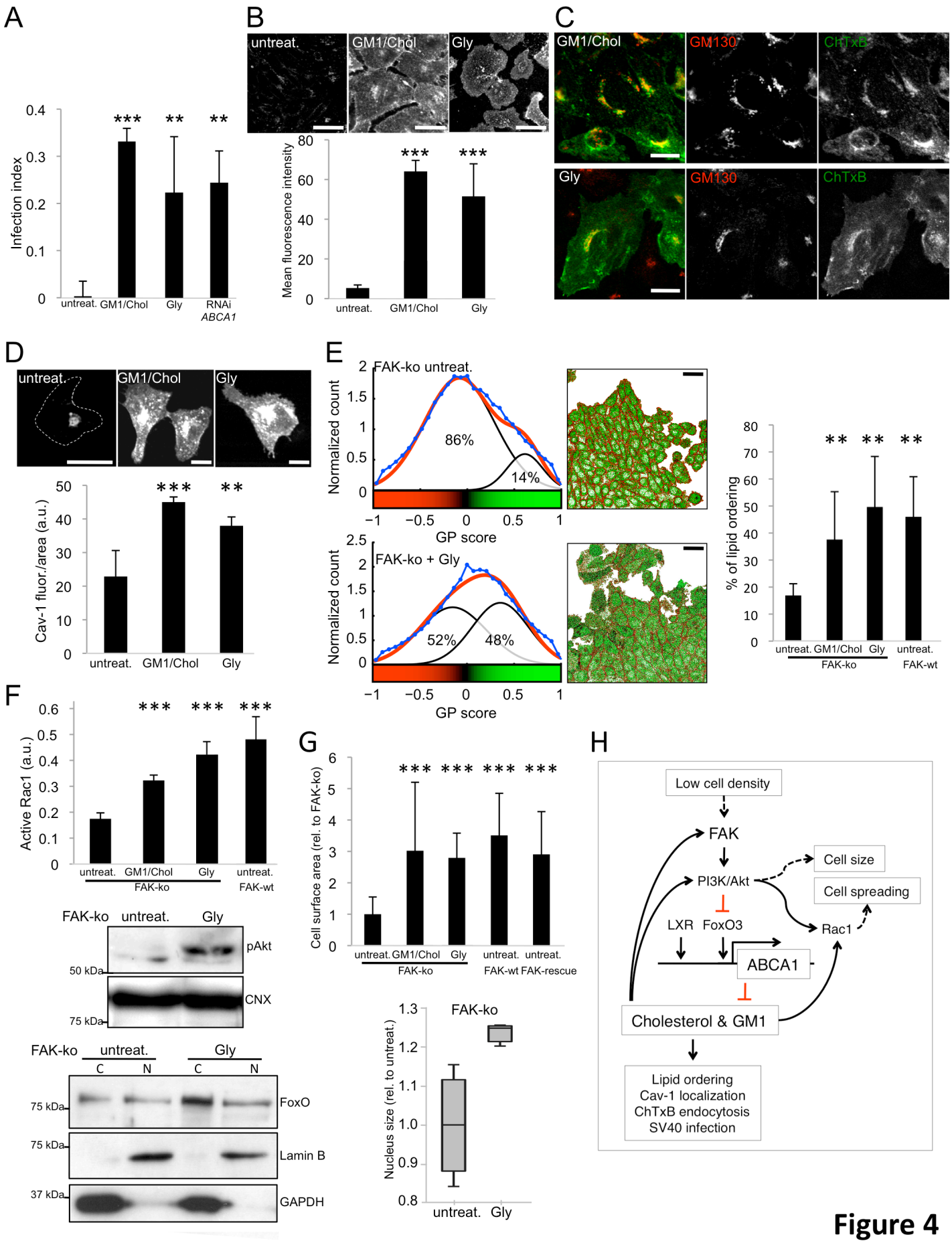
A
B
C
D
E
F
G
H
Infection index
untreat.
GM1/Chol
Gly
RNAi ABCA1
Mean fluorescence intensity
GM130
ChTxB
Cav-1 fluor./area (a.u.)
FAK-ko untreat.
FAK-ko + Gly
Normalized count
GP score
86%
14%
52%
48%
% of lipid ordering
FAK-ko
FAK-wt
Active Rac1 (a.u.)
pAkt
CNX
FoxO
Lamin B
GAPDH
Cell surface area (rel. to FAK-ko)
FAK-rescue
Nucleus size (rel. to untreat.)
Low cell density
FAK
PI3K/Akt
Cell size
Cell spreading
Rac1
LXR
FoxO3
ABCA1
Cholesterol & GM1
Lipid ordering
Cav-1 localization
ChTxB endocytosis
SV40 infection

Figure 4

9 Acknowledgements

This thesis would not have been possible without the help of many people. Again and again, they helped me to take the next step in my research project and in my life. All I can do now is to tell them my appreciation. I would like to mention a few, putting them as pars pro toto for the many more who would deserve it.

I would like to thank Lucas Pelkmans for giving me the possibility to pursue this challenging project. Your visionary attitude made this all happen! I would also like to show my gratitude to my PhD committee, Ernst Hafen and Christoph Thiele. Thanks for asking the right questions and pushing me forward when decisions had to be taken. This also applies for Lilli Stergiou, your attitude of hard working, your sound reasoning, your benevolent personality and honest comradeship will always inspire me. I would also like to thank all other lab members: Berend Snijder, Frank Wippich, Eva-Maria Niemann, Manuel Bauer, Mirko Birbaumer, Pauli Raemoe, Prisca Liberali and Raphael Sacher for all major and minor support during the years. I would also like to mention my "Viennese connection". Thank you Gerhard ("Kommst vorbei, bei mir funktioniert das immer"), Jesse ("Ja, aber dafür braucht man dann. . . ") and Marko ("STRUKTUR!"). You are nerds by nature, but scientists by choice. Thanks for honest and productive criticism and helping hands when I needed them. I would also like to thank the Boehringer Ingelheim Foundation for financial support and creating this cordial atmosphere of true passion for science whenever we gathered together.

All true achievements I my life are rooted in the love I experienced in my family. My parents, Maria and Herbert, have been role models for honesty and benev-

olence for their children and their environment. My sisters, Michaela and Eva Maria, for their care and support whenever their little brother was in need. It for sure requires a self-assured personality to support that inquisitive character of mine.

Finally, words can hardly express my affection and gratitude for Marta. Thank you for every day being there with me.

Pensar uma flor é vê-la e cheirá-la
E comer um fruto é saber-lhe o sentido.

CV of Herbert Georg Polzhofer

Contact Information	Herbert Georg Polzhofer Schaffhauserstrasse 59 8057 Zuerich Switzerland	*Cell:* 077 4259688 *E-mail:* polzbert@gmail.com

Citizenship: Austria

Working Permit: B

Professional Experience

June 2006 - July 2010, PhD student in Systems Biology

ETH Zurich, Institute for Molecular Systems Biology
Screening for Regulators of the Cholesterol Metabolism using RNAi, Automated Microscopy and Quantitative Single-cell Analysis.

I developed a siRNA screen for genes involved in cholesterol regulation. For this, I developed an image-based reporter assay using a GFP-tagged recombinant protein in its chromosomal environment (BAC recombineering), assisted in setting up a newly founded lab with high content screening equipment (Evo series liquid handling roboters from Tecan, various automated microscopes eg: Molecular Devices ImageXpress microscopes), and implemented single cell image analysis and statistical analysis software (CellProfiler and R) for my data.

March 2005 - June 2006, Diploma Student

IMBA Vienna, Institute of Molecular Biotechnology
Cryo-electron tomography on the ultra structure of the actin-cytoskeleton.

In this project, I established an in vitro assay for actin based motility on nano- fibres, set-up a collaboration with the Boulder Laboratory For 3-D Electron Microscopy of Cells and performed comparative analysis to primary fish keratocytes using 3D cryo-electron tomography. Collaboration between:

- Institute of Molecular Biotechnology (IMBA), Vienna , Austria
- The Boulder Laboratory For 3-D Electron Microscopy of Cells, Col , USA
- Centre national de la recherche scientifique, Gif-sur-Yvette, France

November 2004 - February 2005, Rotational student

The Centre for Cell Engineering University of Glasgow, UK
Producing 40nm micro-patterns on plastic chips to study the reaction of skin cells to their nano environment.

September 2004 - November 2004, Research Assistent

Structural Bioinformatics group, University of Glasgow, UK
Bioinformatics on H-bonds of beta-bulged loops in protein structures

I investigated H-bonding patterns of beta bulged loops in beta-propeller containing crystal structures. I mainly worked with bioinformatic tools like the Reduce-package and HBPLUS, for data mining, I got into writing Perl scripts.

1996 - 2004, Various jobs and practica

Including extra (Komparse) at the Volkstheater GmbH (Vienna), steel construction worker at BMW (Munich), and wood refurbisher at the Karlskirche and in the workshop of Mag. Peter Kopp, (Vienna).

Education

October 2006 - July 2010,

PhD at the Institute of Molecular Systems Biology, ETH Zrich, funded by the Boehringer Ingelheim Foundation

October 2000 - May 2006,

Studies of Molecular Biology at the University of Vienna Majors during masters degree: Bioinformatics, Cell Biology, Biophysical Chemistry

September 2004 - February 2005,

Erasmus exchange student at the University of Glasgow, Scotland.

October 2000 - October 2001,

Military Service. Promoted to Rank of Sergeant.

June 2000,

Matura (equivalent in the UK: A levels) passed with distinction (Ausgezeichneter Erfolg).

Interests

Endurance sports (cross country skiing, running, mountaineering), volleyball, medieval and contemporary literature, making and arguing about music (piano, guitar), world peace!